Phytoplankton dynamics and its influence on optical properties in the coastal waters of Southeastern Arabian Sea

Thesis submitted to the

Cochin University of Science and Technology

In partial fulfilment of the requirements

For the Degree Of

DOCTOR OF PHILOSOPHY

IN

MARINE SCIENCES

UNDER THE FACULTY OF MARINE SCIENCES

By

Minu P

(Reg. No. 4282)

Cochin University of Science and Technology
Cochin University Post, Ernakulam
Kerala-682 022

Fishing Technology Division
ICAR-Central Institute of Fisheries Technology
Matsyapuri post, Ernakulam
Kerala-682029

March 2017

Declaration

*I hereby do declare that the work presented in this thesis entitled "**Phytoplankton dynamics and its influence on optical properties in the coastal waters of Southeastern Arabian Sea**" is based on the original work done by me under the supervision of **Dr. P. Muhamed Ashraf,** Principal Scientist, ICAR-Central Institute of Fisheries Technology, Ernakulam-682029 and that no part of this work has previously formed the basis for the award of any degree, diploma or associateship, fellowship or any other similar title or recognition.*

Ernakulam

30-03-2017 *(Minu P)*

Acknowledgements

It is a pleasant task to express my sincere thanks to all those who contributed and supported for the successful completion of this thesis.

I express my deep and sincere gratitude to my supervising guide Dr. Muhamed Ashraf P for conceptualization and implementation of this research topic, in addition to his peerless guidance, motivation and patience all the way through my doctoral research. I was extraordinarily fortunate in having the opportunity to work on this challenging research area on marine bio-optics under his guidance. Dear Sir, your valuable contributions in every turning point in my academic life will always be treasured and I look forward to an exciting acquaintance in the future.

I sincerely place on record my thanks to Dr. C. N. Ravishankar, Director, ICAR-Central Institute of Fisheries Technology for facilitating my research under the Fishing Technology Division.

Words fail me to express my thankfulness to my head of the Fishing Technology Division, Dr. Leela Edwin, for the affection she showered, generous care and the 'thought provoking talk over a cup of tea'. I warmly thank for her excellent mental support during my work in the division. My warm thanks are due to Dr. B. Meenakumari for her kind support, motivation and critical comments during this study. She was approachable at any time and was open to valuable discussion on any matter and I will cherish her fatherly affection forever. Words are insufficient to express my gratitude towards Dr. Aneesh A. Lotliker for his help and encouragement through the course of my research and publications. I express my sincere gratitude for Dr. Trevor Platt and Dr. Shubha Satyendranath for rendering all support for taking part in the 3rd Marine Phytoplankton Identification workshop held at SAHFOS, Plymouth, United Kingdom. It was the fulfilment of a dream that I could participate in the workshop. The help rendered by Dr. Nandini Menon and Dr. Ajith Joseph, Scientist, NERCI Kochi, in fulfilling that dream is invaluable. I thank them from the bottom of my heart.

Sincere gratitude to my colleagues Mr. Shaju SS, Mr. Santhosh Kumar B, Mr. Manu KP, Ms. Souda VP and Mr. Sumith V, Mr. Vishnu and Mr. Prince for their whole hearted support and assistance during the sample collection and analysis.

I gratefully acknowledge all Scientists in the division. Dr. Mr. R Boopendranath, Dr. Saly N Tomas, Dr. Pravin P, Dr. Ramesan MP, Dr. Madhu VR, Mr. MV Baiju for their valuable critiques and advices. I am also grateful to Dr. Suseela Mathew and Mr. Joshi CG for helping me in doing my course work and in arranging all committees associated with PhD submission. I owe my deep gratitude for a life time to all my teachers of the past Dr. R. Indira Nair, Dr. Johny Joseph, Dr. PG Usha, Dr. Radakrishnan and Dr. Alphonsa Xavier the way they molded my life to what I am today.

Thanks are also to my fellow workers Mr. Dhiju Das, Mr. Vipin PM, Mr. Jose T. Fernandez, Mr. Sanjiba Kumar Baliarsingh, Mr. Yunus Ali and M. Kumaraswami for their immense support and advices. I express my thanks to Mr. Pradip Kumar Mahato, Mr. Muhamed Sherief, Mr. Rithin Joseph, Mrs. Sayana, Ms. Remyakumari, Mrs. Rehitha TV, Mrs. Leena Raphel and Msrs. Jolasana Jeevan. I thank my dear friends Dr. Poornima, Dr. Jasin Rahman, Mr. Sabin, Mr. Devaraj, Mr. Lighin, Mr. Ragesh, Mr. Sudheesh, Mr. Bejoy and Mr. Jayesh, who was there in my life, supporting me through all the difficult times and encouraging me whenever I decided to take part in International journeys. I sincerely thank all the research scholars of Central Institute of Fisheries Technology for their help and friendship.

I thank the technical staff of CIFT- Ms. Sasikala, Ms. Archana, Ms. Karthika, Mr. Nikhil Das P and Late Mr. Krishnan. I thank all the boat staffs of commercial trawlers Bharat Darshan, Mosa and CIFT vessels for the unrestricted support, courage and food they provided during each sampling days. I specially thank Mr. Jose Vincent for the arrangements and help he rendered to me for the sampling.

This work would not have been possible without the substantial financial support provided in the form of Research Fellowship for the projects entitled "In-situ time series measurements of Bio-optical parameters off Kochi" and "Retrieval of phytoplankton biomass and associated optical constituents based on long term bio-optical studies" under SATCORE, Indian National Centre for Ocean Information Services, Ministry of Earth Sciences, Government of India, Hyderabad. I express my profound sense of gratitude towards Dr. T. Satheesh C. Shenoi, Director, INCOIS for his benevolent support during his period. I extend my gratitude towards Dr. T. Srnivasa Kumar for the satellite data and facility provided at INCOIS. I thank Science and Engineering Research Board of Department of Science and Technology (DST) for providing me International Travel Grant to participate in the 3rd 3rd Marine Phytoplankton Identification workshop held at SAHFOS, Plymouth, United Kingdom. I also than National Centre for Antarctic and Ocean Research, Goa, for providing facilities and financial support for participating in 7th and 8th Indian Expedition to Southern Ocean onboard ORV Sagar Nidhi.

And most of all, I would like to share this moment of happiness with my loving, supportive, encouraging, family where the most basic source of my life energy resides. The never-ending support of my loving husband Sanuprasad, achan (Venugopalan), Amma (Anandavally) and brother (Athul) and my cute little pie Krish has been unconditional all these years and without their encouragement, prayers and understanding it would have been impossible for me to finish this work. I very fondly acknowledge their love and support. I sincerely thank all my relatives for their love and encouragement…..

Minu P

I deeply acknowledge Dr. Ravi, Dr. Teng, Dr. Karen and Dr. Elena for their endless support in identifying phytoplankton samples throughout my study.

Dr. Ravidas Naik
Research Scientist B
Southern Ocean Group
National Centre for Antarctic and Ocean Research (NCAOR)
Headland Sada, Goa-403 804, India

Dr. Teng Sing Tung
Ph.D. Student
13010134
Faculty Resource Sciences and Technology,
University Malaysia Sarawak.
Tel: 013-8047387
Email: tst861208@hotmail.com

Dr. Karen A. Steidinger
Research Scientist
Ecosystem Assessment and Restoration – Harmful Algal Blooms
Florida Fish and Wildlife Conservation Commission,
Farris Bryant Building
620 S. Meridian St. • Tallahassee, FL 32399-1600 • (850) 488-4676

Dr. Elena Stanca
Temporary Research Fellow
Università del Salento –
Piazza Tancredi, n7 - 73100 Lecce (LE) – Italy

This thesis is dedicated to all my teachers and friends……

Publications

Publications used in this thesis:-

1. **Minu, P**., Shaju, S.S., Ashraf, P.M. and Meenakumari, B., 2014. Phytoplankton community characteristics in the coastal waters of the southeastern Arabian Sea. Acta Oceanologica Sinica, 33(12), pp.170-179.
2. **Minu, P**., Lotliker, A.A., Shaju, S.S., Ashraf, P.M., Kumar, T.S. and Meenakumari, B., 2016. Performance of operational satellite bio-optical algorithms in different water types in the southeastern Arabian Sea. Oceanologia, 58(4), pp.317-326.
3. **Minu, P.,** and Muhamed Ashraf, P.. **2017.** A field guide on Marine phytoplankton along coastal waters off Kochi, South Eastern Arabian Sea. (ready for publication).

Other Publications:-

4. **Minu, P.**, Souda, V, P., Muhamed Ashraf, P., **2017**. Temporal variability of size-fractionated chlorophyll a concentration and influence of associated chemical parameters in coastal waters of southeastern Arabian Sea. Fishery Technology, 54:1-11.
5. Shaju, S.S., **Minu, P.,** Srikanth, A.S., Ashraf, P.M., Vijayan, A.K. and Meenakumari, B., 2015. Decomposition study of in vivo phytoplankton absorption spectra aimed at identifying the pigments and the phytoplankton group in complex case 2 coastal waters of the Arabian Sea. Oceanological and Hydrobiological Studies, 44(3), pp.282-293.
6. **Minu, P**., Shaju, S.S., Souda, V.P., Usha, B., Ashraf, P.M. and Meenakumari, B., 2015. Hyperspectral Variability of Phytoplankton Blooms in Coastal Waters off Kochi, South-eastern Arabian Sea. Fishery Technology, 52(4), pp.218-222.

7. **Minu, P**., Lotliker, A.A., Shaju, S.S., SanthoshKumar, B., Ashraf, P.M. and Meenakumari, B., 2014. Effect of optically active substances and atmospheric correction schemes on remote-sensing reflectance at a coastal site off Kochi. International Journal of Remote Sensing, 35(14), pp.5434-5447.

8. **Minu, P**, Souda, V,P., Mishra, R.K., Anilkumar, N., Muhamed Ashraf, P., 2013. Size fractionated phytoplankton and its optical properties in the Indian sector of Southern Ocean. Southern Ocean Expedition, Technical Report. NCAOR.

9. Ashraf, P.M., Shaju, S.S., Gayatri, D., **Minu, P**. and Meenakumari, B., 2013. In Situ Time Series Estimation of Downwelling Diffuse Attenuation Coefficient at Southern Bay of Bengal. Journal of the Indian Society of Remote Sensing, 41(3), pp.725-730.

10. **Minu, P**. and Ashraf, P.M., 2012. Occurrence of freshwater green algae in coastal waters off cochin during south west monsoon season. Fish Technology Newsletter, vol.23(1) : 3.

11. Shaju, S.S., **Minu, P**., Ashraf, P.M. and Meenakumari, B., 2011. Measurements of bio-optical parameters of southern ocean. Technical Report, 2011. NCAOR.

Table of Contents

List of Table

List of Figures

List of Plates

Chapter 1

The breaking of the wave cannot explain the whole Sea

-Vlamadir Nabokov

1. Introduction

1.1. Background of the study

The marine fisheries sector in India has witnessed a phenomenal growth during the last five decades both quantitatively and qualitatively. India ranks second in position, contributing about 3.59 million tones of marine landings to the world fish production (ICAR 2011; FSI 2012; CMFRI 2013a; FAO 2013, 2014a, b). Maximum marine landings were from Gujarat, Tamil Nadu, and Kerala contributing 54% to the total marine fish landings of the country. Total marine fish landings in Kerala estimated at 5.76 lakh tones (CMFRI 2015). The increase in fish production over the years has been the result of increased vessel number and availability of large and more efficient gear systems, developments in electronic, navigational, and acoustic detection equipment, which increased the area of operation of the mechanized fishing fleet (Edwin et al., 2014).

Advances in satellite-based technologies such as global positioning system (GPS) influenced the precision in fishing and Global Maritime Distress Safety System (GMDSS) based rescue system facilitated safety for fishermen (Edwin et al., 2014). Satellite remote sensing in Indian fisheries helped to map of potential fishing zones (PFZ) which helped the fishermen to reduce search time and significantly increase catch per unit effort (Solanki et al., 2003). Finding schools of fish and productive fishing areas are the main cause of fuel consumption in many commercial fisheries. Accurate prediction and detection of economically fishable aggregations of fish in

space and time lowers the cost of fishing operations. Remote sensing helps management of fisheries at a sustainable level along with guiding fishing fleets to increase their catch. Satellites monitor and the data used to predict potentially favorable areas of fish aggregation based on remotely detectable environmental indicators. These indicators include ocean fronts which separate waters of different temperature or colour, upwelling areas, which are cooler and more productive than background waters, specific temperature ranges preferred by certain fishes (Solanki et al., 2015). The recruitment, survival condition, distribution patterns, and migration of fish stocks are affected by changes due to short and long-term environmental variations. Any use of environmental data for the preparation of oceanographic analysis and forecasts in support of fishery operations will depend on an adequate understanding of the complex linkage between marine environmental and biological processes (Makris et al., 2009). These environmental variations frequently observed in satellite-derived patterns of ocean temperature and productivity (Longhurst 2010; Chassot et al., 2011).

The specific environmental parameters measured from satellite remote sensors include –sea surface temperature (SST), surface optical or bio-optical properties (Ocean colour, diffuse attenuation coefficient (Kd), total suspended matter, coloured dissolved organic matter (CDOM), chlorophyll pigments), salinity, fronts and gyres, oil pollution, wind and sea state (Klemas2013). Satellite data from chlorophyll concentration (Chla) and SST have

been used to identify productive fishing areas (i.e. PFZ). The biological productivity indicated by photosynthetic pigment of phytoplankton –Chla. Gower (1986) reported that Chl *a* above 0.2 mg m^{-3} indicated the presence of sufficient plankton activity to sustain a viable commercial fishery. Examination of fishing grounds on Albacore tuna by using satellite SST and ocean colour data showed that the species were high in locations corresponding to frontal zones and anti-cyclonic eddies (Zynuddin et al., 2006). Satellite measurement of spectral reflectance (ocean colour) is an effective method for monitoring phytoplankton by its index chlorophyll concentration (Schofield et al., 2004).

The spectral radiance emerging from the ocean surface measured at the top of atmosphere (TOA) by satellite remote sensors. The surface radiances converted to reflectances provides the spectral signatures required for identifying Chl and other water constituents (Behrenfeld and Falkowski 1997; Carder et al., 1989). A meticulous calibration and validation approach used for producing valid products such as ocean Chla and other constituents derived from ocean colour data (Robinson 2004; Schofield et al., 2004; Bailey and Werdell 2006). In this study, an approach to understand the phytoplankton dynamics affecting the optical properties of coastal waters off Kochi, Southeastern Arabian Sea (SEAS), and to validate the satellite products on a regional scale carried out.

1.2. Classification of ocean waters

Morel and Prieur (1977) classified oceanic waters into two basic optical types- Case 1 and Case 2 waters. In Case 1 waters, the concentration of phytoplankton is high compared to non-living particles and the phytoplankton pigments and co-varying detrital material play an important role in actual absorption.

Jerlov (1976) classified oceanic waters based on the spectral shape of the diffuse attenuation coefficient, $K_d(z,l)$, defined as:

$$K_d(z,l) = -d[\ln E_d\ (z,l)]/\ dz$$

where Ed(z, l) is the downwelling irradiance at depth 'z' and wavelength 'l'. The variability of diffuse attenuation coefficient depends on the inherent optical properties of water such as total absorption and backscattering and hence considered as a quasi-inherent optical property. Baker and Smith (1979) showed that E_d is insensitive to environmental effects except for extreme conditions, such as of very large solar zenith angles.

The Jerlov's classification of ocean waters is based on water clarity. The types are numbered I (clearest), IA, IB, II and III (most turbid) for open ocean waters and 1 (clearest) through 9 (most turbid) for coastal waters. The

Jerlov types I – III correspond to case 1 waters (Morel & Prieur 1977) and type 1-9 correspond to case 2 waters.

Mobley (1994) reported that 98% of the world's open and coastal waters fall into case 1 category. These waters, where major bio-optical research was oriented, considered as less complex and phytoplankton dominant. Previous studies have developed many models and parameterizations to relate optical properties of water (such as absorption and backscattering) and remote sensing reflectance (Rrs) and Chl (Prieur and Sathyendranath 1981; Gordon and Morel 1983; Gordon et al., 1988; Morel 1991). For case 2 waters, these models developed for case1 waters, are not applicable. Case 2 waters are highly complex, typically near-shore, coastal and estuarine waters. In case 2 waters, significant optical variability is caused by human-induced processes (drainage of water from factories and industries) and natural process (river runoff).

1.3. Optical properties of natural waters

The properties of the air-water interface sea salts, sea spray, aerosols) and the optical properties of water column mainly influence the amount of light that penetrates to a given depth. Cloud cover, wind speed, solar zenith angle and time determines the transmission of solar radiation through the air-water interface whereas the

variability in the angular distribution of incident irradiance and the effect of surface waves are the factors modulating the intensity at particular depth.

Water has two groups of properties viz. apparent and inherent optical properties (Preisendorfer 1976). Apparent optical properties (AOPs) depend on both the water's composition and the geometrical distribution of the light field. They include properties such as reflectance, average angles of incident radiation and irradiance attenuation coefficients. Inherent optical properties (IOPs) depend solely on the water's composition and the optical characteristics of each individual constituent and include absorption, scattering and attenuation coefficients, index of refraction, and scattering phase functions.

1.3.1. Composition of natural waters

Natural waters are considered as highly complex consisting of living and non-living matter. Apart from this, organic, inorganic, particulate, and dissolved matter is also present. Eventhough seawater contains a range of distinct units varying in size from that of large mammals to that of a water molecule, the constituents of seawater traditionally divided into "dissolved", and "particulate" matter. Dissolved material is everything that passes through a ~ 0.2 – 0.4 µm pore sized filter.

a. Pure seawater and its constituent like various dissolved salts increase scattering by about 30%. In visible wavelengths, effect of these constituents on absorption is negligible (Mobley 1994). But absorption by these

components increases at ultraviolet wavelengths and at very long wavelengths (>0.1 mm).

b. Dissolved Organic Matter (DOM) plays a major role in determining underwater light availability in oceans. Major sources of DOM include autochthonous primary production and river run-off of terrestrial organic matter (allochthonous production). Coloured Dissolved Organic Matter (CDOM) is the optically active fraction of DOM. CDOM has a strong absorption in the short, Ultra-Violet (UV) wavelength regions. In coastal environments, its concentration is usually higher when compared to open ocean waters, hence considered as one of the major component controlling the amount of underwater light.

c. Particulate matter consists of living and nonliving organic particles and inorganic particles. Living organic particles comprise of phytoplankton, zooplankton, viruses and bacteria whereas non-living organic particles includes colloids and organic detritus.

Phytoplankton is microscopic, free floating organisms and is the principal primary producers of the oceans. Their size ranges from 0.2 µm to 2mm.

Microplankton-20-200 µm Picoplankton-0.2-2µm

Macroplankton->200 µm Nanoplankton-2-20 µm

The optical properties of most oceanic waters (Case 1) determined primarily by Phytoplankton and its co-varying matter. Phytoplankton contains primary pigments and accessory pigment such as Chl, carotenoids etc. that strongly absorbs the

blue and red light of the visible spectra. Phytoplankton also influences the total scattering properties of seawater. Due to their relatively large size, the larger phytoplankton species contributes relatively little to backscattering in the visible spectrum. The principal phytoplankton taxonomic groups include-

Class Bacillariophyceae	-	Diatoms
Class Pyrrophyceae	-	Dinoflagellates
Class Prymnesiophyceae	-	Coccolithophores
Class Chysophyceae	-	Silicoflagellates
Class Euglenophyceae	-	Euglenoid flagellates
Class Chlorophyceae	-	Green algae
Class Cyanophyceae	-	Blue-green algae
Class Haptophyceae	-	Brown coloured Phytoflagellates

(Kennish 2001)

Zooplankton are small living organisms of animal realm. They have only limited mobility. Their sizes range from 10 mm to 5 cm. They generally considered feeble in modifying the underwater optics. They usually ignored in most watercolour models. This is because of their small concentration compared to higher concentrations of phytoplankton and bacterioplankton. In some locations, zooplankton populations also affect water optical properties. Their large concentration increases the scattering (Mobley 1994). The effects of light on zooplankton deserves more attention (Fortier et al., 2001; Cottier et al., 2006; Batnes et al., 2013) Daase et al., (2008) pointed to the importance of

light and optical water properties for the behaviours, distributions and life histories of the dominant Arctic copepods (*Calanus* spp. and *Metridia longa*) at the end of the productive season. Trudnowska et al., (2013) observed vertical separation of *Calanus* sp. development and showed that the variability in zooplankton distribution and community structure closely related to the hydrographic and optical characteristics of the water.

Microscopic unicellular organisms with size ranging between 0.2-2µm comprise the living bacteria. The free-living heterotrophic bacteria also play a major role in scattering and absorbance of light mainly in blue wavelengths (Spinrad et al., 1989; Morel and Ahn 1990; Stramski and Kiefer 1991) and in oligotrophic waters with low Chl concentrations.

Kepner et al., (1998) and Bergh et al., (1989) reported that the concentration of virus particles range from 10^6 to 10^{15} particles per m^3 in eutrophic marine waters. Viruses have size ranging between 20-250 nm. Viruses control planktonic microorganisms by infecting all members (Proctor and Fuhrman 1990). The absorption and scattering by viruses in marine waters are doubtful eventhough they form large numbers (Mobley 1994). Studies conducted by Balch et al., (2000) reported that there is no possibility of contribution by viruses to the back scattering coefficient. They conducted laboratory experiments in which four bacterial viruses (bacteriophages) of varying sizes measured for their volume scattering functions and suggested that viruses, are not a major source of backscattering.

Trace metals, clay minerals, quartz, sand, silt etc are the main components of inorganic particles. These particles have wide range of sizes. The concentrations of these particles are substantially high in coastal waters due to large river discharges, heavy sediment load, and wind driven transport of dust particles. These particles found significantly affecting the light penetration. Detritus particles are non-living organic particles of various sizes formed from the fragments of decayed plants and animals along with their excretions. Significant contribution by these particles more in the shorter wavelengths and as the wavelength increases it found that the contribution decreases in an exponential manner (Kishino et al., 1985; Roesler et al., 1989). Sub-micron detritus and mineral particles found to be the most significant backscatterers in the ocean (Stramski and Kiefer 1991). Lehahn et al (2014) developed satellite-based approaches to quantify the impact of diverse environmental stresses on the fate of phytoplankton blooms and reveled that high level of specific viruses causes mortality of coccolithophore cells.

1.3.2. Optical characteristics of pure sea water -absorption and scattering

Bukata et al., (1995) defined pure water as a chemically pure substance comprised of a mixture of several water isotopes of various molecular masses. Pure seawater consists of pure water plus various dissolved salts that average about 35‰ (35 psu) by weight (Mobley 1994).

Absorption by water is weakly dependent on temperature, especially in the red and near-infrared region (Pegau and Zaneveld 1993; Hojerslev and Trabjerg 1990; Buiteveld et al., 1994). Absorption by water molecules is dominant relative to scattering by water at wavelengths larger than 550 nm. Water scattering becomes very important at wavelengths smaller than 500 nm (Buiteveld et al., 1994).

1.3.3. Phytoplankton community structure

Marine phytoplankton are considered as important contributors to marine food web thereby regulating global carbon fluxes (Falkowski et al., 1998). In the ocean, many different phytoplankton taxonomic groups existed which together determines the primary production. For the better understanding of structure and dynamics of marine ecosystems from space quantification of phytoplankton biomass and community composition is very important.

Phytoplankton are plant like microscopic organisms that freely float or swim in waters (phytoplankton comes from the Greek words phyton=plant and plankton=to wander). Phytoplankton is one among the major substances

that determine the optical and biological characteristics of open ocean and coastal waters. Phytoplankton is diverse in species, shape, size and numerical abundance. They constitute the basis for the marine food web.

Subrahmanyan (1958) studied the phytoplankton abundance along the South Eastern Arabian Sea (SEAS) and reported high abundance during the southwest monsoon period, with seasonal variation in its composition. Studies by Qasim& Reddy (1967), Radhakrishna (1969), Subrahmanyan et al., (1975), Rajagopalan et al., (1992), and Habeebrehman et al., (2008) reported variability of Chl patterns during monsoon season. During monsoon period, the vertical flux of inorganic nutrients triggers phytoplankton production and lead to high biological productivity (Ryther et al., 1966; Qasim 1982). Along the SEAS, intense phytoplankton production found from May–June to September during the summer monsoon upwelling (Bhattathiri et al., 1996).

Tarran et al., (1999), in their study on phytoplankton community structure in the Arabian Sea (AS) during and after Southwest (SW) monsoon

has found that during SW monsoon diatoms were of greatest diversity and during inter-monsoon coccolithophores were the most diverse phytoplankton. They also showed that during both the SW monsoon and inter-monsoon, phytoplankton abundance and biomass was dominated by prokaryote taxa and *Synechococcus* spp. were the abundant phytoplankton which formed $>10^3$ cells L^{-1}. During SW monsoon, the near shore waters are dominated by mixed community of diatoms and *Synechococcus*.

Shalapyonok et al., (2001) as part of their study in the Arabian Sea during summer southwest and fall northeast monsoon showed that the phytoplankton community structure was strongly linked to water-mass characteristics and was affected by both intense monsoon related environmental forcing and widespread and dynamic mesoscale structures. They also showed that, the prokaryotes *Prochlorococcus* and *Synechococcus* contributed about 50% of phytoplankton carbon biomass measured by flow cytometry during both seasons and the changes in phytoplankton community composition during the SW monsoon were accompanied by characteristic shifts in phytoplankton community structure.

Roy et al., (2006) studied the spatial variation of phytoplankton pigments along the SW coast of India towards the end of upwelling season and inferred that the phytoplankton community shifted from a dominant picoplankton fraction and Prymnesiophytes to diatom dominated microplankton.

Thomas et al., (2013) made an attempt to understand the influence of upwelling events on the phytoplankton community in the inshore as well as shelf waters of SEAS during the upwelling period of the summer monsoon of 2009. They found that centric diatom *Chaetoceros curvisetus* and pennate diatoms *Nitzschia seriata* and *Pseudo-nitzschia sp*. dominated during phase 1 upwelling and during phase 2, pennate diatoms are replaced by centric diatoms. They also reported significant presence of solitary pennate diatoms *Amphora* sp. and *Navicula* sp. in the waters off Kochi. Further, they showed that the proportion of dinoflagellates was comparatively higher and was represented mainly by *Protoperidinium* spp., *Ceratium* spp. and *Dinophysis* spp.

The dinoflagellate *Neoceratium platycorne* was reported for the first time from the Northeastern Arabian Sea (NEAS) (Padmakumar et al., 2014). The species found in the open ocean subsurface waters during late winter monsoon period. Banerjee and Prasanna Kumar (2014) studied the role of dust deposition in enhancing phytoplankton blooms during winter monsoon in the Central Arabian Sea (CAS) by tracking the dust storms using satellite imagery. They showed that during winter monsoon, the CAS away from the realm of active winter convection supports episodic phytoplankton blooms fueled by episodic dust storms that are important in driving the inter-annual variability in chlorophyll in a region away from active winter convection.

1.3.4. Absorption by phytoplankton (a_{ph})

Depending on the phytoplankton species, its cell size and physiological state, light energy absorbed by various photosynthetic pigments present inside them. The light energy converted to chemical energy through the process of photosynthesis. The absorption properties of phytoplankton depend on the species and their pigment composition. The three basic types of photosynthetic pigments are the chlorophylls, the carotenoids and the biliproteins. Chl and carotenoid pigments are present in almost all phytoplankton but biliproteins are present in certain blue-green and red algae.

Chl are the main photosynthetic pigments in plants. Chl pigment is present in distinct types as chlorophyll a, b, c and d (Chla, Chlb, Chlc and Chld respectively). All photosynthetic plants contain Chla, while most classes of plants contain in addition Chlb or Chlc. The role of Chld in photosynthesis is uncertain (Bukata et al., 1995).

Chla and Chlb strongly absorb light in the red region of the spectrum (~675nm for Chla and ~650nm for Chlb), and in blue region of the visible spectra (~440 nm for Chla and ~460 nm for Chlb). Chlc includes of Chlc 1, Chlc 2 and Chlc 3, which are spectrally distinct components and has strong absorption in the blue region of the spectrum while they show some smaller

absorption maxima at larger wavelengths (~580 and ~630nm). The term "Chlorophyll concentration" refers to the sum of Chla and related phaeophytin-a (Phaeoa). This sum often called 'pigment concentration'. Chl ranges from 0.01 mg m^{-3} in the clearest waters, to more than 100 mg m^{-3} in eutrophic estuaries or lakes (Mobley 1994). The carotenoid absorbs mainly between 450nm to 550nm and represents more than 100 different pigments.

Diatoms are the major phytoplankton found in most marine and freshwater environments (Kirk 1994). Division Chrysophyta under the class Bacillariophyta in diatoms are usually yellow-brown coloured due to the presence of two xanthophyll pigments-fucoxanthin and diatoxanthin. Dinoflagellates (Division Pyrrophyta) are the second major group of phytoplankton in total marine environment. They have brownish to reddish colour due to the presence of carotenoid pigment peridinin. They form red tides during bloom conditions. Peridinin strongly absorbs 500-560 nm of the visible spectrum. Open oceans with warm waters are dominant in coccolithophorids (Division Chrysophyta, Class Haptophyceae) which have also yellow-brown cells. Their bloom appears as milky turquoise in the ocean. Phylum Chlorophyceae comprising green algae found mainly in freshwater environments contains Chl *a* and Chl *b* as dominant pigments.

Sathyendranath et al., (1987) found that, for phytoplankton groups of Chlorophyceae, Haptophyceae and Bacillariophyceae, specific absorption at 440 nm [a*ph(440)], varied between 0.019 and 0.047 m^2 mg^{-1}, while a*ph (676) varied between 0.011 and 0.023 m^2 mg^{-1}. Another study by Prieur and Sathyendranath (1981) found that a*ph (440) vary within the range 0.013 to 0.077 m^2 mg^{-1}.

Phytoplankton size and taxonomic information can be inferred from features of the spectral phytoplankton absorption coefficient (Bricaud and Stramski 1990; Ciotti et al., 2002; Bricaud et al., 2004; Vijayan and Somayajula, 2014). In optically-complex waters with high spatial and temporal variability in both phytoplankton and detritus concentration and composition, direct pigment analyses are more sensitive for getting information on phytoplankton size and taxonomy (Bricaud and Stramski1990; Ciotti et al., 2002; Bricaud et al., 2004). The time evolution of phytoplankton size structure over the global ocean was studied (Roy et al., 2012). The light absorption coefficient of phytoplankton was used to retrieve quantitative information about phytoplankton size structure from satellite-derived ocean-colour data. The results showed that, the spatial distribution of the size-spectrum exponent and the biomass fractions of pico-, nano- and micro-phytoplankton estimated are consistent with current understanding of phytoplankton functional types in the global oceans.

The variability in the absorption spectra of phytoplankton and particulate matter of case 2 coastal waters of the SEAS were studied

Table 1.1: Absorption maxima by Chl, carotenoids and biliproteins

Pigment groups main		Absorption Peak	Reference
Chlorophyll a		~ 440 nm ~675 nm	Prezelin and Alberte (1978); Prezlin and Boczar (1986); Aguirre-Gomez et al., (2001)
Chlorophyll b		~ 460 nm ~650 nm	Millie et al., (1997)
Chlorophyll c	c1 c2 c3	~ 460 nm ~ 580 nm ~ 630 nm	Millie et al., (1995); Millie et al., (1997);
Carotenoids		450 - 550 nm	Aguirre-Gomez et al., (2001) Millie et al., (1995);
Biliproteins		480 - 600 nm	Millie et al., (1997); Louchard et al., (2003) Ong et al., (1984)

between June 2010 to November 2011 by Shaju et al., (2015). Their results showed that the phytoplankton specific absorption coefficient, at 440 nm and 675 nm, a^*_{ph} (440) and a^*_{ph} (675) varied from 0.018 to 0.32 m^2 mg^{-1} and from 0.0005 to 0.16 m^2 mg^{-1}. They reported that the amplitude of maxima obtained is proportional to the concentration of the chromoprotein, which absorbed that wavelength. Lorenzoni et al., (2015) examined phytoplankton taxonomic and pigment time series data collected between 2006 and 2012, to understand

how seasonal changes in these parameters relate to bio-optical data. They reported that, the absorption properties exhibited seasonal variations and could not identify diagnostic pigments in a quantitative way using derivative analysis of phytoplankton absorption because of overlapping of absorption spectra among the pigments present.

1.3.5. Absorption by Non-Algal Particulate matter (a_{NAP})

Mixing processes like wind induced turbulence and tidal currents cause re-suspension of sediments, non-living organic and inorganic particles. Detrital particulate matter includes non-living organic particles, fragments of decayed organisms along with their excretions. Minerals such as fine clay, silt particles, sand etc. and precipitates of iron oxide, manganese hydroxide and calcium carbonate form the inorganic particles (Bukata et al1995). a_{NAP} is prominent in the short, ultra-violet wavelengths and the shape of the spectra resembles that of absorption by coloured dissolved organic matter (a_{CDOM}) (Yentch 1962). Studies by Kishino et al (1985), Roesler et al (1989) and Morrow et al (1989) showed that a_{NAP} increases with decreasing wavelength. Roesler et al (1989) found that in the wavelength range 400-750 nm, a_{NAP} reaches upto 0.01 m^{-1}. Various other studies showed that the absorption by NAP ranged between 0.006 and 0.014 m^{-1} (Kishino et al., 1986 (studies in NW pacific); Maske and Haardt 1987 (studies in Kiel harbor); Morrow et al., 1989; Iturriaga and Siegel 1988; Bricaud and Stramski 1990 (studies in the Sargasso Sea)).

The proportion of non-algal particles in the water column is affected by substantial disposal of sewage (Abril et al., 2002; Callahan et al., 2004; Spencer et al., 2007). Rivier et al., (2012) investigated the spatial and temporal variability of non-algal suspended particulate matter (SPM) in surface waters of the English Channel and highlighted that three explanatory variables—the tide, waves and Chl *a* is able to estimate non-algal surface SPM with a coefficient of determination reaching 70% at many locations. Eleveld et al., (2014) investigated, how large-scale estuarine SPM concentrations were affected by tidal and bulk meteorological drivers, and how retrieved SPM is biased by tidal aliasing and sampling under clear sky conditions using optical data from a sun-synchronous satellite. The results showed spatial patterns in SPM as a function of semi-diurnal tidal phase, fortnightly tidal phase, or season and distance to shallow source area, tidal current velocity, and advection of North Sea and estuarine surface waters controls surface Suspended Particulate matter. Minu et al., (2015) studied the hyperspectral variability of phytoplankton blooms in SEAS and reported that, the detrital absorption spectra showed marked difference for different blooms.

1.2.6. Absorption by coloured dissolved organic matter (a_{CDOM})

Varying concentrations of dissolved organic substances found in aquatic environments. The optically active fraction is known as CDOM or chromophoric organic matter or gelbstoff or gilvin. It plays a major role in determining the underwater light field along with phytoplankton and non-algal

particles. CDOM consists of mainly fulvic and humic acids (Jerlov 1976; Leyendekkers 1967). When the concentration of CDOM is large, water may have its yellow or yellowish brown colour. Autochthonous primary production and river runoff of terrestrial organic matter (allochthonous production) considered as the major sources of CDOM in natural waters. Oceanic CDOM formed by the decomposition of phytoplankton (Kopelevich and Burenkov 1977; Bricaud et al., 1981). Mixing, photochemical, and microbial processes as well as human activities like wetland drainage etc. can alter CDOM's composition, structure, and optical properties. Photo bleaching of CDOM and biological production of certain compounds absorb more strongly in ultraviolet region than in visible region (Coble and Brophy 1994; Gao and Zepp1998) resulting in the increase of spectral slope. Vodacek et al., (1997) showed that as distance to off shore increases the CDOM absorption decreases. This is because dissolved materials originating from the land reaches coastal waters thereby increasing their absorption.

CDOM strongly absorbs light in shorter wavelengths especially in the ultraviolet-visible region. Its concentration is more in coastal waters compared to open ocean. Studies related to climate change using modifications in CDOM concentrations showed that cloudiness, intensity and frequency of storm events, mixing processes and river runoff significantly affect biologically destructive UV radiation causing changes in aquatic biota and composition of aquatic food webs and thereby affecting overall structure and dynamics of the ecosystem (Gibson et al., 2000; Pienitz and Vincent

2000). Coastal waters significantly affected by CDOM absorption in shorter wavelengths causing reduction in photosynthetically active radiation (PAR) available to phytoplankton. CDOM also influences the measurements of Chl and primary productivity using global ocean satellites.

As wavelength increases a_{CDOM} spectra typically decrease in an exponential fashion. $a_{CDOM}(355)$ ranges from <0.05 m^{-1} in very clear, oligotrophic waters to >15 m^{-1} in some rivers, lakes, and coastal regions (Blough and DelVecchio 2002). Variability in a_{CDOM} is associated with changes in the composition of the dissolved material present in the water. Various factor influences the absorption and spectral slope of CDOM. Boyd and Osburn (2003) in their studies suggested that bacterial degradation of CDOM components have severe impact on optical properties of CDOM. CDOM strongly absorbs in the blue and its varying proportion in the absorption confuses classical “blue-to-green” band ratio algorithms for the determination of Chla from remote platforms (Siegel et al., 2005; Morel and Gentili 2009a). Zhu et al., (2011) developed a semi analytical algorithm to study the seasonal and spatial variations of CDOM absorption. Bricaud et al (2012) showed that the exponential slope values of CDOM also vary among three major oceanic basins and follow specific seasonal dynamics. Ocean currents transport CDOM over long distances (>1000 km) in a few months (Matsuoka et al 2011; 2012). A semi-analytical algorithm for estimating light absorption coefficients of the CDOM developed using R_{rs} by Matsuoka et al., (2013). They claimed that the

algorithm can be used to separate CDOM and non-algal particles (NAP) using an empirical relationship between NAP absorption and particle backscattering coefficients. A novel algorithm presented by Cao and Miller (2015) for resolving CDOM absorption spectra accurately from ocean colour. The model developed for remotely determining the amount and type of CDOM in the environments of coastal lagoon and the coastal waters around Chennai on the Southeast part of India, recognized healthy phytoplankton cells and macrophytes contributing to the authochthonous production of coloured humic-like substances in variable amounts (Shamnugam et al., 2016).

Since, the geographical extent of the terrestrially dominated regions varies seasonally, depending on the magnitude of freshwater inputs and its dilution by physical mixing processes of the coastal areas, it is very important to understand the performance of sensors in assessing the CDOM on regional scales.

1.3.7. Remote sensing of Phytoplankton community structure

The chlorophyll concentration, considered as an indicator of phytoplankton biomass, determines the optically active constituents altering the underwater light field. Hence in-situ measurements of phytoplankton and their optical characteristics in the coastal areas can provide the database required to develop bio-optical algorithms useful in retrieving chlorophyll from space (Carder et al., 1991; Tassan, 1994; Le et al., 2011). Chlorophyll a (Chl a) is the major pigment in phytoplankton which absorbs blue and red light in the visible spectrum and results in the blue-green color of ocean. Also the regional, seasonal and inter-annual variations of the ocean color products and its retrieval depend on the types of dominant phytoplankton that contribute to the ocean colour. Hence understanding the variations in phytoplankton community structure helps to know its own inherent optical properties and dynamics of complex coastal waters in which they inhabit, thereby to get a clear idea about the water leaving signal reaching the sensor (IOCCG report No.9). Phytoplankton taxonomic studies provide basic information on the phytoplankton species which can be used in pigment marker studies. The contribution of various marker pigments used for the

development of algorithms to determine the contribution of these pigments to the total Chl a concentration

Matondkar et al., (2006) studied the seasonal variation of phytoplankton abundance and types in the NEAS and Lakshadweep Sea using sequential images from IRS P4/OCM satellite and shipboard sampling and found that Chl concentration varied spatially and temporally and from coastal to offshore waters. They reported the sequential transition of blooms from a mixture of dinoflagellates to *Noctiluca miliaris* to *Trichodesmium erythraeum* and *Trichodesmium thiebautii*. The studies conducted in west coast of India showed that nitrogen depletion below detectable limits resulted in the declination of both diatom and prymnesiophytes and gave way to dinoflagellates and in well oxygenated surface waters with non-detectable levels of nitrate and ammonia led to the domination of pico-cyanobacterial populations.

Gonsalves et al., (2011) reported that the water column of slope of EAS is more diverse and dominated by heterotrophic dinoflagellates whereas water column offshore showed low diversity and dominated by diatoms. Inter-annual variability of phytoplankton blooms in northwestern AS and Gulf of Oman studied by Marvasti et al., (2015) using SeaWIFS Ocean colour data. Their study exhibited two climatological blooms in the region. A pronounced anti-correlation between the AVISO sea surface height anomaly (SSHA) and Chl found during the wintertime bloom. They concluded that on a regional scale, inter-annual variability of the wintertime bloom is dominated by cyclonic eddies which vary in location from one year to another.

Species identification of mixed algal blooms, in the Northern Arabian Sea, using remote sensing techniques were done by Dwivedi et al., (2015). The approach developed for detection of bloom-forming algae *Noctiluca scintillans* from diatoms using Moderate Resolution Imaging Spectroradiometer (MODIS)-Aqua data in a mixed-species environment went successful. The phytoplankton pigment signatures and nutrient distribution from a front in the NEAS showed that nutrient concentrations were high within the filament and front compared to the surrounding waters and had a unique phytoplankton assemblage. The study demonstrated that phytoplankton groups respond strongly to nutrient enhancement that

encountered within the vicinity of the SST fronts that characterize the Potential Fishing Zones (Roy et al., 2015). The seasonal and intra annual variation of phytoplankton availability showed that Chl a, concentration was almost identical throughout the year in the northern Arabian sea near the coastline and open sea waters of Pakistan, India, Iran and Oman (Khan et al., 2015). An optical system was developed to detect and monitor three major algal blooms (viz. *Noctiluca scintillans*, *Noctiluca miliaris*, *Trichodesmium erythreum*, *cochlodinium polykrikoides*) over ecologically relevant scales around India. The model were successful in delineating the presence of the blooms in a heterogenous phytoplankton community; but were not able to detect specific species during their pre -bloom conditions and to indicate whether a particular bloom is toxic or harmful (Gokul and Shanmugam 2016). A study of spatial-temporal variability of *Noctiluca scintillans* blooms using satellite data expressed a cyclic pattern of their spread over a period of 13 years (Dwivedi et al., 2016).

Few studies carried out in the coastal waters off Kochi, in the eastern Arabian Sea to know the phytoplankton community characteristics and its influence on other optical properties, even though, the backwaters and Arabian Sea were investigated in detail. Previous studies in the area mainly focused on physical and chemical characteristics of phytoplankton blooms. Every phytoplankton irrespective of their species and size has their own peculiarity, influencing different parts of the visible electromagnetic radiation in terms of absorption. It is important to understand the characteristics and associated bio-optical properties in the area on a regional scale. Hence, a study carried out in the coastal waters of SEAS with the following objectives:-

1.4. Objectives of the work

1. To characterize the phytoplankton community structure in order to assess seasonality and physiological characteristics.
2. To understand the influence of index chlorophyll of dominant phytoplankton species on inherent and apparent optical properties
3. To evaluate the performance of standard empirical algorithms for chlorophyll and coloured dissolved organic matter.

1.5. References

Abril G, Nogueira M, Etcheber H, Cabeçadas G, Lemaire E and Brogueira MJ. 2002. Behavior of organic carbon in nine contrasting European estuaries. Estuarine Coastal and Shelf Science, 54 (2), 241–26

Aguirre-Goméz R, Weeks A R, Boxall S R. 2001. The identification of phytoplankton pigments from absorption spectra. International Journal of Remote Sensing, 22(2–3), 315–338

Bailey S W, &Werdell P J. 2006. A multi-sensor approach for the on-orbit validation of ocean colour satellite data products. Remote Sensing of Environment, 02,12−23

Banerjee P, and Prasanna Kumar S. 2014. Dust-induced episodic phytoplankton blooms in the Arabian Sea during winter monsoon. Journal of Geophysical Research. Oceans, 119, 7123–7138, doi:10.1002/2014JC010304

Baker K S, and Smith R C. 1979. Qasi-inherent characteristics of the diffuse attenuation coefficient for irradiance. Ocean Optics VI, S.Q.. Duntley, Editor, Proc.SPIE, 208, 60.

Balch W M, Drapeau D T, Fritz J J. 2000. Monsoonal forcing of calcification in the Arabian Sea. Deep-Sea Research II, 47, 1301–1337.

Batnes A S, Miljeteig C, Berge J A et al. 2013. Quantifying the light sensitivity of Calanus spp. during the polar night: potential for orchestrated migrations conducted by ambient light from the sun, moon, or aurora borealis. Polar Biology, 1–15, doi:10.1007/s00300- 013-1415-4

Behrenfeld M J, Falkowski P G. 1997. Photosynthetic rates derived from satellite-based chlorophyll concentration. Limnology and Oceanography, 42, 1-20

Bergh O, Bsrsheim K Y, Bratbak G, Heldal M. 1989. High abundance of viruses found in aquatic environments. Nature 340: 467-468.

Bhattathiri P M A, Pant A, Sawant S, Gauns M, Matondkar S G P, MohanrajuR. 1996. Phytoplankton production and chlorophyll distribution in the eastern and central Arabian Sea. Current Science, India, 71 (11), 857–862

Blough N V, and Del Vecchio R. 2002. Chromophoric DOM in the coastal environment. Biogeochemistry of Marine Dissolved Organic Matter. 509-546, D.A. Hansell and C.A. Carlson, eds., Academic Press, San Diego, CA.

Bracher A, Vountas M, Dinter T, Burrows J P, Röttgers R and Peeken I. 2009. Quantitative observation of cyanobacteria and diatoms from space using PhytoDOAS on SCIAMACHY data. Biogeosciences, 6, 751-764

Bricaud A, Claustre H, Ras J, and OubelkheirK. 2004. Natural variability of phytoplankton absorption in oceanic waters: Influence of the size structure of algal populations, Journal of \Geophysical Research, 109, C11010, doi:10.1029/2004JC002419

Bricaud A, Ciotti A M and Gentili B. 2012. Spatial-temporal variations in phytoplankton size and coloured detrital matter absorption at global and regional scales, as derived from twelve years of SeaWiFS data (1998–2009). Global Biogeochemical Cycles, 26(1)

Bricaud A, Prieur L, and Morel A. 1981. Absorption by dissolved organic matter of the sea (yellow substance) in the UV and visible domains. Limnology and Oceanography, 26, 43–53

Bricaud A, and Stramski D. 1990. Spectral absorption coefficients, of living phytoplankton and nonalgalbiogenous matter: a comparison between the Peru upwelling area and the Sargasso Sea. Limnology and Oceanography, 35562-582

Boyd T J, and Osburn C L. 2003. Changes in allochthonous and autochthonous CDOM excitation and emission fluorescence matrices (EEMS) from bacterial degradation. Biogeochemical Cycles. ASLO Meeting.

Bukata R P, Jerome J H, Kondratyev K Y, and Pozdnyakov D V. 1995. Optical Properties and Remote Sensing of Inland and Coastal Waters. CRC Press, Florida, 362 pp.

Buiteveld H, Hakvoort J H M, and DONZE M. 1994. The optical properties of pure water, p. 174–183. In Ocean Optics XIII. Proc. SPIE 2258

Callahan J, Dai M, Chen R F, Li X, Lu Z, Huang W. 2004. Distribution of dissolved organic matter in the Pearl River Estuary. Marine Chemistry, 89, 211–224

Cao F and Miller W L. 2015. A new algorithm to retrieve chromophoric dissolved organic matter (CDOM) absorption spectra in the UV from ocean colour. Journal of Geophysical Research: Oceans, 120(1), 496-516

Carder K L, Steward R G, Harvey G R, and Ortner P B. 1989. Marine humic and fulvic acids: their effects on remote sensing of ocean chlorophyll. Limnology and Oceanography. 34, 68–81

Chassot E, Bonhommeau S, Reygondeau G, Nieto K, Polovina J J, Huret M, Dulvy N K and Demarcq H. 2011. Satellite remote sensing for an ecosystem approach to fisheries management. ICES Journal of Marine Science: Journal du Conseil, 68(4), 651-666

Ciotti A M, Lewis MR and Cullen JJ. 2002. Assessment of the relationships between dominant cell size in natural phytoplankton communities and the spectral shape of the absorption coefficient. Limnology and Oceanography, 47(2), 404-417

CMFRI. 2013a. Annual Report2012-2013. Central Marine Fisheries Research Institute , Cochin 200p

CMFRI. 2015. Annual Report2013-2014. Central Marine Fisheries Research Institute, Cochin 200p

Coble P, Brophy M. 1994. Investigation of the geochemistry of dissolved organic matter in coastal waters using optical properties. SPIE - Ocean Optics XII 2258, 377- 389

Cottier F, Tverberg V, Inall M et al. 2005. Water mass modification in an Arctic fjord through cross-shelf exchange: the seasonal hydrography of Kongsfjorden, Svalbard. Journal of Geophysical Research,110, C12005

Daase M, Eiane K, Aksnes D L et al. 2008. Vertical distribution of *Calanus* spp. and *Metridia longa* at four Arctic locations. Marine Biological Research, 4, 193–207

Dickey TD, Kattawar GW and Voss KJ. 2011. Shedding new light on light in the ocean. Physics Today, 64(4), 44-49

Dwivedi R, Rafeeq M, Smitha B R.Padmakumar K B, Thomas L C, Sanjeevan VN, Prakash P and Raman M. 2015. Species identification of mixed algal bloom in the Northern Arabian Sea using remote sensing techniques. Environmental monitoring and assessment, 187(2), 1-11

Dwivedi R, Priyaja P, Rafeeq M and Sudhakar M. 2016. MODIS-Aqua detects *Noctilucascintillans* and hotspots in the central Arabian Sea. Environmental monitoring and assessment, 188(1), 1-11

Edwin L, Pravin P, Madhu V R, Thomas S N, Remesan M P, Baiju M V, Ravi R, Das D P H, Boopendranath M R and Meenakumari B. 2014. Mechnised Marine Fishing Systems: India, Central Institute of Fisheries Technology, Kochi, 277p

Eleveld M A, Van der Wal D and Van Kessel T. 2014. Estuarine suspended particulate matter concentrations from sun-synchronous satellite remote sensing: Tidal and meteorological effects and biases. Remote Sensing of Environment, 143, 204-215

Falkowski P G, Barber R T, Smetacek V. 1998. Biogeochemical controls and feedback on ocean primary production. Science, 281, 340-343

FAO. 2013. Fisheries and Aquaculture Department. Global capture fisheries production statistics for the year 2011(online) ftp://ftp.fao.org/FI/news/GlobalCaptureProductionstatistics2011.pdf

FAO. 2014a. Fisheries and Aquaculture, Information and Statistics Service http://www.fao.org

FAO. 2014b. Fisheries and Aquaculture, World fisheries production, by capture and aquaculture, by country 2011. http://www.fao.org

FSI. 2012. Marine fisheries census 2010. Union territories of Andaman and Nicobar and Lakshadweep Islands, Department of Animal Husbandary, Dairying and Fisheries and Fishery survey of India, Mumbai 148p

Fortier M, Fortier L, Hattori H, Saito H and Legendre L. 2001. Visual predators and the diel vertical migration of copepods under Arctic sea ice during the midnight sun. Journal of Plankton Research, 23(11), 1263-1278

Gao H Z, Zepp R G. 1998. Factors influencing photoreactions of dissolved organic matter in a coastal river of the southeastern United States. Environmental Science and Technology, 32, 2940-2946

Gibson J A E, Vincent W F, Nieke B, and Pienitz R. 2000. Control of biological exposure to UV radiation in the Arctic ocean : Comparison of the roles of ozone and riverine dissolved organic matter. Arctic, 53, 372-382

Gokul E. A and P. Shanmugam. 2016. An optical system for detecting and describing major algal blooms in coastal and oceanic waters around India. Journal of geophysical research-Oceans,121, 4097-4127

Gonsalves M J, Paropkari A L, Fernandes C E G, LokaBharathi P A, Krishnakumari L, Fernando V, et al., 2011. Predominance of anaerobic bacterial community over aerobic community contribute to intensify 'oxygen minimum zone' in the eastern Arabian Sea. Continental Shelf Research, 31. 1224–1235

Gordon H R, Brown O B, Evans R H, Brown J W, Smith R C, Baker K S, and Clark D K. 1988. A semianalytic radiance model of ocean colour, Journal of geophysical Research, 93, 10909–10924

Gordon H R, and Morel A. 1983. Remote assessment of ocean colour for interpretation of satellite visible imagery- A review. In R. T. Barber, M. J.

Bowman, C. N. K. Mooers, & B. Zetzschel (Eds.), Lecture notes on coastal and estuarine studies . pp. 1–144. New York: Springer- Verlag

Gower J F R (Ed.). 1986. Opportunities and problems in satellite measurements of the sea. Report of SCOR Working Group 70. UNESCO Technical Papers in Marine Science, No. 46, 70 pp

Habeebrehman H, Prabhakaran M P, Jacob J, Sabu P, Jayalakshmi KJ, Achuthankutty CT and Revichandran C. 2008. Variability in biological responses influenced by upwelling events in the Eastern Arabian Sea. Journal of Marine Systems, 74(1), 545-560

Hojerslev N K, and Trabjerg I. 1990. A new perspective for remote measurements of plankton pigments and water quality. Rep. 51, p. 10, Geophysical Institute, University of Copenhagen, Copenhagen

ICAR. 2011. Handbook of Fisheries and Aquaculture (Eds. Ayyappan S, Moza U, Gopalakrishnan A, Meenakumari B, Jena J K, Pandey A K) Directorate of knowledge management in agriculture and Indian council of agricultural research, New Delhi, 1116p

Itturiaga R and Siegel D. 1988. Microphotometric characterization of phytoplankton and detrital absorption properties in the Sargasso Sea. Limnology and Oceanography. 34-8, 1706

Jerlov N G. 1976. Marine Optics. Elsevier, New York. 231p

Kennish M. 2001. Practical Handbook on Marine Science, 3rd Edition. Marine Science Series

Kepner R L, Wharton Jr. R A, and Shuttle C A. 1998. Viruses in Antarctic lakes. Limnology and Oceanography. 43, 1754-1761

Khan, I.A., Ghazal, L., Arsalan, M.H., Siddiqui, M.F. and Kazmi, J.H., 2015. Assessing spatial and temporal variability in phytoplankton concentration through chlorophyll-a satellite data: a case study of northern Arabian Sea. Pakisthan Journal of Botany, 47(2)797-805

Kirk J T O. 1994. Light and Photosynthesis in aquatic ecosystems, 2nd Edition, Cambridge University Press, Cambridge

Kishino M, Takahashi N, Okami N, Ichlmura S. 1985. Estimation of the spectral absorption coefficients of phytoplankton in the sea. Bulletin of Marine Science, 37, 634-642

Kishino M, Okami N, Takahashi M, Ichimura S. 1986. Light utilization efficiency and quantum yield of phytoplankton in a thermally stratified sea. Limnology and Oceanography. 31, 557-566

Klemas V. 2013. Fisheries applications of remote sensing: an overview. Fisheries Research, 148, 124-136

Kopelevich O V, and Burenkov V I. 1977. Relation between the spectral values of the light absorption coefficients of sea water, phytoplanktonic pigments, and the yellow substance. Oceanology, 17, 278-282

Lee Z, Wei J, Voss K, Lewis M, Bricaud A and Huot Y. 2015. Hyperspectral absorption coefficient of “pure” seawater in the range of 350–550 nm inverted from remote sensing reflectance. Applied Optics, 54(3/20)

Lehahn Y, Koren I, Schatz D, Frada M, Sheyn U, Boss E, Efrati S, Rudich Y, Trainic M, Sharoni S and Laber C. 2014. Decoupling physical from biological processes to assess the impact of viruses on a mesoscale algal bloom. Current Biology, 24(17), 2041-2046

Leyendekkers J. 1967. Fluorophores and light absorbing substances in natural waters. KoninklijkNederlands, Meteorologisch Inst. In Debilt. 67-1(IV-4)

Longhurst AR. 2010. Ecological geography of the sea. Academic Press

Lorenzoni L, Toro-Farmer G, Varela R, Guzman L, Rojas J, Montes E and Muller-Karger F. 2015. Characterization of phytoplankton variability in the Cariaco Basin using spectral absorption, taxonomic and pigment data. Remote Sensing of Environment

Louchard E M, Reid R P, Stephens C F, et al. 2003. Derivative analysis of absorption features in hyperspectral remote sensing data of carbonate sediments. Optics Express, 10(26): 1573– 1584

Maske H, and Haardt H. 1987. Quantitative in vivo absorption spectra of phytoplankton: Detrital absorption and comparison with fluorescence excitation spectra. Limnology and Oceanography, 32: 620-633

Makris NC, Ratilal P, Jagannathan S, Gong Z, Andrews M, Bertsatos I, Godø O R, Nero R W and Jech JM. 2009. Critical population density triggers rapid formation of vast oceanic fish shoals. Science, 323(5922), 1734-1737

Marvasti S S, Gnanadesikan A, Bidokhti AA, Dunne JP and Ghader S. 2015. Challenges in modelling spatiotemporally varying phytoplankton blooms in the Northwestern Arabian Sea and Gulf of Oman. Biogeosciences Discussions, 12(13)

Matondkar S G P, Parab S, Dwivedi R M. 2006. Seasonality in sub-surface chlorophyll maxima in the Arabian Sea: detection by IRS-P4/OCM and implication of it to primary productivity, Proceedings of SPIE - The International Society for Optical Engineering, 6406, art. no. 64060X

Matsuoka A, Hill V, Huot Y, Babin M and Bricaud A. 2011. Seasonal variability in the light absorption properties of western Arctic waters: parameterization of the individual components of absorption for ocean colour applications. Journal of Geophysical Research: Oceans (1978–2012), 116(C2)

Matsuoka A, Hooker SB, Bricaud A, Gentili B and Babin M. 2012. Estimating absorption coefficients of coloured dissolved organic matter (CDOM) using a semi-analytical algorithm for Southern Beaufort Sea (Canadian Arctic) waters: application to deriving concentrations of dissolved organic carbon from space. Biogeosciences Discussions, 9, pp.13743-13771

Matsuoka A, Hooker SB, Bricaud A, Gentili B and Babin M. 2013. Estimating absorption coefficients of coloured dissolved organic matter (CDOM) using a semi-analytical algorithm for southern Beaufort Sea waters: application to deriving concentrations of dissolved organic carbon from space. Biogeosciences, 10(2), 917-927

Millie D F, Kirkpatrick G J, Vinyard B T. 1995. Relating photosynthetic pigments and in vivo optical density spectra to irradiance for the Florida red-tide dinoflagellate Gymnodinium breve. Marine Ecology Progress Series, 120: 65–75

Millie D F, Schofield O M, Kirkpatrick G J et al. 1997. Detection of harmful algal blooms using photopigments and absorption signatures: A case study of the Florida red tide dinoflagellate, *Gymnodinium breve*. Limnology and Oceanography, 42(5 Part 2): 1240−1251

Minu P, Shaju SS, Souda VP, Usha B, Ashraf PM and Meenakumari B. 2015. Hyperspectral Variability of Phytoplankton Blooms in Coastal Waters off Kochi, South-eastern Arabian Sea. Fishery Technology, 52(4), 218-222

Mobley C D. 1994. Light and water: Radiative Transfer in Natural Waters, Academic, New York

Morel A. 1991. Light and marine photosynthesis: a spectral model with geochemical and climatological implications. Progress in Oceanography, 26, 263–306

Morel A and Ahn Y H. 1990. Optical efficiency factors of free-living marine bacteria: Influence of bacterioplankton upon the optical properties and particulate organic carbon in oceanic waters. Journal of Marine Research, 48, 145-175

Morel A and Gentili B. 2009. A simple band ratio technique to quantify the coloured dissolved and detrital organic material from ocean colour remotely sensed data. Remote Sensing of Environment, 113(5), 998-1011

Morel A, and Prieur L. 1977. Analysis in variation of ocean colour. Limnology and Oceanography, 22 pp. 709–722

Morrow J H, Kiefer D A, and Gumberlin W S. 1989. A two-component description of spectral absorption by marine particles. Limnology and Oceanography, 34, 1500-1509

Ong L J, Glazer A N, Waterbury J B. 1984. An unusual phycoerythrin from a marine cyanobacterium. Science, 224(4644), 80–83

Padmakumar K B, Cicily L, Vijayan A and Sanjeevan V N. 2014. First record of dinoflagellate Neoceratiumplatycorne from the North Eastern Arabian Sea. Indian Journal of Geo-Marine Sciences, 43(4), pp.504-506

Pegau W S, Zaneveld J R V. 1993. Temperature-dependent absorption of water in the red and near-infrared portions of the spectrum. Limnology and Oceanography 38, 188-192

Peters E, Wittrock F, Richter A, Alvarado LMA, Rozanov VV and Burrows JP. 2014. Liquid water absorption and scattering effects in DOAS retrievals over oceans. Atmospheric Measurement Techniques, 7(12), 4203-4221

Pienitz R and Vincent W F. 2000. Effect of climate change relative to ozone depletion on UV exposure in subarctic lake. Nature,404, 484-487

Pope R M, Fry E S. 1997. Absorption spectrum (380–700 nm) of pure water: II. Integrating cavity measurements. Appled Optics, 36, 8710–8723

Preisendorfer R W. 1976. Hydrological Optics (6 volumes). US Department of Commerce, NOAA, Honolulu, HA

Prezelin B B, Alberte R S. 1978. Photosynthetic characteristics and organization of chlorophyll in marine dinoflagellates. Proceedings of the National Academy of Sciences of the United States of America, 75(4): 1801–1804

Prezelin B B, Boczar B A. 1986. Molecular bases of cell absorption and fluorescence in phytoplankton: Potential applications to studies in optical oceanography. In: Round F E, Chapman D J, eds. Progress in Phycological Research, Vol. 4. Bristol: Biopress Ltd., 350–465

Prieur L, and Sathyendranath S. 1981. An optical classification of coastal and oceanic waters based on the specific spectral absorption curves of phytoplankton pigments, dissolved organic matter, and other particulate materials. Limnology and Oceanography, 26, 671–689

Proctor L M, and Fuhrman J A. 1990. Viral mortality of marine bacteria and cyanobacteria. Nature, 343, 60-62

Qasim SZ. 1982. Oceanography of the northern Arabian Sea. Deep Sea Research Part A. Oceanographic Research Papers, 29(9), 1041-1068

Qasim SZ and Reddy CVG. 1967. The estimation of plant pigments of Cochin Backwater during the monsoon months. Bulletin of Marine Science, 17(1), 95-110

Radhakrishna K. 1969. Primary productivity studies in the shelf waters off Alleppey, south-west India, during the post-monsoon, 1967. Marine Biology, 4(3), 174-181

Rajagopalan MS, Thomas PA, Mathew KJ, Selvaraj GD, George RM, Mathew C V, Naomi TS, Kaladharan P, Balachandran VK and Antony G. 1992. Productivity of the Arabian Sea along the southwest coast of India. CMFRI Bulletin, 45, 9-37

Rivier A, Gohin F, Bryère P, Petus C, Guillou N and Chapalain G. 2012. Observed vs. predicted variability in non-algal suspended particulate matter concentration in the English Channel in relation to tides and waves. Geo-Marine Letters, 32(2) 139-151

Roesler C S, Perry M J, and Carder K L. 1989. Modeling in situ phytoplankton absorption from total absorption spectra in productive inland marine waters, Limnology and Oceanography, 34, 1510–1523

Roy R, Pratihary A, Gauns M, Naqvi S W A. 2006. Spatial variation of phytoplankton pigments along the southwest coast of India. Estuarine, Coastal and Shelf Science, 69, 189–195.

Roy S, Broomhead DS, Platt T, Sathyendranath S and Ciavatta S. 2012. Sequential variations of phytoplankton growth and mortality in an NPZ model: A remote-sensing-based assessment. Journal of Marine Systems, 92(1),16-29

Roy R, Chitari R, Kulkarni V, Krishna MS, Sarma VVSS and Anil AC. 2015. CHEMTAX-derived phytoplankton community structure associated with temperature fronts in the northeastern Arabian Sea. Journal of Marine Systems, 144, 81-91

Ryther JH, Hall JR, Pease AK, Bakun A and Jones MM. 1966. primary organic production in relation to the chemistry and hydrography of the western Indian ocean. Limnology and Oceanography, 11(3), 371-380

Sathyendranath S, Lazzara L, and Prieur L. 1987. Variations in the spectral values of specific absorption of phytoplankton. Limnology and Oceanography, 32, 403–415

Schofield O, Arnone RA, Bissett WP, Dickey TD, Davis C O, Finkel Z, Oliver M and Moline M A. 2004. Watercolours in the coastal zone: what can we see?. Biological Sciences, 144

Shaju SS, Minu P, Srikanth AS, Ashraf PM, Vijayan AK and Meenakumari B. 2015. Decomposition study of in vivo phytoplankton absorption spectra aimed at identifying the pigments and the phytoplankton group in complex case 2 coastal waters of the Arabian Sea. Oceanological and Hydrobiological Studies, 44(3), 282-293

Shalapyonok A, Olson R J, and Shalapyonok L S. 2001. Arabian Sea phytoplankton during Southwest and Northeast Monsoons 1995: composition, size structure and biomass from individual cell proper- ties measured by flow cytometry. Deep-Sea Res. II, Topical Studies in Oceanography, 48, 1231–1261

Shanmugam P, Varunan T, Jaiganesh NSN, Sahay A, Chauhan P. (2016). Optical assessment of coloured dissolved organic matter and its related parameters in dynamic coastal water systems. Estuarine, Coastal and Shelf Science, 175, 126-145

Siegel D A, Maritorena S, Nelson NB, Behrenfeld M J and McClain CR. 2005. Coloured dissolved organic matter and its influence on the satellite-based characterization of the ocean biosphere. Geophysical Research Letters, 32(20)

Smith R C, and Baker K. S. 1981. Optical properties of the clearest natural waters (200–800 nm). Applied Optics, 20, 177– 184

Sogandares F M, and Fry E S. 1997. Absorption spectrum (340-640 nm) of pure water. Photothermal measurements. Applied Optics, v. 36, 8699-8709

Solanki H U, Dwivedi R M, Nayak S R, Somvanshi V S, Gulathi D K and Pattnayak S K. 2003. Fishery forecast using OCM chlorophyll concentration and AVHRR SST: Validation results off Gujarat coast, India. International journal of remote sensing, 25, 3691-3699

Solanki H U, Bhatpuria D and Chauhan P. 2015. Signature analysis of Satellite derived SSHa, SST and Chlorophyll Concentration and their linkage with marine fishery resources. Journal of Marine Systems, 150, 12-21

Spencer R G M, Ahad J M E, Baker A,. Cowie G L, Ganeshram R, Upstill-Goddard R C, Uher G. 2007. The estuarine mixing behaviour of peatland derived dissolved organic carbon and its relationship to chromophoric dissolved organic matter in two North Sea estuaries (U.K.). Estuarine Coastal and Shelf Science, 74, 131–144.

Spinrad RW, Glover H, Ward BB, Codispoti LA and Kullenberg G. 1989. Suspended particle and bacterial maxima in Peruvian coastal waters during a cold water anomaly. Deep Sea Research Part A. Oceanographic Research Papers, 36(5), 715-733

Stramski D and Kiefer D A 1991. Light scattering by microorganisms in the open ocean. Progress in Oceanography, 28, 343–383

Subrahmanyan R. 1958. Phytoplankton organisms of the Arabian Sea off the west coast of India. The Journal of the Indian Botanical Society, 37(4), 435-441

Subrahmanyan R, Gopinathan CP and Pillai CT. 1975. Phytoplankton of the Indian Ocean: some ecological problems. Journal of the Marine Biological Association of India, 17(3), 608-612

Tam A C, and Patel C K N. 1979. Optical absorptions of light and heavy water by laser optoacoustic spectroscopy. Applied Optics, 18, 3348-3358

Tarran G A, Burkill P H, Edwards E S, Woodward E M S. 1999. Phytoplankton community structure in the Arabian Sea during and after the SW monsoon, 1994. Deep-Sea Research II 46, 655–676

Thomas L C, Padmakumar K B, Smitha B R, Devi C A, Nandan S B and Sanjeevan VN. 2013. Spatio-temporal variation of microphytoplankton in the upwelling system of the south-eastern Arabian Sea during the summer monsoon of 2009. Oceanologia, 55(1), 185-204

Trudnowska E, Sagan S, Kwasniewski S,Darecki M, and Blachowiak-Samolyk K. 2015. Fine-scale zooplankton vertical distribution in relation to hydrographic and optical characteristics of the surface waters on the Arctic shelf. Journal of Plankton Research, 37 (1), 120-133

Vijayan AK and Somayajula SA. 2014. Effect of accessory pigment composition on the absorption characteristics of dinoflagellate bloom in a coastal embayment. Oceanologia, 56(1), 107-124

Vodacek A, Blough N V, DeGrandpre M D, Peltzer E T, and Nelson R K. 1997. Seasonal variation of CDOM and DOC in the Middle Atlantic Bight: Terrestrial inputs and photooxidation. Limnology and Oceanography, 42, 674-686

Yentch C S. 1962. Measurement of visible light absorption by particulate matter in the ocean. Limnology and Oceanography, 7, 207-217

Zainuddin M, Kiyofuji H, Saitoh K and Saitoh SI. 2006. Using multi-sensor satellite remote sensing and catch data to detect ocean hot spots for albacore (Thunnusalalunga) in the northwestern North Pacific. Deep Sea Research Part II: Topical Studies in Oceanography, 53(3), 419-431

Zhu W, Yu Q, Tian Y Q, Chen R F, and Gardner G B. 2011.Estimation of chromophoric dissolved organic matter in the Mississippi and Atchafalaya river plume regions using above surface hyperspectral remote sensing, Journal of Geophyical Research, 116, C0, doi:10.1029/2010JC006523

Chapter 2

All the rivers run into the sea; yet the sea is not full.

-King Solomon

2. Field Observations of physical, chemical and optically active substances in coastal waters

2.1 Study area

Bio-optical measurements were carried spatially, once in a month from coastal waters off Kochi. The sampling stations are shown in Figure (2.1). The study area forms part of SEAS. The area has a strong monsoonal influence resulting in seasonal changes of hydrographic conditions influenced by river water discharge and surface circulation. During Pre-monsoon (February-May) wind-induced upwelling along with a northward undercurrent and a southward surface flow associated with strong vertical mixing is observed off Kochi waters (Kumar and Kumar 1995). Upwelling process supported by the southerly current is also observed along the coastal waters during monsoon season (Joshi and Rao 2012). After monsoon season, the hydrographic features change causing very strong freshwater discharge from backwaters (Srinivas and Kumar 2006). During monsoon period, the nutrient input of the coastal waters increases along with detrital load and surface salinity and water temperature falls down diminishing light penetration. These rapid changes often lead to high production at primary and secondary levels (Devassy 1983; Madhupratap et al., 1990; Honjo et al., 1999; Jyothibabu et al., 2008). During the transition period of monsoon to the post-monsoon season, the freshwater containing high levels of nutrients are transported through the Cochin inlet or Barmouth, thus making a

significant contribution to the nutrient budget of the coastal waters (Balachandran 2008). At certain locations, during the southwest monsoon period, seasonal phytoplankton blooms (Srinivas and Kumar 2006) were also observed. Usha et al.,(2014) pointed that increase of influx of nutrients contributes to the domination of a single species of phytoplankton and results in a high pelagic fishery.

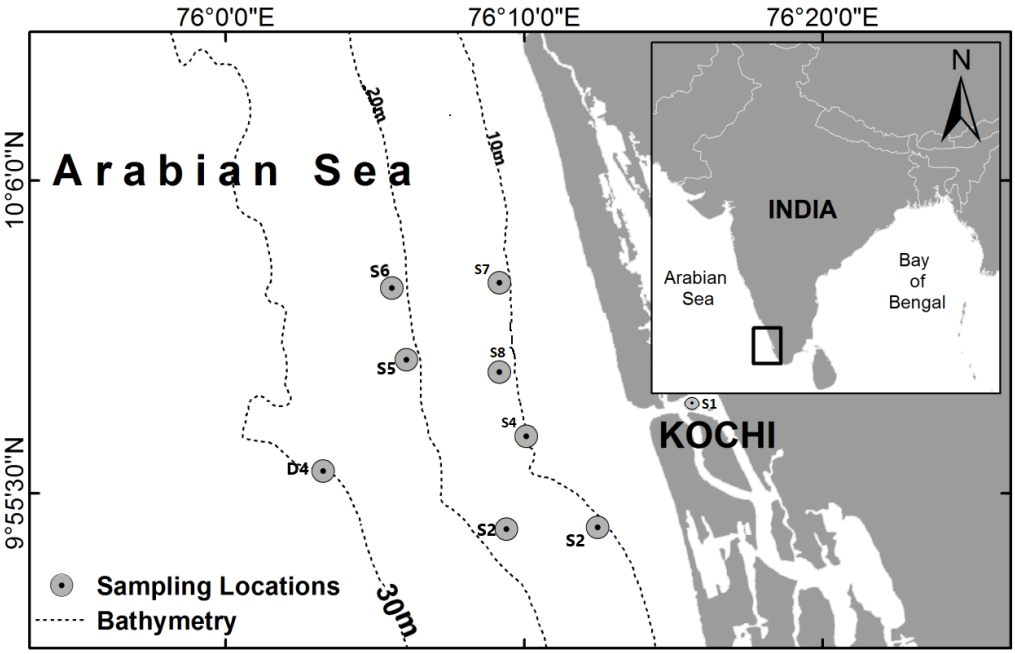

Figure 2.1. Map showing the study area and station locations

2.2. Sample Collection, Preservation and Storage

Station 1 is in the nearby estuarine area, where increased nutrient-rich freshwater influx occurs during monsoon season. Station 4 is represented by the area where mixing of

marine and freshwater occurs. Other stations were on the northern and southern parts of an inlet to the Kochi estuary.

Surface water samples were taken on a monthly basis from 8 sampling sites during April 2010 to December 2015. Sampling was done using a commercial purse seiner. Samples collected using Niskin water sampler and clean bucket (for surface samples) were stored in clean, dark polyethene bottles and kept in cold and transported to the laboratory where further analysis was carried out. a_{CDOM} was measured within 8 hours after sample collection and absorption by particulate matter (a_p) and Chla concentration within 48 hours after sample collection. For analysis of hydrographic parameters samples were stored in -40 and -20°C.

2.3. Chlorophyll *a* Concentration

Seawater samples were collected from the surface for Chla analysis. Seawater was filtered (2 litres) through Whatman GF/F filters (0.7µm pore size and 47 mm diameter) at a vacuum of less than 0.5 atm. The filters were extracted with 10 ml of 90% acetone solution. The samples were allowed to extract overnight (about 12 hours) in the dark at 4 °C (in the refrigerator). Samples were centrifuged at 3500 rpm for 10 minutes to remove cellular debris. Chla concentration was measured using a 10AU Turner Design fluorometer with 90% acetone as blank. Chla standard obtained from Sigma was used to calibration the instrument. A standard

stock solution was prepared and a minimum of five dilutions prepared from the standard (Strickland and Parsons 1972).

$$Chla = \frac{m * F0 * Volume\ of\ Acetone\ used\ for\ extraction}{Volume\ of\ water\ filtered}$$

m= slope of regression obtained from the calibration

F0= Fluorescence value

Table 2.1: Location of sampling sites

Station No.	**Station Code**	**Latitude**	**Longitude**
1	S1	09^0 58' 160'' N	76^0 15' 323'' E
2	S2	09^0 54' 34'' N	76^0 12' 47'' E
3	S3	09^0 54' 28'' N	76^0 09' 40'' E
4	S4	09^0 57' 40'' N	76^0 10' 10'' E
5	S5	10^0 00' 02'' N	76^0 06' 05'' E
6	S6	10^0 02' 37'' N	76^0 05' 58'' E
7	S7	10^0 02' 58'' N	76^0 09' 15'' E
8	S8	09^0 59' 57'' N	76^0 09' 15'' E
9	D4	09^0 56' 15'' N	76^0 03' 15'' E

2.4. Total Suspended Matter

Total Suspended Matter (TSM) concentration (mg L^{-1}) was determined gravimetrically following the procedures by Strickland and Parsons (1972) and JGOFS protocols

(UNESCO 1994). 0.7µm GF/F filters (Whatman) are used for filtering suspended particles. Before filtration, the glass fibre filters are pre-weighed and pre-dried at 90° C for 3 hours. A known volume of water (1.5 L) was filtered through filters. After filtration, the filters are rinsed with Milli-Q water to remove salts followed by drying (90° C for 3 hours) and then reweighed on a high precision balance.

TSM by using the equation below

$$TSM\left(\frac{mg}{L}\right) = \frac{[(A-B)*1000]}{C}$$

where

A = final dried weight of the filter (in milligrams = mg)

B = Initial weight of the filter (in milligrams = mg)

C = Volume of water filtered (in Litres)

2.5. Absorption by Coloured dissolved organic matter (a_{CDOM})

a_{CDOM} was measured spectrophotometrically following Kowalczuk and Kaczmarek (1996). Seawater samples were filtered through 0.2 µm cellulose nitrate membrane filters (Whatmann). The sample transparency was measured using Shimadzu™double beam UV-2450 spectrophotometer, over the spectral range 400 to 700 nm at a 1 nm resolution, in 10cm quartz cuvette relative to a bi-distilled Milli-Q reference blank. a_{CDOM} was calculated

from the optical density of the sample and the cuvette path-length following the methods are given in Twardowski et al., (2004).

$$\mathbf{a_{CDOM}(\lambda) = a_{CDOM}(440) \exp[-s(\lambda - 440)]\ [m^{-1}]}$$

where, a_{CDOM} (440) is the absorption measured at 440 nm and s is the slope coefficient which was calculated as the slope of the curve resulted by plotting the logarithm of a_{CDOM} against wavelength (λ). The magnitude of a_{CDOM} (440) indicates the concentration while the spectral slope (s) indicates its composition (Stedmon and Markager 2003). The absorption coefficients were then corrected for backscattering of small particles and colloids, which pass through filters (Green and Blough 1994).

$$\mathbf{a_{CDOM\_corr}(\lambda) = a_{CDOM}(\lambda) - a_{CDOM}(700) * (\lambda/700)\ [m^{-1}]}$$

2.6. Absorption by phytoplankton (a_{ph})

Seawater samples (2-5 litres) are filtered under low vacuum (<25 hPa) through 25 mm Whatman GF/F filters of pore size 0.7µm. The volume of seawater taken for filtration varies depending on the season and stations. All filtration done under low light conditions. After the sample is filtered, each filter is transferred to a pre- washed and dried filter case. The light absorption spectrum of phytoplankton is measured by the quantitative filter technique (QFT) method (Mitchell 1990). The absorption spectra of total particulate matter, relative to a blank filter saturated with seawater are measured in the wavelength range 400 to 750 nm with a resolution of 1 nm using a double-beam spectrophotometer equipped with an integrating

sphere. For each of the measured spectra, the optical density obtained at 750 nm was subtracted from that of all other wavelengths. Optical density of the total suspended matter was corrected for the pathlength amplification (effect) and converted into light absorption coefficients by the total particulate matter and detrital matter, viz. $a_p(\lambda)$ and $a_d(\lambda)$ respectively according to Cleveland and Weidemann (1993).

The particulate ($a_p(\lambda)$) and detritus absorption ($a_d(\lambda)$) were determined using the equation

$$a_{ph}(\lambda)=a_p(\lambda)-a_d(\lambda)$$

$$a_p(\lambda)=\frac{[2.303\,[OD]\_s(\lambda)]}{(V/S)}$$

$$a_d(\lambda)=\frac{[2.303[OD]\_s(\lambda)]}{(V/S)}$$

$$OD\_s(\lambda)=0.378OD\_f(\lambda)+0.523[[OD\_f(\lambda)]]\,2$$

where ODs is the optical density of total suspended particulate matter or detritus matter, V is the filtration volume (m^3) and S is the filtration area (m^2). The filtration area is calculated by the formula $S=\pi r^2$, where 'r' is the radius of filter area of filtration. The coefficients 0.378 and 0.523 are the path-length correction factors caused by multiple scattering in the glass fibre filter. Following this extraction, the absorption of the filters relative to blank filters also treated with methanol and re-saturated with filtered seawater was determined in the spectrophotometer. These spectra represent absorption by non-methanol extractable detrital material ($a_d(\lambda)$).

$$a_d(\lambda) = \frac{[2.303\ ODs(\lambda)]}{(v/s)}$$

where ODs (λ) is calculated using the same equation as described for particulate absorption. The terms 'v' and 's' stand for the filtration volume (m^3) and filtration area (m^2) respectively. The filtration area is calculated using the diameter of the filter paper where the residue is concentrated. An estimate of phytoplankton component of the total particulate absorption ($a_{ph}(\lambda)$) was determined by subtracting $a_d(\lambda)$ from $a_p(\lambda)$ (Kishino et al., 1985). The chlorophyll-specific light absorption coefficients of phytoplankton ($a^*_{ph}(\lambda)$) were obtained by dividing ($a_{ph}(\lambda)$) by the Chla concentration.

2.7. Phytoplankton taxonomy

Surface water samples of 1-2 L were collected onboard and then filtered through 20 µm mesh of bolting silk material to concentrate microphytoplankton. The filtration volume varied depending on seasons and stations. The filtrate was concentrated in 5-10 ml of filtered seawater and preserved in 4% buffered formalin/Lugol's Iodine solution. Phytoplankton numerical abundance was estimated by counting the number of cells of each species of phytoplankton in one millilitre of seawater using Sedgewick Rafter counting chamber. The total number of microphytoplankton cells present was calculated per litre using the formula (Santhanam et al., 1989)

$$N = \frac{n * v}{V}$$

Where,

N = Total number of microphytoplankton cells present per litre

n = Number of microphytoplankton cells in one ml

v = volume of plankton sample preserved in ml

V = Total volume of water filtered in litre

Species identification using standard identification keys was done with Leica™ Generic DMIL inverted microscope attached to camera. Photographs of phytoplankton species were taken for confirmation and identification. Small sized fractionation of phytoplankton was not included in this study. Identification was carried according to Cupp (1943), Tomas (1997) and Subrahmanyan (1959).

2.8. Hyperspectral Radiometer

At each station, a standalone hyperspectral radiometer of Satlantic™ Instruments was operated. The hyperspectral radiometer provided by Indian National Centre for Ocean Information Services under the SATCORE programme. The Satlantic hyperspectral ocean colour radiometer (Hyper OCR) is a sensor which can measure radiations up to 255 channels of optical data with the wavelength ranging from 300 – 1200 nm. It is a standalone instrument capable of measuring spectral energy in the oceanic environment. The profiler design includes hyperspectral sensors of OCR – 3000 series, temperature, pressure, tilt, Chla, CDOM and salinity sensors. The instrument

was deployed in the sea from the aft of the ship in free falling mode. The data was collected when the tilt and descending speed was less than 3° and 0.5 m s^{-1}, respectively. The continuous data were collected in the deck unit which was connected to the instrument via power telemetry cable. The data was recorded using SatView™ software and multilevel processing carried out using the Prosoft™ software. The radiometer was deployed 3 times away from the boat shadow (Muller and Fargion 2002).

The reference sensor is connected at the point where direct sunlight is falling on the sensor. The reference and profiler are connected to the MDU unit and then to the laptop using USB terminals. After all the connections are done, the profiler is kept onboard vertically to perform the pressure tare. Pressure Tare is required to “zero” the pressure sensor in all Satlantic optical systems that measure depth. SatView™ subtracts this offset from the depth field and provides actual depth of the profiler. This data is also used by ProSoft™ to correct for the pressure offset during post-processing. The pressure tare must be performed every time the instrument's power is cycled and if the data acquisition software is re-launch. After pressure tare is done, the profiler is deployed in the water in a free falling mode by continuously monitoring the depth, velocity and tilt of the instrument.

Plate 1. Identification of Phytoplankton using Leica™ Inverted Microscope and analysis done using Shimadzu™ UV-VIS Spectrophotometer

Plate 2. Photos of Satlantic™ Hyperspectral Radiometer Operation and Turner™ 10 AU Fluorometer analysis.

The operation was performed three times at each station. The data recorded by the SatView™ software is processed using ProSoft™. ProSoft™ is available as a Windows™ application and is supplied as a single self-extracting install program on CD-ROM. It can be downloaded directly from (http://www.satlantic.com/software.asp?CategoryID=3) Satlantic website. The data were processed as a single level or as multi-level (from raw data to level-4). Initial processing of the '.raw' files create '.hdf' files. The '.hdf' files were converted to Ascii files for easier analysis of the data (Lotliker et al., 2009).

2.9. Hydrographic parameters

During the study period, the hydrographic parameters affecting the phytoplankton were investigated. Turbidity was measured using Nephelometer (NTU), water temperature (degree Celsius) with thermometer and pH with pH meter. Dissolved Oxygen (DO) was determined using Winkler method and Salinity determined by Mohr-Knudsen titration method (Grasshoff et al., 1983).

a. *Determination of silicate*

Silicate was determined by treating the 25ml of water sample (taken in plastic containers) with reagents- acid molybdate solution (1 ml), oxalic acid (1 ml) and ascorbic acid (0.5ml). The mixture forms a blue complex and

the concentration was measured using spectrofluorometer at 810 nm within 30minutes of preparation of the sample for analysis (Grasshoff et al., 1983).

b. *Determination of phosphate*

Phosphate concentration was determined by taking 15 ml sample and treating with 0.5ml ascorbic acid reagent and 0.5ml mixed reagent. The absorbance was measured at 880 nm within 30 minutes of complex formation (Grasshoff et al., 1983).

c. *Determination of Nitrate*

Nitrate concentration was determined using Resorcinol method. 10ml of the sample is treated with 1.2 ml resorcinol, 10ml H_2SO_4 (conc) reagents taken in 50 ml standard flask and kept in dark for 30 minutes. After that the mixture is made up to 50 ml and absorbance measured at 505 nm (Grasshoff et al., 1983).

d. *Determination of Nitrite*

15ml sample is treated with 0.5 ml sulphanilamide and 0.5 ml NNED (N-naphthyl ethylene diamine hydrochloride) and kept for 15 minutes. The absorbance is measured at 540 nm (Grasshoff et al., 1983).

2.10. References

Balachandran K K, Laluraj C M, Jyothibabu R, Madhu N V, Muraleedharan K R, Vijay J G, Maheswaran P A, Ashraff T T M, Nair K K C, Achuthankutty CT. 2008. Hydrography and biogeochemistry of the north western Bay of Bengal and the north eastern Arabian Sea during winter monsoon. J. Marine Syst. 73, 76–86.

Cleveland J S and Weidemann A D. 1993. Quantifying absorption by aquatic particles: A multiple scattering correction for glass-fiber filters. Limnology and Oceanography, 38, 1321-1327

Cupp E E. 1943. Marine Plankton Diatoms of the West Coast of North America. University of California Press, Berkeley and Los Angelos; Reprint 1977, Koeltz Science Publishers, Koenigstein.

Devassy V P. 1983. Plankton ecology of some estuarine and marine regions of the west coast of India. Ph.D. Thesis University of Kerala, Trivandrum.

Grasshoff K, Ehrhardt M, Krembling K.1983. Methods of seawater analysis. pp, 125–183.

Green, S and Blough, N. 1994. Optical absorption and fluorescence properties of chomophoric dissolved organic matter in the natural waters. Limnology and Oceanography, 39, 1903 – 1916

Joshi M, Rao A D. 2012. Response of Southwest monsoon winds on shelf circulation off Kerala coast, India. Continental shelf Research, 32, 62-70.

Kishino M, Takahashi M, Okami N and Ichimura S. 1985. Estimation of the spectral absorption coefficients of phytoplankton in the sea. Bulletin of Marine Science, 37, 634-642

Kowalczuk P, Kaczmarek S. 1996. Analysis of temporal and spatial variability of 'yellow substance' absorption in the Southern Baltic. Oceanologia ,38-1, 3-32.

Kumar H P V, and Kumar M N. 1996. On the flow and thermohaline structure off Cochin during pre-monsoon season Continental Shelf Research, 16(4), 457-468.

Lotliker A, Dudeja G, Kumar S T. 2009. Technical report on Hyperspectral Radiometer – Data Acquisition and Post Processing. Indian National Centre for Ocean Information Services. Report No. : INCOIS-ASG-OCAT-TR-02-2009

Madhupratap M, Nair S R, Haridas P, Gadi Padmavathy. 1990. Response of Zooplankton to physical changes in the environment: coastal upwelling along the Central West Coast of India.Journal of Coastal Research, 62, pp. 413–426.

Mitchell B G. 1990. Algorithms for determining the absorption coefficient of aquatic particulates using the quantitative filter technique (QFT). Soc. Photo-Opt. Instr. Eng., Ocean Optics, X, 137-148

Mueller J M, and Fargion G S. 2002. Ocean optics protocols for satellite ocean color sensor validation, Revision 3, Part I and II, NASA Tech. Memo. 2002-210004, 308 pp., NASA Goddard Space Flight Cent., Greenbelt, Md.

Santhanam R P, Velayutham and Jegathesan G. 1989. A Manual of Freshwater Ecology. Daya Publishing House, New Delhi

Srinivas K, Dineshkumar P K. 2006. Atmospheric forcing on the seasonal variability of sea level at Cochin, South west of India. Continental Shelf Research, 26: 1113-1133.

Stedmon C A and Markager S. 2003. Behaviour of the optical properties of coloured dissolved organic matter under conservative mixing. Estuarine, Coastal and Shelf Science, 57, 1 – 7

Strickland J D H, Parsons T R. 1972. A practical Handbook of Seawater Analysis, II ed. Bulletin of Fisheries Research Board Canada. 167. 310 pp.

Subrahmanyan R. 1959. Studies on the phytoplankton of the west coast of India—I and II. Proceedings of the Indian Academy of Science B 50, 113–252.

UNESCO. 1994. Protocols for the Joint Global Ocean Flux Study (JGOFS) core measurements, IOC/SCOR Manual and Guides, 29, 128–134.

Usha B, Shaju SS, Ragesh N, Menakumari B and Muhamed Ashraf P. 2014. Observations on bio-opticalproperties of a phytoplankton bloom in coastal waters off cochin during the onset of southwest monsoon. Indian journal of Geo-marine Sciences. Vol.43(2), 289-296.

Utermöhl H. 1958. Zur Vervollkommung der quantitativen Phytoplankton-Methodik. Mitteilung Internationale Vereinigung fuer Theoretische unde Amgewandte Limnologie., 9, 1–38.

Tomas C R. 1997. Identifying Marine Phytoplankton. Academic Press, USA, 858pp.

Twardowski M S, Boss E, Sullivan J M, and Donaghay P L. 2004. Modeling the Spectral Shape of Absorption by Chromophoric Dissolved Organic Matter. Marine Chemistry, 89: 69– 88.

Chapter 3

The sea, once it casts its spell, holds one in its net of wonder forever
-Jacques Yves Cousteau,

3. Phytoplankton Diversity and Abundance

3.1. Introduction

Phytoplankton refers to the autotrophic component of the plankton that drifts in the water column. They are single celled and microscopic (0.5 to 250µm) plants that form the base of aquatic food web (Wikipedia). They undergo the process of photosynthesis, like plants in the terrestrial area, and produce carbohydrates and oxygen using carbon dioxide and solar radiation. They are known as primary producers of the ocean. Phytoplankton lives near the surface of water where they get enough sunlight for the process of photosynthesis and are mostly limited to the top 100-200m in the euphotic zone (Woodshole Institution). In addition to carbon dioxide and sunlight, they also require inorganic nutrients such as nitrates, phosphates, and silicate which they convert into proteins, fats, and carbohydrates.

Phytoplankton are some of earth's most critical organisms and so it is vital to study and understand them. They generate about half the atmosphere's oxygen and form the base of virtually every ocean food web making most other ocean life possible. They play an essential part of Earth's carbon cycle, by taking up carbon dioxide from the atmosphere and carrying this atmospheric carbon to the deep sea when they die and sink to the bottom. In a balanced ecosystem, phytoplankton provides food for a wide range of sea creatures including whales, shrimp, snails, and jellyfish. Since phytoplankton depends upon certain conditions for growth, they are a good indicator of changes in their environment. For these reasons, and because

they also exert a global-scale influence on climate, phytoplankton are of primary interest to oceanographers and Earth scientists around the world. Phytoplankton are ubiquitous and abundant (up to 10^5cells per ml). They contain a green pigment, Chl, which helps in the process of photosynthesis. Although microscopic, phytoplankton blooms in such large numbers that they can change the colour of the ocean that can be measured from space. The presence of more phytoplankton in the water imparts green colour and less phytoplankton imparts blue colour to the ocean.

Insitu measurements of phytoplankton and their optical characteristics in the coastal waters provide the database required to develop bio-optical algorithms useful in retrieving Chl from space (Carder et al., 1991; Tassan, 1994; Le et al., 2011). The regional, seasonal and inter-annual variations of the ocean colour products and its retrieval depend on the types of dominant phytoplankton that contribute to the ocean colour (Minu et al., 2014). Phytoplankton taxonomic studies provide basic information on the phytoplankton species which can be used in pigment marker studies. The contribution of various marker pigments is used for the development of algorithms to determine the contribution of these pigments to the total Chla concentration. Hence, understanding the variations in phytoplankton community structure helps to understand its own inherent optical properties and dynamics of complex coastal waters in which they inhabit, thereby to get a clear idea about the water leaving signal reaching the sensor (IOCCG report No.9).

Several studies are available from Cochin backwaters (Qasim 1970; Qasim et. al., 1972 a, b; Devassy and Bhattathiri 1974; Qasim et. al., 1974; Madhupratap and Haridas 1975; Madhupratap 1987; Joy et. al., 1990; Menon et.al., 2000; Haridevi et. al., 2004; Jyothibabu et. al., 2006; Madhu et. al., 2007 and 2010; Martin et. al.,2013; Mohan et al., 2016) on plankton ecology. Studies conducted in the coastal waters mainly focused on physical and chemical characteristics of phytoplankton and their numerical abundance during single season (Kaladharan et al., 1990; Selvaraj et al., 2003; Jugunu 2006; Roy et al., 2006; Madhu et al., 2010; Padmakumar et al., 2010, 2012; Sarangi and Mohammed 2011; D'Silva et al., 2012; Thomas et al., 2013; Martin et al., 2013; Robin et al., 2013) and on phytoplankton blooms (Thomas et al., 2014; Bhagirathan et al., 2014; Jagadeesan et al., 2017). A complete record of intra annual variation in phytoplankton diversity and community structure based on different seasons within 20m bathymetry are limited. Hence a study was carried out in coastal waters to understand the phytoplankton community structure, its diversity and abundance in relation to its diversity index.

Previous studies on the community structure, during the onset and establishment of southwest monsoon, confirmed nanoplankton, having maximum photosynthetic efficiency in coastal waters, as the major contributor to the total Chla and primary production in the region (Madhu et al., 2010). The response of microzooplankton (20–200 µm) to coastal upwelling and summer stratification in the SEAS showed abundance of phytoflagellates in the inshore waters and diatoms followed by dinoflagellates

in the offshore waters. Presence of *Trichodesmium erythraeum* in the high temperature and nitrate-depleted surface waters were also reported (Jyothibabu et al., 2008). The studies on diversity, abundance, biomass of phytoplankton and primary productivity in the shelf waters of four stations along the southwest coast of India during May - June 2005 revealed phytoplankton community comprising 67 species of phytoplankton belonging to bacillariophyceae (49 species), pyrrophyceae (17 species) and cyanophyceae (1 species). The study also reported that *Chaetoceros lorenzianus* constituted maximum abundance throughout the water column (Robin et al., 2010). An assessment of phytoplankton standing crop along the SEAS during the different phases of coastal upwelling in 2009 was done in detail (Thomas et al., 2013). Their study reported significant presence of solitary pennate diatoms *Amphora* sp. and *Navicula* sp. in the waters off Kochi during phase 2 of upwelling.

Anthropogenic influence shaping the nutrient dynamics and phytoplankton biomass in the coastal waters of southwest India studied by Kumar et al., (2014). They explained that, for most of the diatom variability, silicate supply acts as a driving force. 185 species of phytoplankton were identified in a study conducted on phytoplankton diversity, abundance and distribution in the AS waters off Kerala and Karnataka coasts. The diatoms, namely *Cymbella aspera*, *Licmophora abbreviata* and *Skeletonema costatum* were found to be dominant while *Oscillatoria limosa* was the prevailing cyanobacterium identified in the study (Rai and Rajasekhar 2015). Godhe et al., (2015) studied on 21 years of

phytoplankton and environmental monitoring data from the surface waters of coastal southeast AS showed a shift in phytoplankton community towards higher sample genus richness and diatom abundance.

3.2. Materials and Methods

Phytoplankton taxonomy, abundance, diversity and evenness studies were carried out in 8 stations (S1-S8) in the study area. To demonstrate annual variations in phytoplankton abundance the study area was divided into two transects along 10m and 20m bathymetry. Taxonomical difference along both transects were also studied.

3.2.1. Phytoplankton taxonomic composition and abundance

Phytoplankton taxonomic studies were carried out and a detailed methodology adopted for identification and calculation of numerical abundance is presented in Chapter 2, Section 2.7. For studies on monthly variations, common phytoplankton found along the 10m and 20m bathymetry selected.

3.2.2. Phytoplankton diversity and evenness

Species diversity is the number of different species in a particular area, which is an important index in characterizing the community structure and community importance in ecosystem. Changes in phytoplankton dynamics examined using Shannon-Wiener diversity index (H') (Zar, 1984).

$$H' = -\sum_{i=1}^{R} p_i \ln p_i$$

where 'p_i' is the proportion of characters belonging to the i^{th} type of letter in the string of interest.

Evenness, a measure of the relative abundance of the different species constituting the richness of an area, is an indicator of whether the community structure is developed and stable. Species evenness indicated by Pielou's evenness index (Pielou 1966).

$$J' = \frac{H'}{H'_{\max}}$$

Where H' is the number derived from the Shannon diversity index and $H'_{\max}$ is the maximum value of H',

3.3. Results and Discussion

3.3.1. Phytoplankton taxonomy

The composition of different phytoplankton species were shown in Table 3.1.A total of 73genera of phytoplankton from 19 orders and 41 families were identified. Main orders identified were Biddulphiales with 11 family and 23 genera, Bacillariales with 5 family and 15 genera and Gonyaulacales with 5 family and 6 genera. The largest community identified was Thalassiosiraceae with 5 genera, Fragilariaceae and Gymnodiniaceae with 4 genera each. The principal species of the family Thalassiosiraceae were *Skeletonema* spp., *Planktionella* spp.and *Thalassiosira* spp. Representation of diatoms, dinoflagellates and Phytoflagellates, Green algaeand Blue Green Algae were shown in Plates 3.1, Plate 3.2 and Plate 3.3. respectively.

Table 3.1. List of phytoplankton species identified during the study

***1. Diatoms*:-**

Centric diatoms: -

Skeletonema costatum, *Cyclotella*, *Lauderia annulata*, *Planktionella* spp., *Thalassiosira subtilis*, *Melosira*, *Leptocylindrus danicus*, *Corethron* spp., *Coscinodiscus* spp., *Hemidiscus*, *Azpeitia*, *Asteromphalus*,*Guinardia*, *Eucampia* spp., *Hemiaulus, Triceratium*, *Ditylum brightwelltii*, *Streptotheca*, *Odontella*, *Climacosphenia*, *Licmophora*, *Cyclophora*

*Rhizosolenia*spp.:- *R. setigera*, *R. delicatula*, *R. imbricate*, *R. styliformis*, *R. stolterfothii*, *R. alata*

Bacteriastrum spp.:-*B. hyalinum*, *B. delicatulam*, *B. furcatum*,

Chaetoceros spp.:- *C. decipiens*, *C. curvisetus*,

Biddulphia spp.:-*Biddulphia sinensis*, *B. mobiliensis*, *B. aurita*

Pennate diatoms:-

Amphiprora, *Navicula* spp., *Striatella*, *Pseudoeunotia*, *Asterionella japonica*, *Fragilaria*, *Thalassiothrix*, *Synedra*, *Thalassionema* spp., *Phaeodactylum*, *Nanoneis*, *Pseudonitzschia* spp., *Cylindrotheca closterium*

*Pleurosigma*spp.:-*Pleurosigma elongatum*, *P. directum*

Nitzschia spp.:- *N. longissima*, *N. seriata*, *N. sigma*

2. Dinoflagellates: -

Mesoporos, *Gymnodinium*, *Gyrodinium*, *Chochlodinium*, *Katodinium*, *Pyrocystis*, *Pyrophacus*, *Alaxandrium, Gonyaulax*, *Lingulodinium*, *Peridinium*, *Preperidinium, Scripisella*, *Noctiluca, Heterocapsa*

Prorocentrum spp.:- *P.micans*, *P.lima*

Dinophysis spp.:- *D. caudata*, *D. acuminate*, *D. fortii*, *D. tripos*, ,

Ceratium spp.:-*Ceratium fusus*, *C. tripos*, *C. furca*, *C. inflatum*, *C. horridum*,,

Protoperidinium sp.:- *P. ovatum*, *P. leonis*,

3. Green algae:-

Agmenellum, *Oscillatoria*, *Lyngbya*, *Anabaena*, *Nostoc*, *Staurastrum*

4. Blue green algae: -*Trichodesmium erythraeum, Synecococcus*

5. Phyto flagellates: - *Euglena*, *Pediastrum* spp., *Senedesmus*, *Actinastrum*, *Dictyocha*

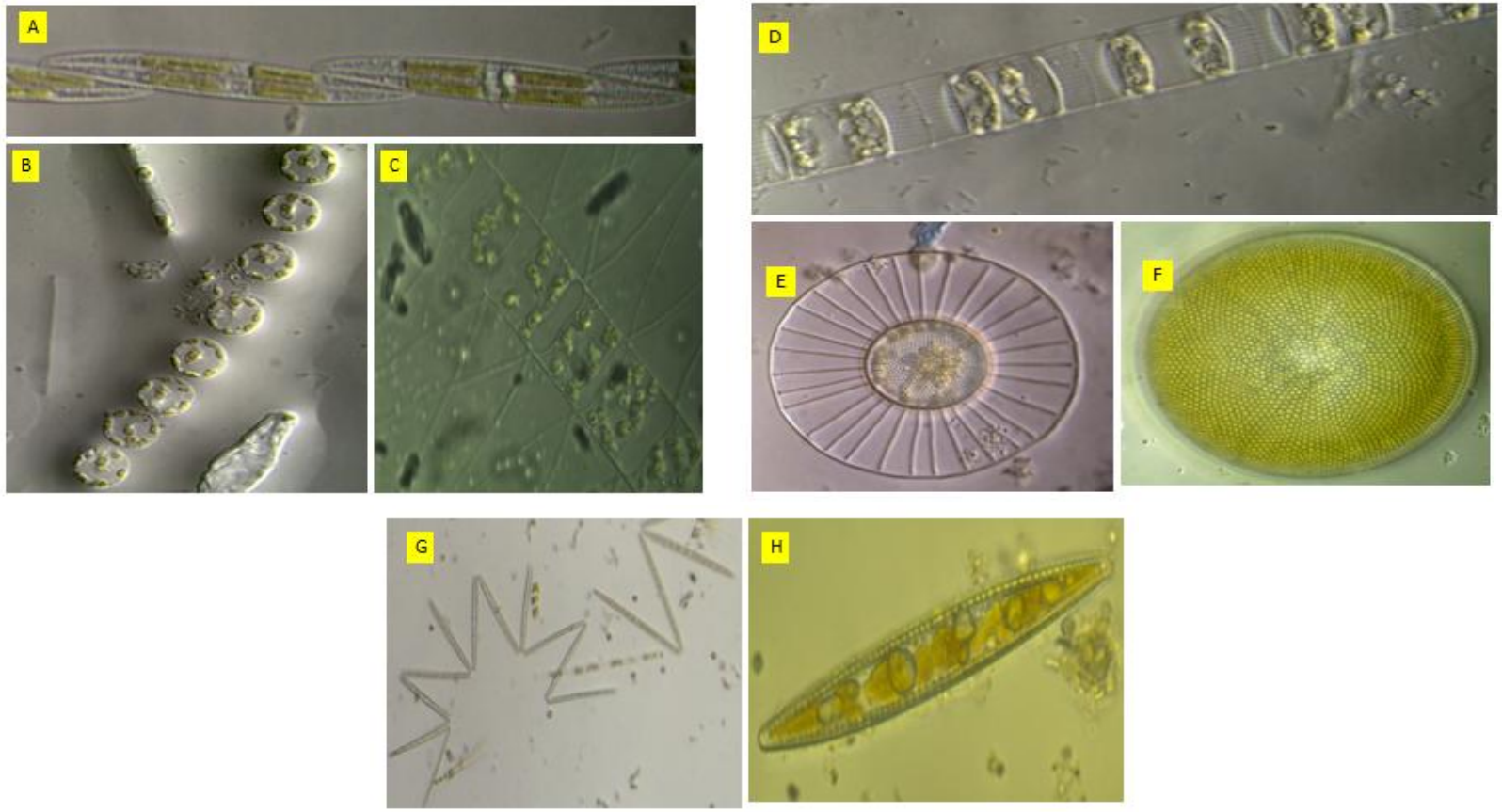

Plate 3.1. Photographs showing major Diatoms observed along the coast off Kochi.

A. *Pseudionitzschia pungens*, B. *Thalassiosira* species in chain form,C. C*haetoceros lorenzianus*, D. *Skeletonema indicum*, E. *Planktionella sol*, F. *Coscinodiscus granii*, G. *Thalassionema nitzschioides*, H. *Navicula lanceolata*

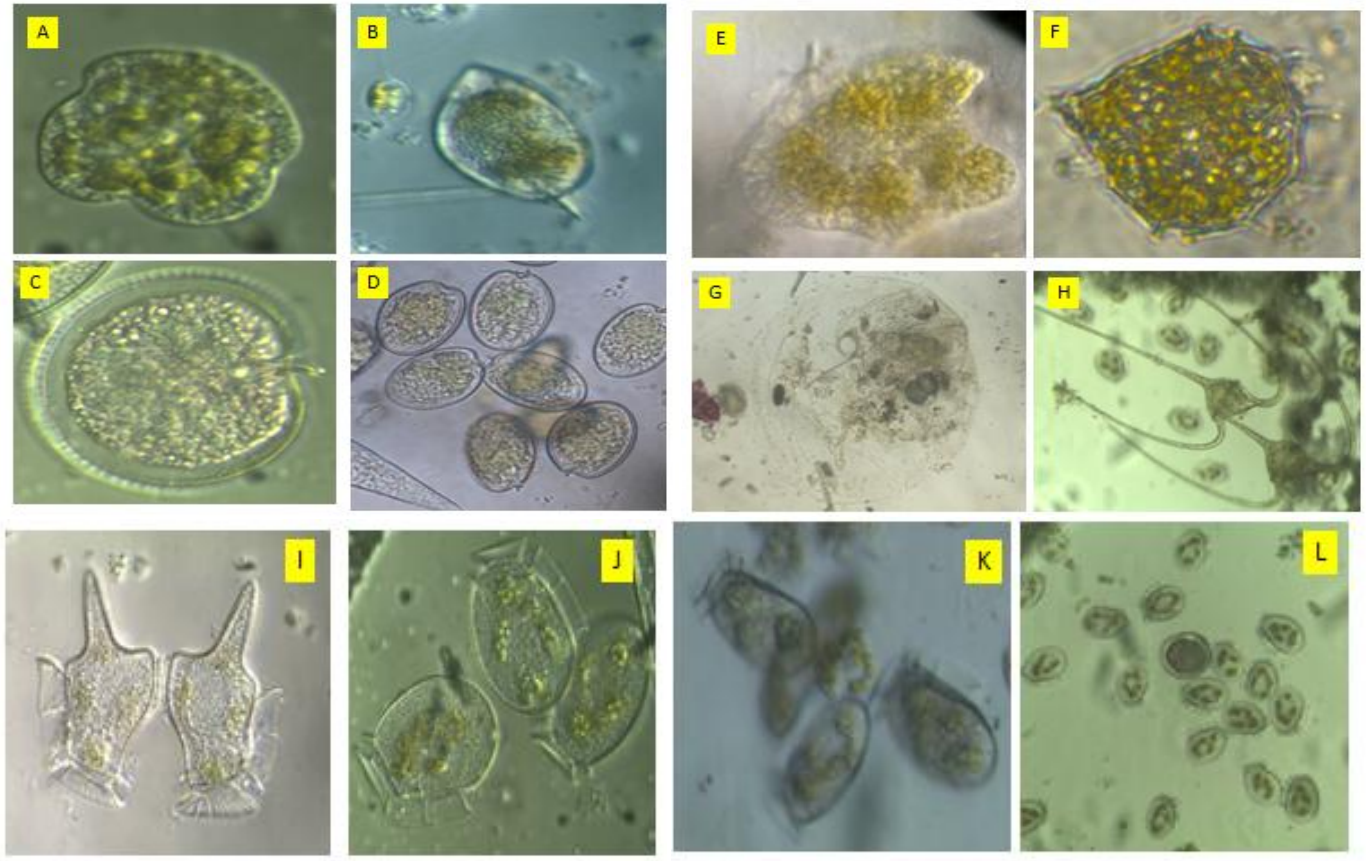

Plate 3.2. Photographs showing Major Dinoflagellates observed along the coast off Kochi.

A. *Karenia mikimotoi*, B. *Prorocentrum micans*, C. *Preperidinium meunieri*, D. *Prorocentrum mexicanum*, E. *Akashiwo sanguinum* F. *Peridinium quinquecorne*, G. *Noctiluca scintillans*, H. *Ceratium massiliense*, I. *Dinophysis caudate*, J. *Dinophysis acuminate*, K. *Dinophysis fortii*, L. *Dinophysis* bloom.

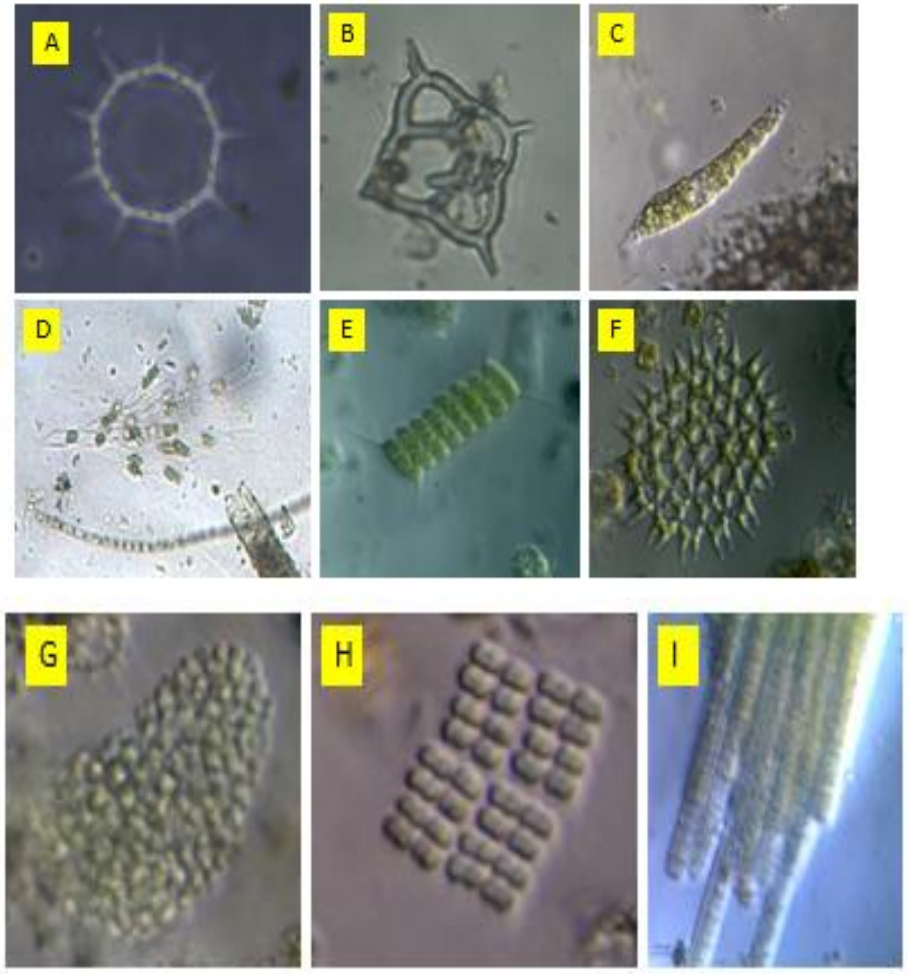

Plate 3.3. Photographs showing Phytoflagellates, Green algae and Blue Green Algae observed along the coast off Kochi.

A. Octactis octonaria, B. Dictyocha fibula, C. Euglena acusformis, D. Dinobryon sp., E. Scenedesmus quadricauda, F. Pediastrum clathratum, G. Microcystis sp., H. Agmenellum quadruplicatum, I. Trichodesmium erythraeum

Table 3.2. Table showing the average numerical abundance of phytoplankton along 10m bathymetry from 2010 to 2013.

Sl. No.	Phytoplankton along **10m** bathymetry	January	February	March	April	May	June	August	September	October	November	December
Diatoms												
1	Asterionella	++	++	++	++	++	+++	+	++	+	++	+++
2	Fragialria	-	+	+	+	+	++	+	+	+	-	+
3	Navicula	+	+	+	+	+	+	+	+	+	+	+
4	Pleurosigma	-	+	++	+	+	++	+	+	+	++	+
5	Nitzschia	++	+	+	+	+	+	+	+	+	+	+
6	Cylindrotheca	+	+	+	+	+	+	+	+	+	-	+
7	Pseudonitzschia	+++	++++	+++	+++	+++	++	+	+	+	+++	++
8	Hemiaulus	++	+	+++	-	+	++	-	+	+	-	++
9	Biddulphia	+	++	+	-	+++	+	+	+	+	+	++
10	Chaetoceros	++++	++++	++++	++++	++++	++++	++++	++++	++++	++++	++++
11	Bacteriastrum	++++	++	++	-	+	-	-	-	-	-	+
12	Leptocylindrus	++	++	+++	++	++	++	+	++	+	++++	+
13	Rhizosolenia	+	+	+	+	+	+	+	+	+	+++	+
14	Guinardia	++++	++	+++	+++	++	+	+	+	+	++++	+
15	Skeletonema	+++	++++	++	+	+++	++++	+	++	+	++++	++++
16	Lauderia	-	+++	++	++	++	+	+	-	+	+	++
17	Thalassiosira	++	++	++	++	+	++++	++	++++	+	+++	++
18	Coscinodiscus	++	++++	+++	++	++	++	+	+	++	+	+++
19	Hemidiscus	-	+	-	-	+	+	-	+	++	-	-
20	Eucampia	++	++	+	-	+	+	++++	-	++	-	+
21	Ditylum	+	-	-	-	+	+	+	-	++	-	-
22	Striatella	-	-	-	-	+	+	+	-	+	-	+
23	Thalassionema	++++	+++	+	+++	+	+	+	++++	+	++++	++

Dinoflagellates												
24	Prorocentrum	++++	++	+	+	+	++	+	+	+	+++	++
25	Akashiwo	-	-	-	++	-	+	+	+	+	+	+
26	Gyrodinium	+	-	-	-	+	-	+	+	+	-	-
27	Preperidinium	-	+	+++	+++	++	++	+	+	+	-	+++
28	Protoperidinium	+	+	+++	++	+	+	+	+	+	++++	+++
29	Peridinium	-	-	++	-	+	-	+	-	-	-	++
30	Dinophysis	-	+	++	-	+++	+	+	-	+	-	++
31	Ceratium	++	+++	+	+	++	++	+	+	+	++	++
Phytoflagellates, Green algae and Cyanophytes												
32	Dictyocha	+	+	++	+	+	-	+	-	-	-	++
33	Euglena	++	+++	-	+	-	+	-	-	-	-	-
34	Pediastrum	-	-	-	-	-	-	-	+	-	-	-
35	Trichodesmium	-	++++	+++++	+++	-	+++	+++	+++	+++	-	-

- Absent
+ < 1, 00,00 cells per litre
++ 10,000-20,000 cells per litre
+++ 20,000-1,00,000 cells per litre
++++ >1,00,000 cells per litre

Monthly variations in phytoplankton taxonomy were carried out from 2010 to 2013. The average abundance of phytoplankton at genus level along 10m bathymetry is shown in Table 3.2. 35 number of phytoplankton were selected at genus level along 10m bathymetry for the study. These include 23 diatoms, 8 Dinoflagellates, 4 from other groups such as phytoflagellates (1), green algae(2) and blue-green algae(1). Among diatoms, *Asterionella* sp. *Navicula* sp., *Nitzschia* sp., *Pseudonitzschia* sp., *Chaetoceros* sp., *Leptocylindrus* sp., *Rhizosolenia* sp., *Guinardia* sp., *Skeletonema* sp., *Thalassiosira* sp., *Coscinodiscus* sp., and *Thalassionema* sp. comprising 12 diatoms occurred throughout the year. Out of 8 dinoflagellates observed, 3 were seen permanently throughout the year. They were *Prorocentrum* sp., *Protoperidinium* sp., and *Ceratium* sp. Among phytoflagellates, green algae and blue-green algae, no member was seen throughout the year.

The average abundance of phytoplankton at genus level along 20m bathymetry is shown in table 3.3. Total of 25 diatoms, 7 dinoflagelates 4 others including phytoflagellates, green algae and cyanobacteria were taken for understanding monthly variations along 20m bathymetry. Out of 25 diatoms, 11 species of diatoms existed throughout the year. Only 1 species of dinoflagellate existed all year round along 20m bathymetry. None among the phytoflagellates, green algae and cyanobacteria was seen throughout the year.

Table 3.3. Table showing numerical abundance of phytoplankton along 20m bathymetry

Sl. No.	Phytoplankton along **20m** bathymetry	January	February	March	April	May	June	August	September	October	November	December
Diatoms												
1	Asterionella	++	++	++++	+++	+++	+++	+	+++	+	+	+
2	Fragialria	-	++	+	+++	+	+	+	+	+	-	+
3	Navicula	+	+	+	+	+	+	+	+	+	++	+
4	Pleurosigma	+++	++	++	-	+	++	+	-	-	++	-
5	Nitzschia	+	+	+	+	+	+	+	+	+	+++	++
6	Cylindrotheca	+	+	+	++	+	+	+	+	-	+++	++
7	Pseudonitzschia	+	+	+	+	+	+	+	-	-	++++	+
8	Hemiaulus	+	-	+++	+	++	++	+	+	+	-	+
9	Biddulphia	+	+++	++	+	++	++	+	+	+	-	+
10	Triceratium	-	-	-	-	-	-	-	-	+	-	+
11	Chaetoceros	+++	+++	++++	+++	++++	++++	++	+++	+++	++++	+++
12	Bacteriastrum	-	+	+	++	+	+	+	+	-	-	-
13	Leptocylindrus	+++	+++	++++	+++	++	++	+	++	+	++	++
14	Rhizosolenia	++++	++++	+++	++	+++	+	+	+	+	++	+
15	Guinardia	++++	++	+++	++	++	+	+	+	+	++	+
16	Skeletonema	+++	+	+++	++	+++	++++	+	+	+	+++	+
17	Lauderia	++	+++	++	++	+	+	-	+	+	+++	++
18	Cyclotella	++	+	+	+	+	+	+	+	-	-	+
19	Thalassiosira	++	+	++	+	+	++	+	++	+	++++	++
20	Corethron	-	+	-	-	-	++	-	-	-	-	++++
21	Coscinodiscus	++	+	+++	++	+	+	+	+	++	+++	+
22	Hemidiscus	-	+	-	-	+	+	+	+	+	+	+
23	Eucampia	-	+	+	_	++	+	++	+	+++	-	-
24	Ditylum	-	-	+	-	++	+	+	-	-	-	+
25	Thalassionema	++++	++	++++	++	++	++++	+	+++	++	+++	+++

Dinoflagellates												
26	Prorocentrum	++++	+	+	+	+	+	-	+	+	++	+
27	Gyrodinium	++	-	+	-	+	+	++	++++	+++	++	-
28	Preperidinium	-	+	++	++	+	+	+	+	+	++	+
29	Protoperidinium	++++	++	++	+	+	++	+	+	+	+++	+
30	Peridinium	-	+	+	-	+	+	-	-	+	++	+
31	Dinophysis	-	+	+	+	++	+	+	-	+	-	+
32	Ceratium	++	++	++	-	+	++	+	+	+	+++	++
Phytoflagellates, Green algae and Cyanophytes												
31	Dictyocha	+	+	+	+	-	-	-	+	-	-	+
32	Euglena	+	++	-	+	+	+	+	-	-	-	-
33	Pediastrum	-	-	-	-	-	+	+	-	-	-	+
34	Trichodesmium	-	++++	++++	+++	-	+++	+++	+++	+++	-	-

- **Absent**

+ < 1, 00,00 cells per litre

++ 10,000-20,000 cells per litre

+++ 20,000-1,00,000 cells per litre

++++ >1,00,000 cells per litre

Seasonal variation of phytoplankton along entire study area was analysed. *Cyclotella* spp., *Striatella* spp., *Paralia* spp., *Fragilaria* spp., *Euglena* spp., *Alexandrium* spp. and green algae were not seen during monsoon season whereas it occurred in the other two seasons. Phytoplankton such as *Climacosphenia*, *Licmophora, Gyrosigma* and *Pediastrum* were seen only during monsoon season. *Gonyaulax* spp. was not seen during the postmonsoon season while *Staurastrum* spp. occurred only during postmonsoon season. Phytoplankton species such as *Azpeitia* spp., *Streptotheca* spp., *Odontella* spp., *Amphiprora* spp., *Synedra* spp., *Nanoneis* spp., *Agmenellum* spp., and *Noctiluca* spp. were identified during premonsoon season only but *Senedesmus* spp. observed during other two seasons was not seen in premonsoon. *Trichodesmium* were absent during postmonsoon season.

Matondkar et al.,(2006) reported the dominance of green algae and Noctiluca during premonsoon season and *Trichodesmium* and flagellates during post monsoon seasons in the northeastern Arabian Sea. Dominance of *Trichodesmium* and *Noctiluca* were reported during premonsoon season and diatoms and coccolithophores during monsoon season along the eastern Arabian Sea by Parab et al., (2006) and Martin et al., (2013). They also reported the dominance of dinoflagellates and picobacteria soon after the monsoon season. The presence of *Licmophora gracilis, Gyrosigma littorale,* during summer monsoon in the coastal waters were reported (Habeebrahman 2009; Shunmugaraj et al., 2002). Occurrence of *Pediastrum* species, primarily a freshwater form during

monsoon season has been reported in Cochin backwaters by several authors (Devassy and Gopinathan 1970; Joseph and Pillai 1975; Madhu et al., 2007; Dayala et al., 2013). The presence of *Pediastrum* in the coastal waters is reported during the study period. The presence of this phytoplankton in the coastal waters is a result of high river flow during monsoon season from estuary to sea (Minu and Ashraf 2012). With respect to earlier reports, this study also confirms the dominance of *Trichodesmium* during Premonsoon season.

3.3.2. Spatial and Temporal Analysis of Phytoplankton abundance

Station wise analysis of phytoplankton numerical abundance showed that Stn. S4 (46 genera) had the highest phytoplankton species richness index followed by Stn. S8 (45 genera). The species richness in the estuarine Stn. S1 was 39 genera. The changes in species richness of phytoplankton with respect to seasons were also studied. Monsoon season recorded 43 genera of phytoplankton whereas post-monsoon recorded 48 genera. High species richness with highest numerical abundance occurred during pre-monsoon season with 57 species. As a tropical coastal region, the dominant ecotype of phytoplankton was at estuarine region (Stn. S1) with higher abundance during pre-monsoon season followed by post-monsoon and monsoon seasons, and the second dominant ecotypes were at Stn. S6 and Stn. S8 during pre-monsoon season. Low numerical density of phytoplankton was exhibited in all the stations during monsoon. Even though post-monsoon recorded high species richness, numerical abundance of phytoplankton in this region during the season was comparatively low. The cell abundance of

phytoplankton varied from 14.23×10^3 to 55.07×10^6 cells L^{-1} (Fig. 3.1). The predominant abundance was by centric diatoms which ranged from 27.84×10^3 to 25.10×10^5cells L^{-1}throughout the year. The lowest and highest density of centric diatoms was in Stn. S1 during monsoon (27.84×10^3 cells L^{-1}) and pre-monsoon seasons (25.10×10^5cells L^{-1}). On examining the Nitrite and Phosphate dynamics in Stn. S1, it was found that nitrite concentration was 0.65 µmol $L^{-1}$and 0.25 µmol L^{-1} respectively during monsoon and pre-monsoon season, and phosphate concentration was 2.45 µmol L^{-1} and 1.57 µmol L^{-1} respectively during both the seasons.

Pennate diatoms ranged from 48.95×10^2 to 21.47×10^5cells L^{-1} during the entire study. Spatial analysis recognized the lowest numerical abundance of pennate diatoms in Stn. S1 during monsoon season and highest in Stn. S8 during premonsoon. Dinoflagellate abundance ranged from 44.10×10^2 to 44.92×10^4cells L^{-1} in the study area.

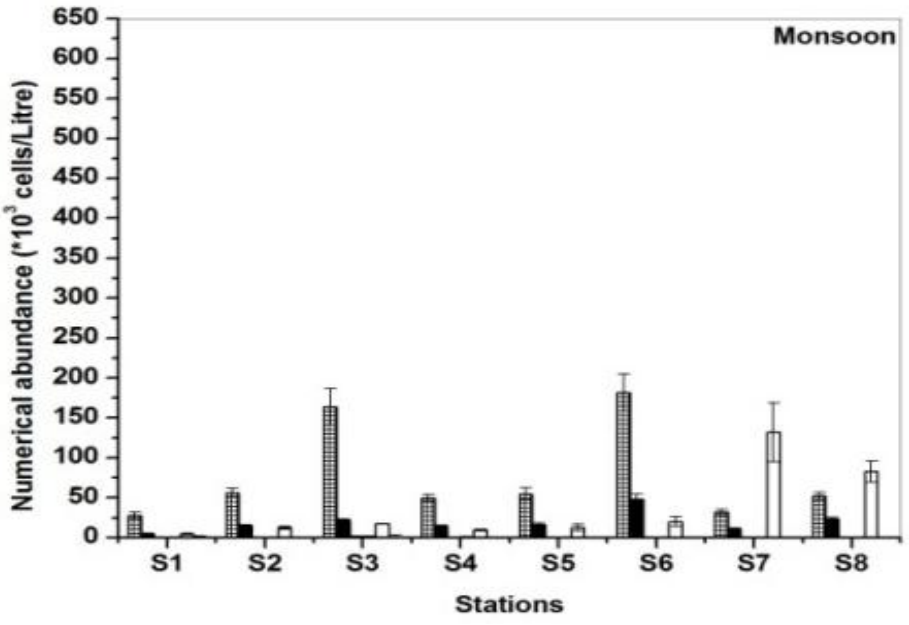

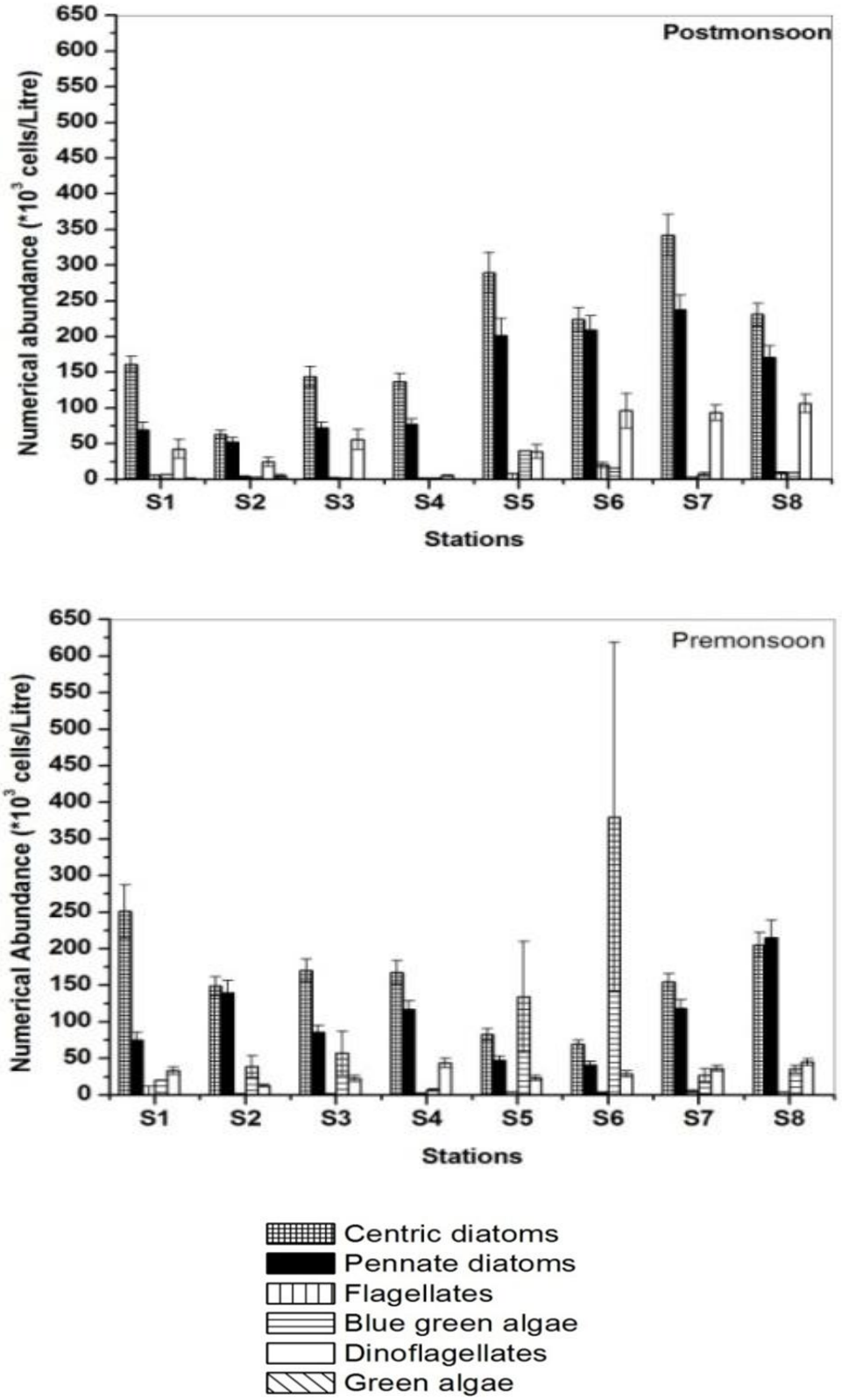

Figure. 3.1. Spatial and temporal analysis of numericalabundance of phytoplankton species in the study area. X axis represented by stations and Y axis by numerical abundance expressed in cells L^{-1}.

Lowest abundance of dinoflagellate was recorded during monsoon season in Stn. S1 and highest was during pre-monsoon season in Stn. S8. Phytoflagellates ranged from 2.23×10^{2} to 5.05×10^{4}cells L^{-1} and it exhibited lowest numerical density during monsoon season in Stn. S5. The highest abundance of phytoflagellate was recorded during pre-monsoon season in Stn. S7. Monsoon season showed lowest abundance and pre-monsoon season showed highest abundance of blue-green algae which ranged from 33×10^{3} to 3.80×10^{6}cells L^{-1}. Lowest abundance of blue green algae was seen in Stn. S4 and highest in Stn. S6.

The study showed that the during monsoon season the numerical abundance of all groups of phytoplankton identified in this study area are lower. The physico-chemical factors such as pH, salinity, temperature, DO and nutrients played a significant role in determining the abundance of phytoplankton in this region. Low numerical density of phytoplankton exhibited during the monsoon season was influenced by the low pH and temperature along with highest nitrite and silicate concentration and lowest phosphate concentration prevailed in the area (Shaju et al., 2015; Qasim 2003; Menon et al., 2000; Qasim et al., 1968; Pinker and Laszlo 1992; Banse and English 2000; Choudhary and Pal 2010). Contradictory to these findings, Gopinathan et al., (1974) highlighted the high numerical abundance of phytoplankton in the inshore and estuarine areas of Cochin backwaters during monsoon season which coincided with low salinity and temperature along with high nutrient concentration. Marked decrease in

nutrient and phytoplankton pigment levels due to mixing with marine waters was reported in later studies (Sankaranarayanan and Qasim 1969; Saraladevi et al., 1991; Lierheimer and Banse 2002).

During pre-monsoon season river runoff decreases and the transparency level increases. During pre-monsoon season, marked decreased in NO_3 and SiO_4 levels lead to increased phytoplankton diversity in the coastal waters. The low NO_3 and SiO_4 levels in the coastal waters decreased the ecological advantage of certain species and favour the co-occurrence of others in the environment (Niemi 1973; Hobro 1979; Rinne et al., 1981; Kononen and Niemi 1984; Niemisto et al., 1989; Martin et al., 2013). During pre-monsoon season, solar radiation, salinity, and temperature favoured blue-green algal growth especially *Trichodesmium* growth (Capone et al., 1998; Hegde et al., 2008).The results from this study agree with the findings that phytoplankton numerical abundance is positively correlated to pH and phosphate and negatively related to nitrite and silicate.

3.3.3. Percentage composition of Phytoplankton communities

Centric diatoms were identified as the dominant groups in the study, but their percentage contribution during pre-monsoon was lower than that of other seasons (Table 3.4.). Centric diatoms contributed to an average of 59.09% during monsoon season whereas during post-monsoon and pre-monsoon seasons, the average percentage composition was 47.64 and 38.96 % respectively. In contrast, pennate diatoms showed high percentage

composition during post-monsoon season (31.25%) and least during monsoon season (14.87%). Dinoflagellates had higher abundance during monsoon season (average of 24.63%) and lowest during pre-monsoon season (average of 7.69%). Stn. S7 exhibited highest percentage of dinoflagellates (75.35%) during monsoon season whereas Stn. S2 exhibited lowest percentage (3.58%) during pre-monsoon season. Phytoflagellates and blue-green algae were minor contributors to the entire phytoplankton community in the region (≤1%) during monsoon and post-monsoon seasons. In case of phytoflagellates, highest percentage was observed in Stn. S6 during postmonsoon season and in case of blue green algae, it was in the same station during premonsoon season (71%). The occurrence and highest contribution of blue green algae during premonsoon season was attributed to the presence of *Trichodesmium erythraeum* bloom prevailed during the season.

Table 3.4. Table showing the dominant group during different seasons

Phytoplankton	Monsoon Order/Family/ Genera	Postmonsoon Order/Family/ Genera	Premonsoon Order/Family/ Genera
Centric diatoms	3/13/21	1/11/20	1/11/23
Pennate diatoms	1/4/9	1/4/12	1/5/14
Dinoflagellates	5/8/9	5/8/9	7/11/12
Phytoflagellates	1/1/1	3/3/3	2/2/2
Blue green algae	1/1/1	1/1/1	3/3/3
Other communities	1/2/2	2/2/2	1/1/1

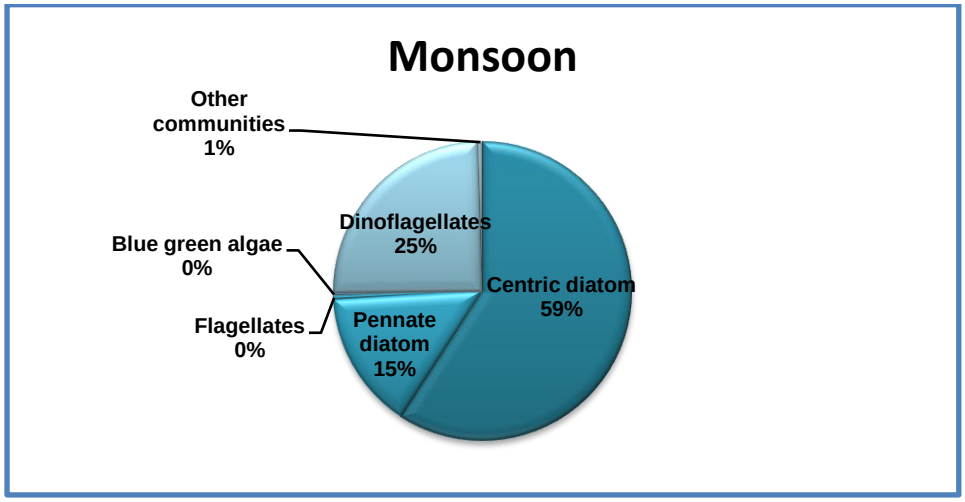
Monsoon
Other communities 1%
Dinoflagellates 25%
Blue green algae 0%
Centric diatom 59%
Flagellates 0%
Pennate diatom 15%

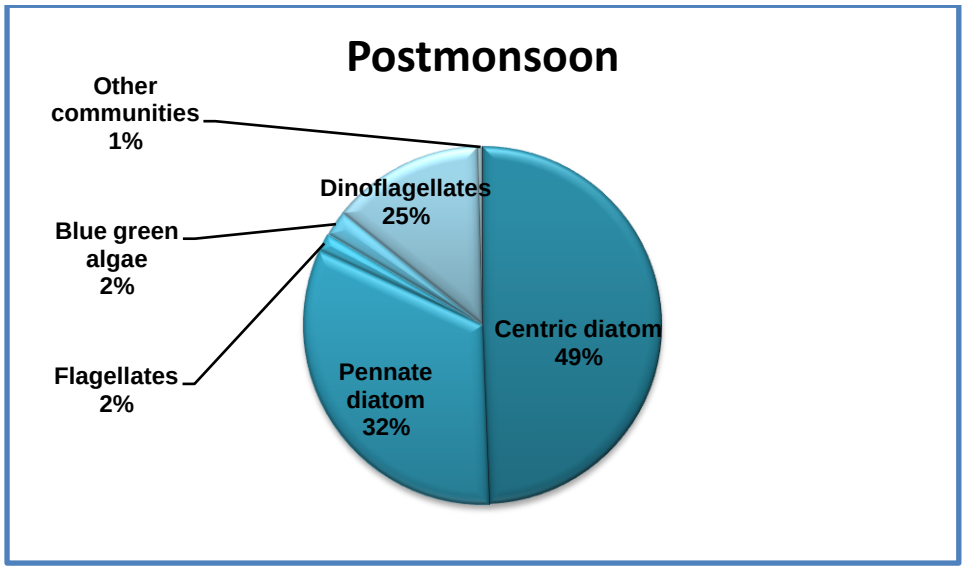
Postmonsoon
Other communities 1%
Dinoflagellates 25%
Blue green algae 2%
Centric diatom 49%
Flagellates 2%
Pennate diatom 32%

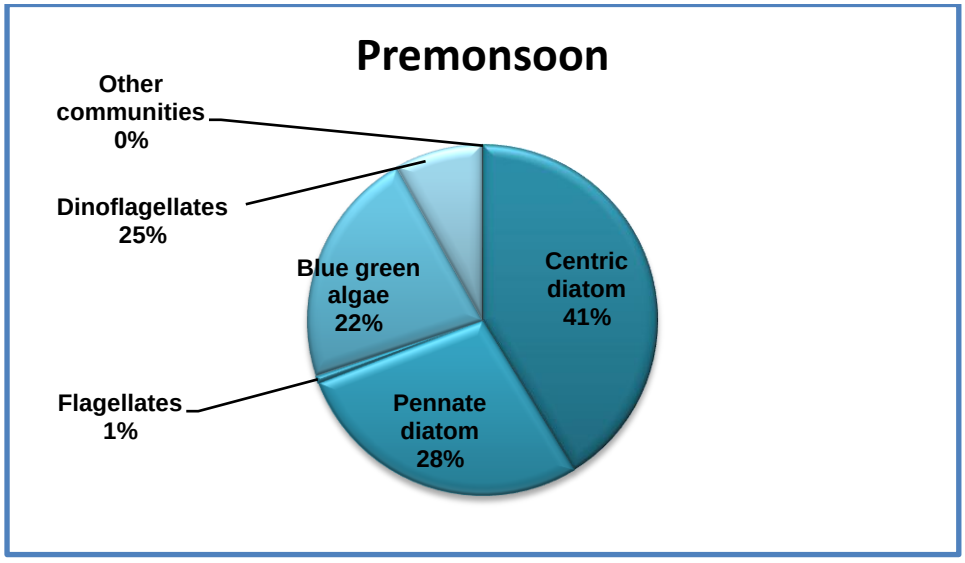
Premonsoon
Other communities 0%
Dinoflagellates 25%
Blue green algae 22%
Centric diatom 41%
Flagellates 1%
Pennate diatom 28%

Figure 3.2 Percentage compositions of phytoplankton communities in the study area during the three seasons

The percentage composition of centric diatoms during monsoon season was 59%, while it decreased to 49% and 41 % during postmonsoon and premonsoon seasons. The pennate diatoms showed an increase of 15% to 35% from monsoon to postmonsoon and then decreased during premonsoon season (28%). Dinoflagellate contribution (25%) remained same irrespective of seasons. A remarkable change was observed in the percentage contribution by bluegreen algae from monsoon to premonsoon through postmonsoon. The contribution was 0.2 %, 2% and 22% respectively in monsoon, postmonsoon and premonsoon seasons. Flagellate contribution was high during postmonsoon season.

Proliferation and high abundance of diatoms during monsoon season has been reported in earlier studies (Madhupratap and Haridas 1990; Nair et al., 1992; Sawant and Madhupratap 1996). This study reveals that centric diatoms are the major contributors during monsoon season. They are known for their fast growth responses to nutrient enrichments (Harrison and Davis 1979; Sanders et al., 1987; Kuosa et al., 1997) and dominate often in natural eutrophic waters. Kochi coastal waters are considered to be among one of the highly productive regions in the world because of its high eutrophication due to upwelling and wind driven water mixing (Rao et al., 1992; Gopinathan et al., 2001). Pennate diatoms generally have lower growth rates than the centric species (Grover 1989; Sommer 1989). Late monsoon season (September – October), encounters the weakening of the upwelling process, favouring the green flagellates and dinoflagellates to form a major component of the phytoplankton community in SEAS (Ramaiah et

al., 2005; Sahayak et al., 2005; and Roy et al., 2006). Contradictory to this, Jyothibabu et al., (2008) reported that diatoms, followed by dinoflagellates dominated in the SEAS during Southwest monsoon season, except for area between 10° and 13° N latitudes. According to them, phytoflagellates are the dominant group occurred between 10° and 13° N latitudes. The phytoplankton community during premonsoon consists mainly of smaller diatoms and cyanobacteria (Nair et al., 1992; Sawant and Madhupratap, 1996; Anoop et al., 2007). This study shows that waning of centric diatoms encouraged proliferation of pennate diatoms and blue-green algae in postmonsoon and declining of both centric and pennate diatoms encouraged proliferation of blue green algae during premonsoon. There is no change in dinoflagellate community in all seasons.

The present study showed some variations in the contribution by dominant species, the sequence of dominance and cell abundance when compared with the previous studies carried out in the region. The study revealed the composition of dominant species of phytoplankton as complex and centric diatoms as the most common constituent. Diatoms are normally associated with high production rates and elevated organic matter export. The alteration of dominance between the groups from diatoms to dinoflagellate and cyanobacteria, in different seasons can result in significant changes in the light absorption by phytoplankton pigments in the region. This inturn affects the ocean color estimation used for various applications. Thus the data on the phytoplankton numerical abundance and diversity along with its absorption properties in the present study will provide insight to

community dynamics and to the phytoplankton pigment composition of this water mass. This can also be used to indicate that major differences in phytoplankton absorption spectra, which forms the basis of ocean colour remote sensing, with respect to seasons in the area.

3.3.4. Shannon-Weiner species diversity index (H index)

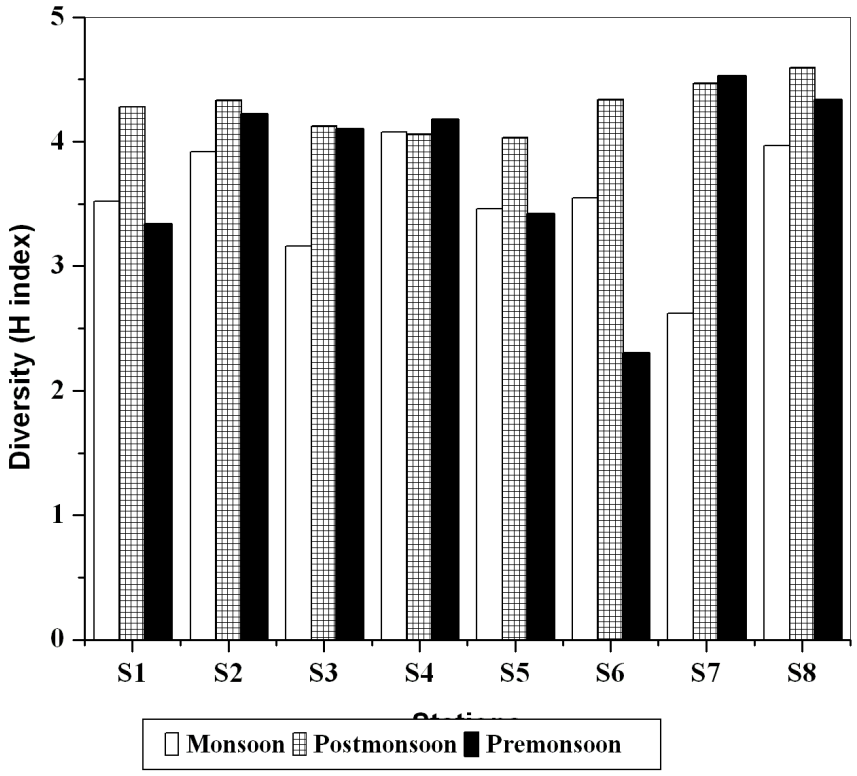

Figure 3.3. Spatial and temporal analysis of Shannon-Weiner Species Diversity index (H index) of phytoplankton in 8 stations during three seasons.

Species diversity is the number of different species in a particular area, which is an important index in characterizing the community structure and community importance in ecosystem. The Shannon-Wiener diversity index (H index) was relatively high during monsoon, postmonsoon and premonsoon seasons (Fig. 3.3). The maximum index obtained was 4.08 (S4) during monsoon, 4.59 (S8) during postmonsoon and 4.52 (S5) during

premonsoon. The minimum diversity index observed during monsoon season was 2.62 (S7), and 4.03 (S5) during postmonsoon and 2.30 (S6) during premonsoon seasons.

Station wise analysis of Shannon-Weiner diversity indices (Fig. 3.3) showed that Stn. S8 had highest diversity during all the seasons. In Stn. S1 and S6, diversity index during monsoon season was higher than postmonsoon season. In Stn. S4 diversity index seemed to be unchanged in all the seasons whereas in Stn. S7, monsoon season showed lower diversity index and during postmonsoon and premonsoon season the diversity remained the same. Station S5 exhibited the same diversity index during monsoon and premonsoon season. Other two Stn. S2 and S3 showed the lowest values during monsoon season followed by premonsoon and the highest values during postmonsoon season.

Phytoplankton diversity was lowest during premonsoon season. Pre-monsoon season along eastern and central Arabian Sea was associated with toxic algal blooms. This causes one species to dominate over others. Hence the diversity was lower. Also, high transparency and low nutrient condition in the coastal waters during premonsoon favours algal blooms dominated by one or two phytoplankton species resulting in decreased phytoplankton diversity (Padmakumar 2010; Martin et al., 2013; Dwivedi et al., 2015). A study conducted in a coastal waters off Kasargode, Kerala exhibited diverse diatom and cyanobacteria community during post-monsoon and pre-monsoon seasons respectively (Rai and Rajashekhar 2014).

The increased abundance of phytoplankton during post-monsoon and pre-monsoon seasons was attributed to the increased salinity, pH, temperature, high nutrient content and high intensity of light penetration (Martin et al., 2010; Badsi et al., 2012). Thestratified water column due to heavy rainfall, reduced salinity, high turbidity, decreased temperature and pH resulted in lowest total count of phytoplankton during monsoon (Perumal et al., 2009). The study concludes that lowest species diversity occurs in monsoon season and highest in postmonsoon season. The phytoplankton diversity in the barmouth remains same throughout the year.

3.3.5. Pielou's evenness index

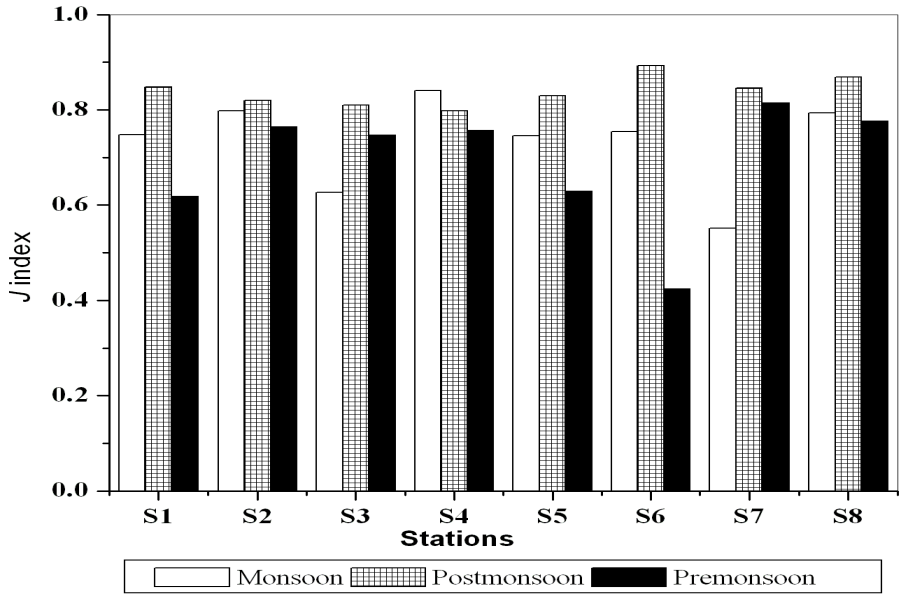

Figure 3.4. Spatial and temporal analysis of Pielou's evenness index (J) of 8 stations during three seasons.

Evenness is an indicator of whether the community structure is developed and stable. It is measured as relative abundance of the different species constituting the richness of an area. The Pielou's evenness index was high in all the stations except S4 during postmonsoon season followed

by monsoon (except in Stn. S3 and S7) and premonsoon seasons (Fig. 3.3). In Stn. S4, high evenness was during monsoon followed by postmonsoon and premonsoon seasons. Stn. S3 and S7 exhibited high evenness during postmonsoon followed by premonsoon season. The abundance of each species varies highly on the basis of its relationship with other species thereby affecting the patterns of assembling or groupings are established at locations throughout the region (Paul et al., 2007).

Decreased salinity, low temperature and mixing of fresh water favoured the rapid growth of both freshwater and marine species thereby creating a favourable environment for the even distribution of phytoplankton during postmonsoon season.

3.4. Conclusion

- The present study determined 73 phytoplankton genera from 19 orders and 41 families. Biddulphiales evolved as the dominant order and the dominant family was Thalassiosiraceae.
- The dominant phytoplankton identified were Skeletonema spp. during the entire study period.
- In terms of abundance and diversity, diatoms formed the major groups compared to other taxonomic groups.
- This study shows that waning of centric diatoms encouraged proliferation of pennate diatoms and blue-green algae in postmonsoon and declining of both centric and pennate diatoms encouraged proliferation of blue green algae during premonsoon. There is no change in dinoflagellate community in all seasons.

- The study concludes that lowest species diversity occurs in monsoon season and highest in postmonsoon season. The phytoplankton diversity in the barmouth remains same throughout the year.
- The study concludes that phytoplankton community structure is well developed and stable during postmonsoon season in the coastal waters and estuarine station.

3.5. References

Badsi H, Ali H O, Loudiki M, Aamiri A. 2012. Phytoplankton diversity and community composition along the salinity gradient of the Massa estuary. American Journal of Human Ecology.1(2):58-64.

Bhagirathan U, Shaju S S, Ragesh N, Meenakumari B, Ashraf M P. 2014. Observations on bio-optical properties of a phytoplankton bloom in coastal waters off Cochin during the onset of southwest monsoon. IJMS. 43:289-96.

Banse K, English D C. 2000. Geographical differences in seasonality of CZCS-derived phytoplankton pigment in the Arabian Sea for 1978–1986. Deep Sea Research II, 47: 1623–1677.

Capone D G, Subramaniam A, Montoya J P, Voss M, Humborg C J, Johansen A M, Siefert R L, Carpenter E J. 1998. An extensive bloom of the N sub (2)-fixing cyanobacterium *Trichodesmium erythraeum* in the central Arabian Sea. Marine Ecology Progress Series. 172:281-92.

Carder, K.L., Hawes, S.K., Baker, K.A., Smith, R.C., Steward, R.G. and Mitchell, B.G., 1991. Reflectance model for quantifying chlorophyll a in the presence of productivity degradation products. Journal of Geophysical Research: Oceans, 96(C11), pp.20599-20611.

Choudhury, A.K. and Pal, R., 2010. Phytoplankton and nutrient dynamics of shallow coastal stations at Bay of Bengal, Eastern Indian coast. Aquatic Ecology, 44(1), pp.55-71.

Dayala V T, Salas P M, Sujatha C H. 2014. Spatial and seasonal variations of phytoplankton species and their relationship to physicochemical variables in the Cochin estuarine waters, Southwest coast of India. Indian Journal of Geo-Marine Sciences. 1; 43:937-47.

Devassy, V.P. and Bhattathiri, P.M.A., 1974. Phytoplankton ecology of the Cochin backwaters.

Devassy V P, Gopinathan C K. 1970. Hydrobiological features of the Kerala backwaters during pre-monsoon and monsoon months. Fishery Technology. 7(2):190-4.

D'Silva M S, Anil A C, Naik R K, D'Costa P M. 2012. Algal blooms: a perspective from the coasts of India. Natural Hazards. 1; 63(2):1225-53.

Dwivedi R, Rafeeq M, Smitha B R, Padmakumar K B, Thomas L C, Sanjeevan V N, Prakash P, Raman M. 2015. Species identification of mixed algal bloom in the Northern Arabian Sea using remote sensing techniques. Environmental monitoring and assessment. 1; 187(2):1-1.

Godhe A, Narayanaswamy C, Klais R, Moorthy K V, Ramesh R, Rai A, Reddy H V. 2015. Long-term patterns of net phytoplankton and hydrography in coastal SE Arabian Sea: What can be inferred from genus level data?. Estuarine, Coastal and Shelf Science. 5;162:69-75.

Gopinathan C P, Nair P V, Kesavan A K. 1974. Studies on the phytoplankton of the Cochin backwater A tropical estuary. Indian Journal of Fisheries. 21(2):501-13.

Gopinathan C P, Gireesh R, Smitha K S. 2001. Distribution of chlorophyll 'a' and 'b' in the eastern Arabian Sea (west coast of India) in relation to nutrients during post monsoon. Journal of Marine Biological Association of India, 43: 21–30.

Grover J P. 1989. Effects of Si: P supply ratio, supply variability, and selective grazing in the plankton: an experiment with a natural algal and protistan assemblage. Limnology and Oceanography, 34(2): 349–367.

Habeebrehman H. 2009. Biological responses to upwelling and stratification in the eastern Arabian Sea. Cochin University of Science and TechnologyKerala, India Ph.D. thesis.

Haridevi C.K., Houlath, K.H., Varma K.K., Renjith K.R., Vijayakumar C.T and Joseph P. 2004. Seasonal variation of zooplankton in relation tohydrographic parameters in the Panagad region of Vembanad Lake.Proceedings of Marine Biology Research, 2004 : 501-511.

Harrison P J, Davis C O. 1979. The use of outdoor phytoplankton continuous cultures to analyze factors influencing species selection. Journal of Experimental Marine Biology and Ecology, 41(1): 9–23.

Hobro R. 1979. Stages of the annual phytoplankton succession in the Askö area (northern Baltic Sea). Acta Botanica Fennica, 110: 79–80.

Hegde S, Anil A C, Patil J S, Mitbavkar S, Krishnamurthy V, Gopalakrishna V V. 2008. Influence of environmental settings on the prevalence of *Trichodesmium* spp. in the Bay of Bengal. Marine Ecology-Progress Series-. 1; 356:93.

Jagadeesan, L., Jyothibabu, R., Arunpandi, N. and Parthasarathi, S., 2017. Copepod grazing and their impact on phytoplankton standing stock and production in a tropical coastal water during the different seasons. Environmental Monitoring and Assessment, 189(3), p.105.

Joseph K J, Pillai V K. 1975. Seasonal and spatial distribution of phytoplankters in Cochin backwater. Bulletin of the Department of Marine Sciences, CUSAT. 7(1):171-80.

Jugnu, R., 2006. Studies on the prevalence of algal blooms along Kerala coast, India (Doctoral dissertation, Cochin University of Science and Technology, Cochin).

Joy, C.M., Balakrishnan, K.P. and Joseph, A., 1990. Effect of industrial discharges on the ecology of phytoplankton production in the river Periyar (India). Water Research, 24(6), pp.787-796.

Jyothibabu R., Madhu N.V., Jayalakshmi K.V., Balachandran K.K., Shiyas C.A., Martin G.D. and Nair K.K.C. 2006. Impact of freshwater influx on microzooplankton mediated food web in a tropical estuary (Cochin backwaters–India). Estuarine, Coastal and Shelf Science, 69(3), pp.505-518.

Jyothibabu R, Devi C A, Madhu N V, Sabu P, Jayalakshmy K V, Jacob J, Habeebrehman H, Prabhakaran MP, Balasubramanian T, Nair K K. 2008. The response of microzooplankton (20–200µm) to coastal upwelling and summer stratification in the southeastern Arabian Sea. Continental Shelf Research. 28(4):653-71.

IOCCG report 9. Ed. Dowell, M. and Platt, T., 2009. Reports and Monographs of the International Ocean-Colour Coordinating Group. Partition of the Ocean into Ecological Provinces: Role of Ocean-Colour Radiometry.

Kaladharan, P., Alavandi, S.V., Pillai, V.K. and Balachandran, V.K., 1990. Inhibition of primary production as induced by heavy metal ions on phytoplankton population off Cochin. Indian Journal of Fisheries, 37(1), pp.51-54.

Krishnan, A.A., Krishnakumar, P.K. and Rajagopalan, M., 2007. Trichodesmium erythraeum (Ehrenberg) bloom along the southwest coast of India (Arabian Sea)

and its impact on trace metal concentrations in seawater. Estuarine, Coastal and Shelf Science, 71(3), pp.641-646.

Kononen K, Niemi A. 1984. Long-term variation of the phytoplankton composition at the entrance to the Gulf of Finland. Ophelia Supplement, 3: 101–110.

Kumar U, Chandran A, Jean Jose J, Shibu R, Krishnan A. 2014. Nutrient-Characteristics, Stoichiometry and Response Stimulus of Phytoplankton Biomass along the Southwest Coastal Waters of India. Marine Biology & Oceanography.

Kuosa H, Autio R, Kuuppo P, et al. 1997. Nitrogen, silicon and zooplankton controlling the baltic spring bloom: An experimental study. Estuarine, Coastal and Shelf Science, 45(6): 813–821.

Le C., Li Y., Zha Y., Sun D., Huang C. and Zhang H., 2011. Remote estimation of chlorophyll a in optically complex waters based on optical classification. Remote Sensing of Environment, 115(2), pp.725-737.

Lierheimer L J, Banse K. 2002. Seasonal and interannual variability of phytoplankton pigment in the Laccadive (Lakshadweep) Sea as observed by the Coastal Zone Color Scanner. Proceedings of the Indian Academy of Sciences-Earth and Planetary Sciences. 111(2):163-85.

Madhupratap M. 1987. Status and strategy of zooplankton of tropical Indian estuaries: a review. Bulletin of Plankton Society of Japan, 34, pp. 65–81

Madhupratap, M. and Haridas, P., 1975. Composition & Variations in the Abundance of Zooplankton of Backwaters from Cochin to Alleppey.

Madhupratap, M. and Haridas, P., 1990. Zooplankton, especially calanoid copepods, in the upper 1000 m of the south-east Arabian Sea. Journal of Plankton Research, 12(2), pp.305-321.

Madhu N V, Jyothibabu R, Balachandran K K, Honey U K, Martin G D, Vijay J G, Shiyas C A, Gupta G V, Achuthankutty C T. 2007. Monsoonal impact on planktonic standing stock and abundance in a tropical estuary (Cochin backwaters–India). Estuarine, Coastal and Shelf Science. 73(1):54-64.

Madhu N V, Jyothibabu R, Balachandran K K. 2010. Monsoon induced changes in the size fractionated phytoplankton biomass and production rate in the estuarine and coastal waters of southwest coast of India. Environmental Monitoring and Assessment, 166(1–4): 521–528.

Martin G D, Muraleedharan K R, Vijay J G, Rejomon G, Madhu N V, Shivaprasad A, Haridevi C K, Nair M, Balachandran K K, Revichandran C, Jayalakshmy K V. 2010. Formation of anoxia and denitrification in the bottom waters of a tropical estuary, southwest coast of India. Biogeosciences Discussions. 7(2):1751-82.

Martin G D, Jyothibabu R, Madhu N V, et al. 2013. Impact of eutrophication on the occurrence of Trichodesmium in the Cochin backwaters, the largest estuary along the west coast of India. Environmental Monitoring and Assessment, 185(2): 1237-1258.

Matondkar S G P, Parab S, Dwivedi R M. 2006. Seasonality in sub-surface chlorophyll maxima in the Arabian Sea: detection by IRS-P4/OCM and implication of it to primary productivity. Proceedings of SPIE- The International Society for Optical Engineering. Society of Photo-Optical Instrumentation Engineers 6406, Art. no. 64060X, 0277-786X/06/$15 • doi: 10.1117/12.693691 .

Menon N N, Balchand A N, Menon N R. 2000. Hydrobiology of the Cochin backwater system–a review. Hydrobiologia. 430(1-3):149-83.

Minu P. and Muhamed Ashraf P. 2012. Occurrence of Freshwater Green Algae in Coastal Waters off Cochin During South West Monsoon Season' published Fish Technology Newsletter, vol.23(1) : 3.

Minu, P., Shaju, S.S., Ashraf, P.M. and Meenakumari, B., 2014. Phytoplankton community characteristics in the coastal waters of the southeastern Arabian Sea. Acta Oceanologica Sinica, 33(12), pp.170-179.

Mohan, A.P., Jyothibabu, R., Jagadeesan, L., Lallu, K.R. and Karnan, C., 2016. Summer monsoon onset-induced changes of autotrophic pico-and nanoplankton in the largest monsoonal estuary along the west coast of India. Environmental monitoring and assessment, 188(2), p.93.

Niemi Å. 1973. Ecology of phytoplankton in the Tvarmlnne area, SW coast of Finland: I. Dynamics of hydrography, nutrients, chlorophyll a and phytoplankton. Acta Botanica Fennica, 100: 1–68.

Niemisto L, Rinne I, Melvasalo T, et al. 1989. Blue-green algae and their nitrogen fixation in the Baltic Sea in 1980, 1982 and 1984. MERI, 17: 1–59.

Padmakumar K B, Smitha B R, Lathika C T, et al. 2010. Blooms of Trichodesmium erythraeum in the South Eastern Arabian Sea during the onset of 2009 summer monsoon. Ocean Science Journal, 45(3): 151–157.

Padmakumar K B, Menon N R, Sanjeevan V N. 2012. Is occurrence of harmful algal blooms in the exclusive economic zone of India on the rise? International Journal of Oceanography, 2012: Article ID 263946, doi: 10.1155/2012/263946.

Parab S G, Matondkar S G P, Gomes H, et al. 2006. Monsoon driven changes in phytoplankton populations in the eastern Arabian Sea as revealed by microscopy and HPLC pigment analysis. Continental Shelf Research, 26(20): 2538–2558.

Paul, J.T., Ramaiah, N., Gauns, M. and Fernandes, V., 2007. Preponderance of a few diatom species among the highly diverse microphytoplankton assemblages in the Bay of Bengal. Marine Biology, 152(1), pp.63-75.

Perumal, N V, Rajkumar M, Perumal P. and Thillai Rajasekar K. 2009. Seasonal variations of plankton diversity in the Kaduviyar estuary, Nagapattinam, southeast coast of India. Journal of Environmental Biology. 30, 1035-1046.

Pielou, E.C., 1966. The measurement of diversity in different types of biological collections. Journal of theoretical biology, 13, pp.131-144.

Pinker R T, Laszlo I. 1992. Global distribution of photo synthetically active radiation as observed from satellites. Journal of Climate, 5(1): 56–65.

Qasim S Z, Bhattathiri P M, Abidi S A. 1968. Solar radiation and its penetration in a tropical estuary. Journal of Experimental Marine Biology and Ecology. 2(1):87-103.

Qasim, S.Z., 1970, June. Some characteristics of a Trichodesmium bloom in the Laccadives. In Deep Sea Research and Oceanographic Abstracts (Vol. 17, No. 3, pp. 655-660). Elsevier.

Qasim, S.Z., Bhattathiri, P.M.A. and Devassy, V.P., 1972. The influence of salinity on the rate of photosynthesis and abundance of some tropical phytoplankton.

Qasim, S.Z., Bhattathiri, P.M.A. and Devassy, V.P., 1972. The effect of intensity and quality of illumination on the photosynthesis of some tropical marine phytoplankton. Marine Biology, 16(1), pp.22-27.

Qasim, S.Z., Vijayaraghavan, S., Joseph, K.J. and Balachandran, V.K., 1974. Contribution of microplankton and nannoplankton in the waters of a tropical estuary. Indian Journal of Marine Sciences, 3, pp.146-149.

Qasim SZ. Indian estuaries. Allied publishers; 2003.

Rai S V, Rajashekhar M. 2014. Seasonal assessment of hydrographic variables and phytoplankton community in the Arabian Sea waters of Kerala, southwest coast of India. Brazilian Journal of Oceanography. 62(4):279-89.

Rai S V, Rajashekhar M. 2015. Ecological measurements of phytoplankton communities in the Arabian Sea water off Kerala and Karnataka coasts (South India). Algological Studies. 149(1):39-60.

Ramaiah, N., Paul, J.T., Fernandes, V., Raveendran, T.V., Raveendran, O., Sundar, D., Revichandran, C., Shenoy, D.M., Gauns, M., Kurian, S. and Gerson, V.J., 2005. The September 2004 stench off the southern Malabar coast-A consequence of holococcolithophore bloom. Indian Academy of Sciences.

Rao D S, Ramamirtham C P, Murty A V S, et al. 1992. Oceanography of the Arabian Sea with particular reference to the southwest monsoon. Bulletin of Central Marine Fisheries Research Institute, 45: 4– 8.

Rinne J N, Minckley W L, Bersell P O. 1981. Factors influencing fish distribution in two desert reservoirs, Central Arizona. Hydrobiologia, 80(1): 31–42.

Robin R S, Vardhan K V, Muduli P R, Rajkumar J S, Swaminathan P. 2010. Vertical distribution of biological characteristics and phytoplankton community structure in the shelf waters off southwest coast of India. International Journal of Current Research. 8:016-34.

Robin R S, Kanuri V V, Muduli P R, Mishra R K, Jaikumar M, Karthikeyan P, Suresh Kumar C, Saravana Kumar C. 2013. Dinoflagellate bloom of *Karenia mikimotoi* along the Southeast Arabian Sea, bordering western India. Journal of Ecosystems. Article ID 463720, 11 pages.

Roy, R., Pratihary, A., Mangesh, G. and Naqvi, S.W.A., 2006. Spatial variation of phytoplankton pigments along the southwest coast of India. Estuarine, Coastal and Shelf Science, 69(1), pp.189-195.

Sahayak, S., Jyothibabu, R., Jayalakshmi, K.J., Habeebrehman, H., Sabu, P., Prabhakaran, M.P., Jasmine, P., Shaiju, P., Rejomon, G., Threslamma, J. and Nair, K.K.C., 2005. Red tide of Noctiluca miliaris off south of Thiruvananthapuram subsequent to the 'stench event'at the southern Kerala coast. Indian Academy of Sciences.

Sanders J G, Cibik S J, D'Elia C F, et al. 1987. Nutrient enrichment studies in a coastal plain estuary: Changes in phytoplankton species composition. Canadian Journal of Fisheries and Aquatic Sciences, 44(1): 83–90.

Sankaranarayanan V N, Qasim S Z. 1969. Nutrients of the Cochin backwater in relation to environmental characteristics. Marine Biology. 2(3):236-47.

Saraladevi K, Sankaranarayanan V N and Venugopal P. 1991. Distribution of nutrients in the Periyar River estuary. Indian Journal of Marine Sciences, 20, 49–54.

Sarangi R K, Mohamed G. 2011. Seasonal algal bloom and water quality around the coastal Kerala during southwest monsoon using insitu and satellite data. Indian Journal of Geo-Marine Sciences. 40(3):356-69.

Sawant, S.S. and Madhupratap, M., 1996. Seasonality and composition of phytoplankton in the Arabian Sea.

Selvaraj, G.S.D., Thomas, V.J. and Khambadkar, L.R., 2003. Seasonal variation of phytoplankton and productivity in the surf zone and backwater at Cochin. Journal of the Marine Biological Association of India, 45(1), pp.9-19.

Shaju S S, Minu P, Srikanth A S, Ashraf P M, Vijayan A K, Meenakumari B. 2015. Decomposition study of in vivo phytoplankton absorption spectra aimed at identifying the pigments and the phytoplankton group in complex case 2 coastal waters of the Arabian Sea. Oceanological and Hydrobiological Studies. 44(3):282-93.

Shunmugaraj T, Ravi V, Rajaguru S, Balamurugan M V, Sundaramoorthy S, Radha M K, Subramanian B R. 2002. A Project report on Critical Habitat Information System for Cochin Backwaters. Integrated coastal and Marine Area Management (ICMAM). DOD. Government of India.

Sommer U. 1989. The role of competition for resources in phytoplankton succession. In: Sommer U, ed. Plankton Ecology–Succession in Plankton Communities. Brock/Springer Series in Contemporary Bioscience. Berlin: Springer, 57–106.

Tassan, S., 1994. Local algorithms using SeaWiFS data for the retrieval of phytoplankton, pigments, suspended sediment, and yellow substance in coastal waters. Applied optics, 33(12), pp.2369-2378.

Thomas L C, Padmakumar K B, Smitha B R, Devi CA, Nandan S B, Sanjeevan V N. 2013. Spatio-temporal variation of microphytoplankton in the upwelling system of the south-eastern Arabian Sea during the summer monsoon of 2009. Oceanologia. 55(1):185-204.

Thomas A M, Sanilkumar M G, Vijayalakshmi K C, Hatha A A, Saramma A V. 2014. Dynamic Changes in Bacterial Population and Corresponding Exoenzyme Activity in Response to a Tropical Phytoplankton Bloom *Chattonella marina*. Journal of Marine Biology.

Zar J H. 1984. Biostatistical Analysis. Englewood Cliffs, NJ: Prentice-Hall.

Chapter 4

In one drop of water are found all the secrets of all the oceans; in one aspect of You are found all the aspects of existence."

-Kahlil Gibran

4. Apparent and Inherent Optical Properties in coastal waters off Kochi

4.1. Introduction

Ocean Optics is the branch of physics concerned with the interactions of light with ocean, as the light propagates through the ocean. There are two types of optical properties-Apparent optical properties and Inherent optical properties.

An optical property of the water body that is dependent upon the spatial distribution of the incident radiation is apparent optical property (AOP) and an optical property of the water body which is totally independent of the spatial distribution of the radiation is known as inherent optical property (IOP). These properties determine the 'colour' of the oceans. When light hits the water surface, the different colours are absorbed, transmitted, scattered, or reflected in differing intensities by water molecules and optically-active constituents in suspension in the upper layer of the ocean.

Chla is considered as the main optically active variable affecting ocean colour. For case 2 waters apart from phytoplankton, other optically active substances (OAS) such as CDOM, total suspended matter (TSM) contribute significantly to the water leaving reflectance (Morel and Prieur 1977; Gordon et al., 1988). Links between optical properties, pigment composition of phytoplankton and other photosynthetic parameters are reported recently (Morel 1997; Kahru and Mitchell 1998; Stuart et al.,1998; Stramski et al., 2001;Aiken et al., 2004; Barlow et al., 2002, 2004; Moore et al., 2005; Fishwick et al., 2006). But these links are seriously affected by

phytoplankton communities including species, differing in size structure and pigment composition. Optical properties of surface waters, affected by variability in phytoplankton communities, can be described by identifying factors that are co-varying with Chla (Ciotti et al., 2002). The relationships among optical properties and phytoplankton community structure were evaluated and showed that many optical characteristics varied significantly by a change in phytoplankton community structure (Barron et al., 2014).

The absorption characteristics of three optically-distinct phytoplankton classes from measurements of total phytoplankton absorption coefficient and Chla concentration showed a representation of three phytoplankton classes pico-, nano- and microphytoplankton (Devred et al., 2011). Remote sensing of size structure of phytoplankton communities using optical properties suggested that phytoplankton size was responsive to changes in SST (Fujiwara et al., 2011), to mixing, stratification, and stability within different regions of the Gulf of Maine (Sauer and Roesler 2013), to both dissolved and particle absorption and scattering properties (Barron et al., 2014). High variability in microphytoplankton a^*_{ph} coefficients between 400 and 500 nm was revealed by Brito et al., (2015).

Satellite remote sensing of ocean colour is the only method currently available for synoptic measurements of phytoplankton Chl biomass. Phytoplankton cells contain Chl that absorbs light and contributes green colour to ocean waters. Chla, specific form of chlorophyll used in oxygenic photosynthesis absorbs most energy from wavelengths of violet-blue and orange-red light and reflects green or yellow light. Several empirical and semi-analytical algorithms have been proposed for the retrieval of Chl

from satellite ocean colour data (Gordon et al., 1983; Carder et al., 1999; O'Reilly et al., 2000; Lee et al., 2002). These algorithms were based on the non-linear relationship between oceanic reflectance and in-situ measured Chla (Marghany and Hashim 2010), more precisely the ratios of reflectance in blue and green bands or their combinations (Gordon and Morel 1983; O'Reilly et al., 1998, 2000; Montres- Hugo et al., 2008).

Remote sensing reflectance (R_{rs}) is an apparent optical property in which the electromagnetic radiation reflected or emitted from an object is identified, measured or analysed by a sensor without direct contact. The reflectance properties of an object depend on the particular material and its physicochemical characteristics, surface roughness and geometric circumstances. The reflectance spectrum shape characteristics are highly affected by the trophic and humic state of the waters (Pulliainen et al., 2001). Variations in radiance reflectance in Case 2 waters are affected by the concentrations of OAS (Pierson and Strombeck 2001). Kutser et al., (2006) reported an 'abnormal' shape of the remote sensing reflectance spectra when concentrations of OAS were high. The study carried out by Cannizaro and Carder (2006) showed that, in non-coastal oligotrophic waters, the peak R_{rs} was at 400 nm which was shifted to ~490 nm in highly reflective, optically shallow, mesotrophic waters and ~560nm in optically deep eutrophic waters. Ouillon and Petrenko (2005) also reported peak R_{rs} at 443 and 490 nm in case 1 water and at 560 nm in case 2 waters. Thus the apparent optical properties (AOP) of aquatic media, such as R_{rs}, largely affected by OAS along with the geometry of ambient light field and the effect can be quantified using IOP's of the OAS (Morel1991; Mobley 1994; Mishra and Mishra 2012). The

fundamental IOP influencing the R_{rs} are absorption (a), scattering (b) and volume scattering function (β). The volume scattering describes the angular distribution of light scattered from an incident beam. In the absence of inelastic scattering, IOP of a medium is completely determined by the absorption coefficient and β. These when combined with the angular and spectral distribution of the incident radiance field just below the surface, the full radiative flux balance of the ocean can be simulated. It also works as a key to current applications measured from remote airborne and satellite platforms (Lee and Lewis 2003). Studies using hyperspectral radiometers, on the relationships between IOP and concentration of OAS, indicated the presence of identifiable sub-types of coastal water within the conventional Case 2 classification (Mckee and Cunningham 2006). The detection and differentiation between phytoplankton size classes based on their optical signatures carried out by a new model showed that nanophytoplankton and microphytoplankton populations are high in surface waters of Arabian Sea (Varunan and shanmugam 2015). In SEAS, so far no attempts were done to study the link between IOP and concentration of OAS using hyperspectral radiometers. In this Chapter efforts were taken to understand, how the different communities of phytoplankton categorized according to their size and dominant taxa affect the shape of phytoplankton absorption and remote sensing reflectance spectra.

4.2. Materials and Methods

4.2.1. Optically active substances

The data collected on a monthly frequency from 8 stations during 2010 and 2011 were used for absorption studies. The data for the distribution of OAS and reflectance studies carried out using Hyperspectral radiometer operated in the study area from 2009 to 2011.

OAS such as Chla, CDOM and β measured using Satlantic™ hyperspectral radiometer. The radiometer was equipped with ECO triplet

sensor (WetlabsTM ECO series) which measures chlorophyll fluorescence, CDOM fluorescence (measures as Quinine sulphate dehydrate equivalent) and β at 650 nm. The data from hyperspectral radiometer was recorded using SatViewTM software and multi-level processing was carried out using ProsoftTM software (Details are given in chapter 2).

4.2.2. Phytoplankton absorption

For measuring phytoplankton absorption, 0.2 to 2 L of seawater were filtered through 25 mm Whatman GF/F filters of 0.7µm pore size, with low pressure (25mm Hg pressure) and measured using Shimadzu UV-2450 attached with integrating sphere (Mitchell and Kahru 1998). Detailed methodology explained in Chapter 2.

4.2.3. Remote sensing Reflectance (R_{rs})

Remote sensing reflectance is the upwelling radiance emerging from the ocean divided by the downwelling irradiance reaching the water surface. It is proportional to the ratio of backscattering (bb), and absorption (a), coefficients, [bb/(a+bb)] (Morel and Prieur 1977). Remote sensing reflectance was measured using hyperspectral radiometer.

The spectral R_{rs} was computed as

$$Rrs(0^+,\lambda) = \frac{Lw(0^+,\lambda)}{Ed(0^+,\lambda)} \quad \text{---------- (1)}$$

where L_w $(0^+, \lambda)$ is water leaving radiance and E_d $(0^+, \lambda)$ is downwelling irradiance above the sea surface. Further, the upwelling radiance and downwelling radiance were computed as follows.

$$Ed(0^+,\lambda) = \frac{Ed(0^-\lambda)}{1-\alpha} \quad \text{---------- (2)}$$

where

α – Fresnel reflection albedo for irradiance from sun and sky

And

$$Lw(0^+,\lambda) = Lu(0^-,\lambda)\frac{[1-\rho(\lambda,\theta)]}{\eta_w^2(\lambda)} \quad \text{---------- (3)}$$

where

ρ(λ,θ) – Fresnel reflectance index of seawater

ηw(λ) – Fresnel refractive index of seawater

The derivative analysis was performed to identify the absorption and reflectance peaks of each pigment. The convexity and concavity of a given absorption curve from the derivative analysis is useful for separating the secondary absorption peaks and shoulders produced by algal pigments in regions of overlapping absorption. The 4th derivative analysis was concentrated, since the magnitude of the 2nd derivative does not provide a reliable measure of the concentration of photosynthetic pigments, due to the absorption contributed by overlapping pigments effect (Gomez et al., 2001). The maxima of the 4th derivative occur close to or at wavelengths where there are absorption peaks attributable to photosynthetic pigments. The procedure was carried out using Microcal Origin 8.0 Scientific analysis software. The fourth derivative of the $a^*_{ph}(\lambda)$ and $R_{rs}(\lambda)$ was calculated by applying a 41 point fourth-degree polynomial smoothing and then differentiating using the Savitzky- Golay method (Savitzky and Golay 1964). The polynomial smoothing was applied because differentiation tends to amplify the effects of high-frequency noise in the spectra (Aguirre- Gomes et al., 2001). Peaks in the fourth derivative curves were selected using the peak finder tool in the software.

4.3. Results and Discussion

4.3.1. Distribution of Optically Active Substances

The analysis of spatio-temporal variability in OAS (Chla and CDOM) and their IOP (β at 650 nm) has been carried out based on the frequency distribution of these substances (Fig. 4.1). The volume scattering function, β, when integrated into backward direction provides estimates of backscattering (Beardsley and Zaneveld 1969; Balch et al., 2001). The backscattering at a longer wavelength, especially in red, is more sensitive to the suspended matter. Hence by analyzing 'β', we can interpret the effect of suspended sediment. The frequency distribution showed large variability in the OAS over the sampling period in the study area. The Chla concentration varied between 0.077 and 23 mg m^{-3} (Fig. 4.1.a). The maximum concentration of Chla was recorded during the month of October 2010 (23.99mg m^{-3}) whereas the minimum was during November 2010 (St-02, 0.077 mg m^{-3}). Further, it was also observed that number of stations encountered within the Chla range of 0.077 to 5 mg m^{-3}. The coefficient of volume scattering function, β, ranged between 0.0002 m^{-1} sr^{-1} (November 2010) and 0.0070 $m^{-1}sr^{-1}$(April 2009) (Fig. 4.1.b). The β values between 0.0002 to 0.002 m^{-1} sr^{-1} occurred most frequently.

The frequency distribution of CDOM (QSDE) showed the range of 0.39 to 2.75 ppb L^{-1} (Fig. 4.1.c). The maximum value of 2.75 ppb L^{-1} was recorded during April 2009 whereas the minimum value of 0.39 ppb L^{-1} was during January 2011. High frequency was observed in concentrations ranging from 0.8 to 2.4 ppb L^{-1}.The distribution of these OAS was controlled

by hydrography of the study area. The study area is subjected to coastal upwelling and heavy freshwater discharge from the estuary of Periyar River in monsoon period which enhances nutrient uptake resulting in the increased biological production (Nair et al., 1992; Jyothibabu et al., 2006). Studies by Srinivas et al., (2003) also reported that the coastal waters of SEAS are the recipient of approximately 1.9×10^{10} m^3 of freshwater annually from the Cochin backwaters. The study concludes that Chla in the study area far high along with β and CDOM (QSDE).

4.3.2. Seasonal variations in Absorption by Phytoplankton based on high and low Shannon Weiner index

Absorption by phytoplankton in 3 seasons from stations with high and low Shannon-Weiner index described in Chapter 3 was shown in Fig. 4.2. The phytoplankton absorption at blue and red wavelengths depends on the species diversity and seasons. During monsoon season, when the phytoplankton species diversity was high, maximum absorption, measured was at 440 nm (0.760 m^{-1}) and it shifted to 430 nm when the diversity was low. The absorption coefficient during low diversity was 0.689 m^{-1}.

In postmonsoon, the absorption coefficients were 0.508 m^{-1} at 436 nm during high diversity and 0.397 m^{-1} at 439 nm during low diversity. During premonsoon, the absorption was comparatively low and it was 0.150 m^{-1} at 437 nm and 0.047 m^{-1} at 436 nm during high and low phytoplankton diversity. Postmonsoon season showed lower absorption coefficient compared to monsoon season and the difference in a_{ph} values at blue and red region was clear in the stations with high and low diversity index.

Compared to monsoon and postmonsoon, the lowest a_{ph} values were observed during the premonsoon season. The phytoplankton absorption peak showed a shift from the usual 440 nm towards shorter wave length.

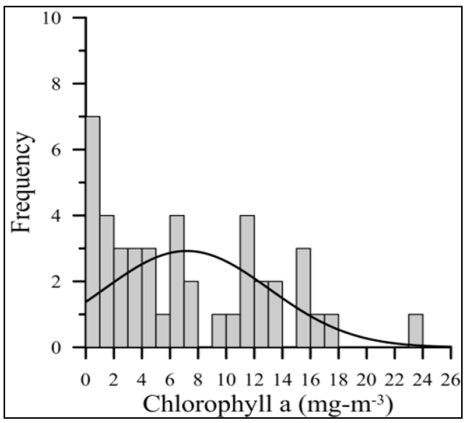

Figure 4.1.a: Frequency distribution of chlorophyll *a* concentration. The solid curve indicates the normal gaussian distribution

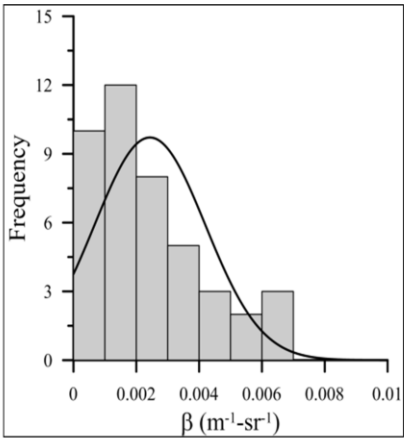

Fig 4.1.b: Frequency distribution of volume scattering function (β) at 670 nm The solid curve indicates the normal Gaussian distribution.

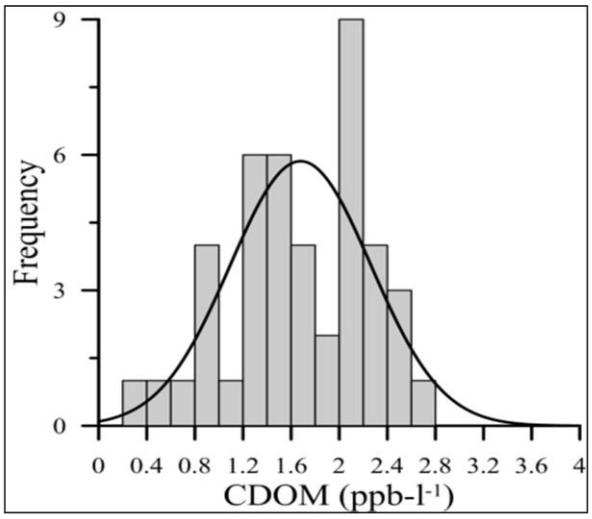

Fig 4.1.c: Frequency distribution of ChromophoricDissolved Organic Matter (CDOM) concentration equivalent to quinine sulfate dehydrate (qsde). The solid curve indicates the normal Gaussian distribution.

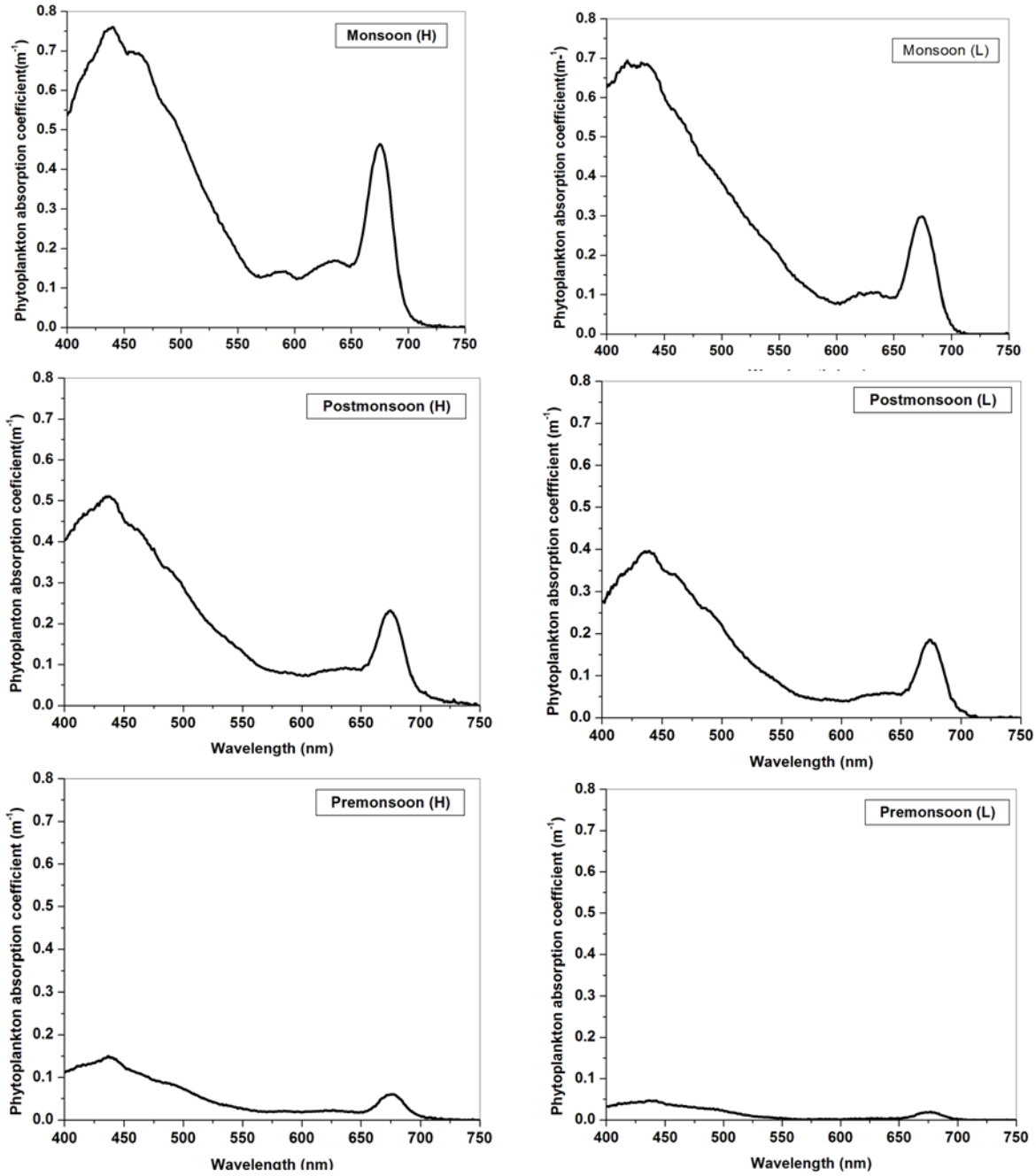

Figure 4.2. Phytoplankton absorption spectra from the stations with highest (H) and lowest (L) Shannon-Weiner diversity index during the three seasons (monsoon, postmonsoon and premonsoon). X-axis represented by wavelength ranging from 400-750 nm and Y axis by phytoplankton absorption coefficient expressed as m^{-1}.

Table 4.1. Summary of photosynthetic pigment absorption maxima determined by fourth derivative analysis in this study

Wave lengths (nm) of absorption in seasons in high (H) or low (L) concentrations						Pigment Group	Reference
Monsoon		Postmonsoon		Premonsoon			
High	Low	High	Low	High	Low		
438	438	438	440	439	441	Chlorophyll a	Prezelin and Alberte (1978); Prezlin and Boczar (1986); Gomez et al., (2001)
467	465	467	467	465	466	Chlorophyll c Peridinin	Millie, Kirkpatrick and Vinyard (1995); Millie et al., (1997); Goericke and Repeta (1993)
497	493	495	495	491	495	Phycourobilin	Millie, Kirkpatrick and Vinyard (1995); Millie et al., (1997): Louchard et al., (2002)
-	546	-	541	542	542	Phycoerythrobilin	Ong et al., (1984)
588	-	590	592	585	584	Chlorophyll b	Millie et al., (1997)
641	639	641	641	641	646	Chlorophyll c	Millie, Kirkpatrick and Vinyard (1995); Millie et al., (1997)
677	674	675	675	676	675	Chlorophyll a	Prezelin and Alberte (1978); Gomez et al., (2001)

A fourth derivative analysis was performed to identify the pigment peak contributions other than Chla (Fig.4.3). The fourth derivative analysis identified peaks at 438-441 nm and 674-677 nm for Chla, 465-467,639-641 nm for Chlc, 491-497 nm for phycourobilin and 541-546 nm for phycoerythrobilin. Peaks at 584-592 nm were identified for Chlb (Table 4.1.). The results of the derivative analysis showed that Cochin coastal waters are dominated by phytoplankton containing pigments such as Chla, Chlb and Chlc, peridinin, diadinoxanthin, fucoxanthin, β-carotene and phycoerythrobilin. Pigment phycoerythrobilin was present during monsoon

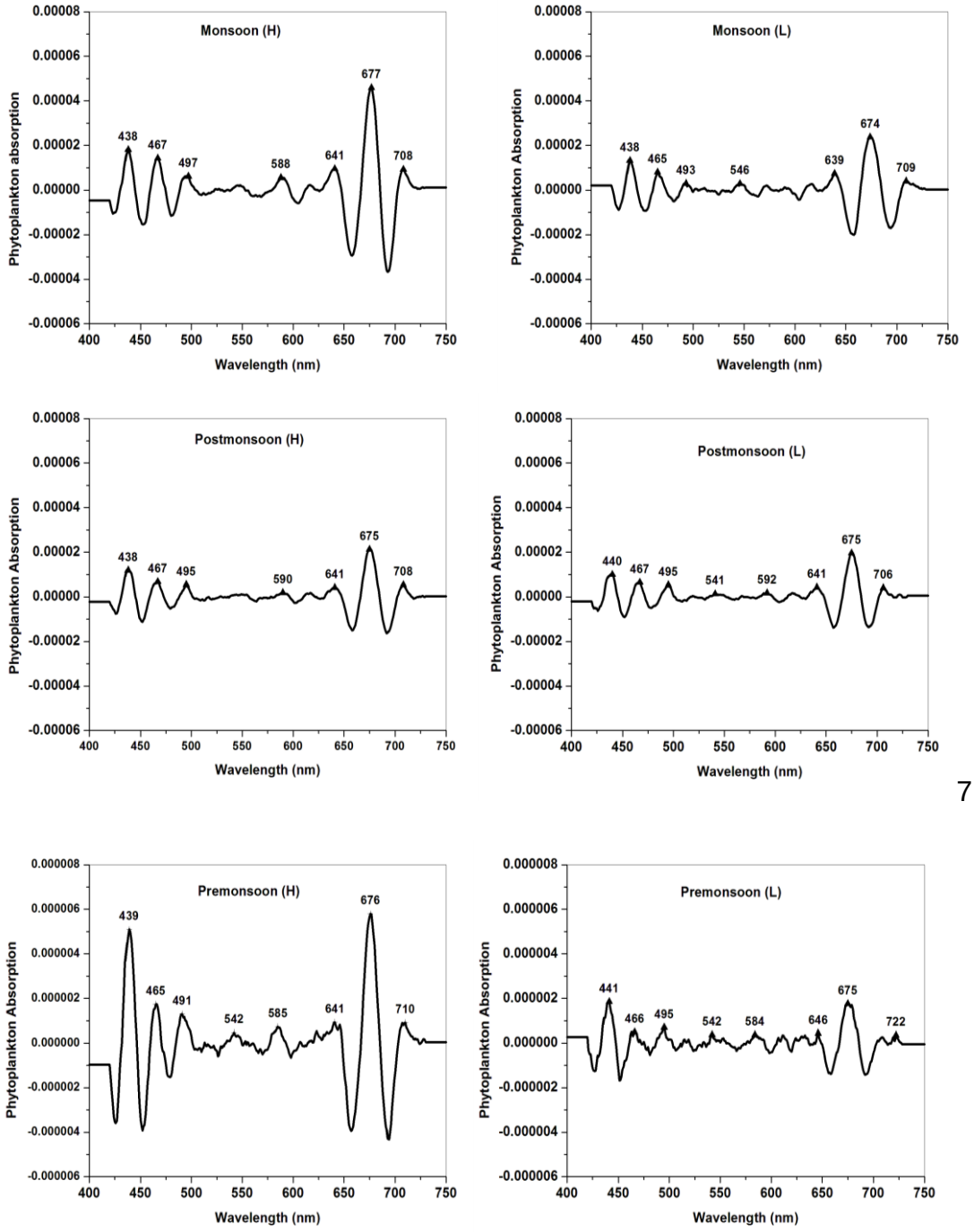

7

Figure 4.3. Fourth derivative analysis of phytoplankton absorption spectra from the stations exhibited with highest (H) and lowest (L) Shannon-Weiner diversity index during three seasons (monsoon, postmonsoon and premonsoon). X axis represented by wavelength ranging from 400-750 nm and Y axis by phytoplankton absorption coefficient after performing 41 point Savitsky–Golay polynomial smoothing and differentiation.

and postmonsoon seasons when the Shannon-Weiner diversity (H' index) was low, while premonsoon season showed the pigment during both high and low phytoplankton diversity index. (Bricaud and Stramski 1990; Morel and Ahn 1990; Babin et al., 1993). Peridinin is the biomarker pigment of dinoflagellates. Phycoerythrobilin, a subtype of the pigment phycobiliproteins are the light harvesting pigment found in cyanobacteria, rhodophytes and cryptophytes. Fucoxanthin and diadinoxanthin are carotenoid pigments found in diatoms, prymnesiophytes, raphidophytes, and chrysophytes (Hsiu-Ping et al., 2002). The pigment β carotene is found in cyanobacteria. Shaju et al., (2015) identified Fucoxanthin and diadinoxanthin, the carotenoid pigments found in the diatoms using the derivatives peaks from the study area.

From the peaks of the fourth derivative analysis, pigments contributing to the phytoplankton absorption were identified. Chlorophyll *a*, chlorophyll *b*,chlorophyll *c*, peridinin, phycourobilin and phycoerythrobilin are the pigments identified using the 4th derivative analysis. Shifting of absorption to shorter wavelengths in different seasons and diversity variation was due to the influence of the high amount of non-algal particles by the decomposition of Chl or the superimposition of some other pigments. These studies provide an insight into the presence of diverse phytoplankton species in the region.

4.3.3. Remote Sensing Reflectance

The R_{rs} data measured using hyperspectral radiometer exhibited three different types of spectra and their spectral variability was shown in Fig. 4.4. Based on the variability in R_{rs} spectra, the coastal waters off Cochin are optically classified into three types. Type-I (T1) waters had spectra (Fig 4.4.a) with flatter curve between 400 to 450 nm which then increased to a maximum at 482 nm. After 482 nm, R_{rs} decreased gradually to 608 nm and then the curve flattened again till 700 nm indicating no reflectance in the region.

The spectral R_{rs} in Type-II (TII) waters (Fig 4.4.b) was found to be distinct from that of T1. The average R_{rs} increased gradually from shorter wavelength (400 nm) and showed almost flat region between 532 nm and 566 nm with marginally higher value at 560 nm. Beyond 560 nm a steep decrease was observed till 610 nm. After which the decrease was gradual till 670 nm. A secondary maximum was also present at 681 nm. The R_{rs} spectra in Type-III (TIII) waters (Fig 4.4.c) showed similarity to that of the Type-II at a longer wavelength. In this type, a steep increase in R_{rs} was seen from 400 nm till 570 nm. The peak R_{rs} was more prominent. The spectral behaviour of R_{rs} from 570 nm to 700 nm in TIII was similar to that of Type-II. However, the secondary maximum was more prominent at 684 nm with high magnitude.

The distribution of OAS within different water types were analysed for evidencing the difference in R_{rs} spectral shapes. In Type-I waters, R_{rs} spectra showed the maximum in the blue (400 to 480 nm) and almost negligible in the red region (beyond 600 nm). The variability in the concentration of Chla and CDOM was very low in this water type with a standard deviation of less than 50% of the average value. The β_{650} also showed less variability in this water types. The low concentration in the distribution of OAS in Type-I waters was responsible for least absorption in the shorter wavelength resulting in high R_{rs}. However, the lower R_{rs} in the longer wavelength may be attributed to the strong absorption due to water molecules. This shows that the water molecules were the principal light absorbing component in this water type along with Chla.

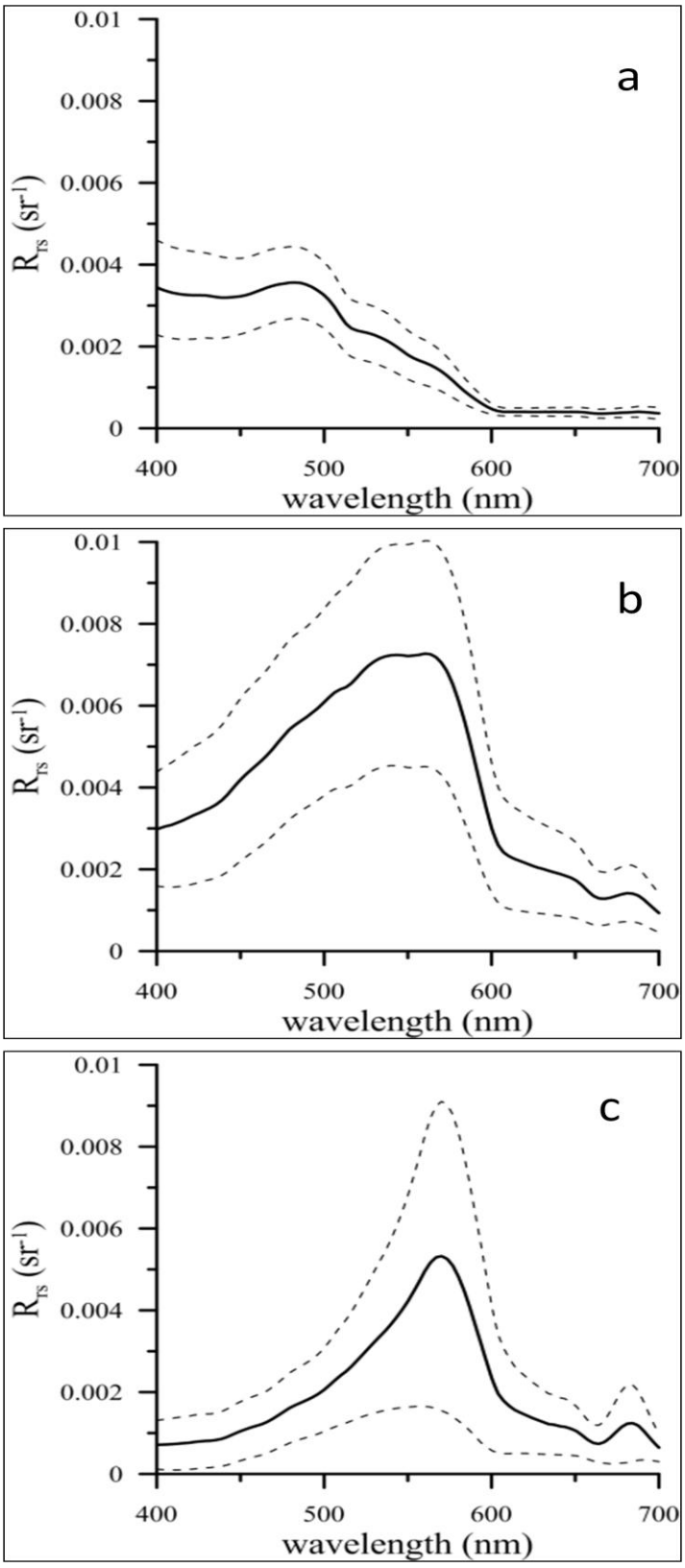

Figure 4.4. Mean and standard deviation of three classes of reflectance spectra obtained during the study. X axis represents wavelength (nm) and Y axis represents coefficient of reflectance (Sr^{-1})

The result was is in agreement with the previous studies carried out in oligotrophic waters of Lakshadweep Islands, hyper oligotrophic waters in the South Pacific gyre and in the Chesapeake Bay wherein the authors have shown that the water molecules are the major component responsible for the absorption in longer wavelength resulting in minimal variability of R_{rs} (Menon et al., 2005; Morel et al., 2007; Tzortziou et al., 2007).

The spectral signature of R_{rs} in Type-II waters showed the significant difference at the shorter wavelength. In Type-II, waters Chla concentration and β_{650} was tenfold higher than in Type-I waters. Also, the CDOM concentration was almost twice in magnitude. The phytoplankton pigment, Chla, has a primary absorption peak in the blue region (~ 440 nm). Apart from this CDOM also has a tendency for strong absorption in UV and blue region (Jorgenson, 1999; Siegal et al., 2002; Menon et al., 2005). Therefore, the respective signature of R_{rs} in Type-II waters was predominantly due to the combined effect of absorption due to Chla and CDOM.

In Type-III waters, the peak in the R_{rs} spectra was shifted more towards the longer wavelength as compared to that in Type-II waters. In addition, the peak R_{rs} was more prominent as compared to Type-I and II waters. In this water type, β_{650} was comparable with Type-II waters. However, Chla and CDOM concentration were found to be increased by 64% and 76% respectively. The impact of Chla and CDOM absorption has further increased in this type of waters which resulted in still lower R_{rs} at the shorter wavelength. The results showed that CDOM significantly influences the water leaving radiance at the shorter wavelengths and its impact can be spread up to 650 nm (Menon et al., 2006). Kutser et al., (2006) reported an 'abnormal' shape of the R_{rs} spectra when the concentrations of optically

active substances were high. The study carried out by Cannizaro and Carder (2006) showed that, in non-coastal oligotrophic waters, the peak R_{rs} was at 400 nm which was shifted to ~490 nm in highly reflective, optically shallow, mesotrophic waters and ~560nm in optically deep eutrophic waters. Ouillon and Petrenko (2005) also reported peak R_{rs} at 443 and 490 nm in case 1 water and at 560 nm in case 2 waters.

The study concludes that concentration of OAS plays an important role in determining the R_{rs} signals in the study area. In Type-I waters Chla, CDOM and β_{650} were very low indicating that these were pure Case-I waters and the peak R_{rs} was in the blue band. In Type-II waters, the peak R_{rs} shifted to the green band which was attributed to the elevated concentration of Chla, CDOM and β_{650}. In Type-III waters, the peak R_{rs} further shifted to longer wavelengths due to an increase in Chla and CDOM.

4.3.4. Performance of 4th Derivative analysis

Differences between optical signatures between phytoplankton species are reflected in the location of local maxima and minima in the reflectance spectrum and changes in the relative height of characteristic peaks with changes in phytoplankton concentration. The different pigment composition of different phytoplankton species results in different location of local maxima and minima in the reflectance spectrum (Soja-Wozniak et al., 2017). It is under the assumption that the positive peaks in the absorption spectra corresponding to a negative peak in the reflectance spectra. In order to understand the contribution of different pigments to the reflectance spectrum, a 4th derivative analysis of remote sensing reflectance spectra were carried and is shown in Figure 4.5. The noise level in the 4th derivative analysis of remote sensing reflectance spectra was minimum for wavelength ranging from 400 nm to 553 nm). Towards the red region of the visible spectra, the noise level was higher especially at wavelengths ranging between 665 nm to 711 nm. Figure 4.6 showed the derivative spectra for 3 types of remote sensing reflectance corresponding to Chla 0.2516 mg m^{-3} (± 0.174), 7.403 mg m^{-3} (± 4.81) and 11.491 mg m^{-3} (± 6.778) respectively for Type-I, II and III waters.

As the Chla concentration increased, the shape of the derivative spectra also became distinct.

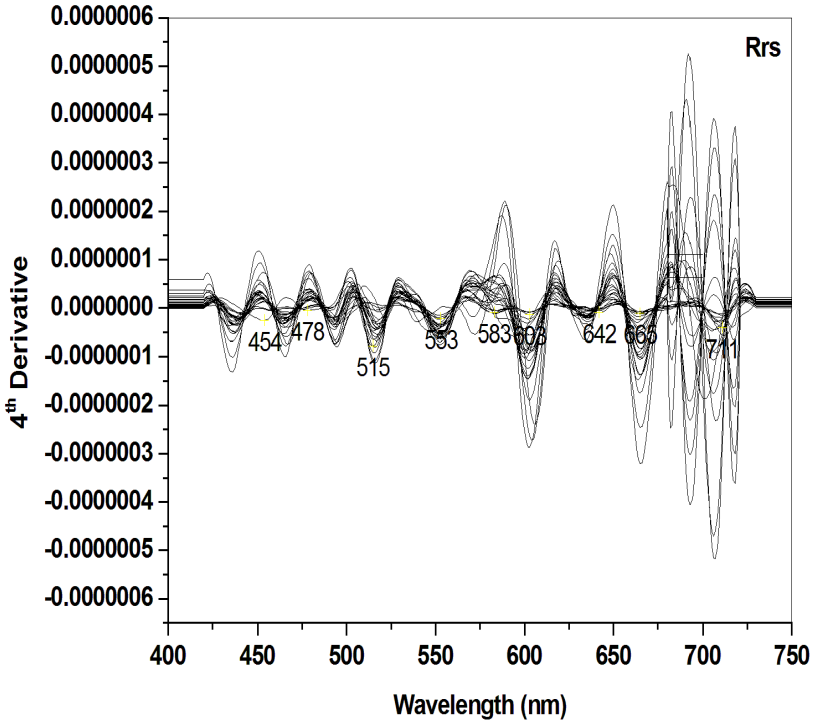

Figure 4.5. Fourth derivative analysis of the Remote sensing reflectance spectra from the study area. X axis represented by wavelength ranging from 400-700 nm and Y axis by remote sensing reflectance after performing 41 point Savitsky–Golay polynomial smoothing and differentiation.

Derivative analysis of Type-I reflectance spectra differed in the blue region with that of Type-II and Type-III. The positive peaks at 451±1 nm, 480 ±1 nm and negative peaks at 465±1 nm and 493±1 nm in Type-II spectra were absent in Type-I waters. The intensity of peaks was comparatively less for Type-I waters except for at wavelength 515±1 nm. No markable difference was observed between Type-II and Type-III spectra. The only difference attributed to distinguish Type-III spectra from Type-II is the intensity of the negative peak at 665 nm. The positive peak at 685 nm reported by Kirk (2011) corresponding to the sum of irradiance produced through

natural fluorescence emission by Chla and elastic scattering were absent in the derivative data.

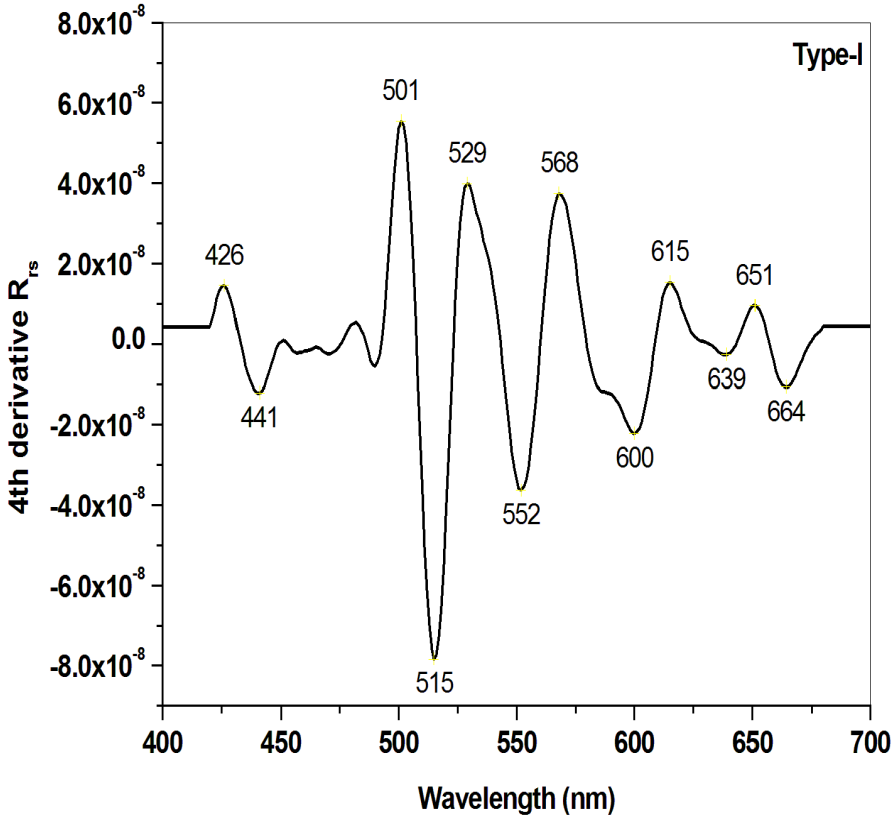

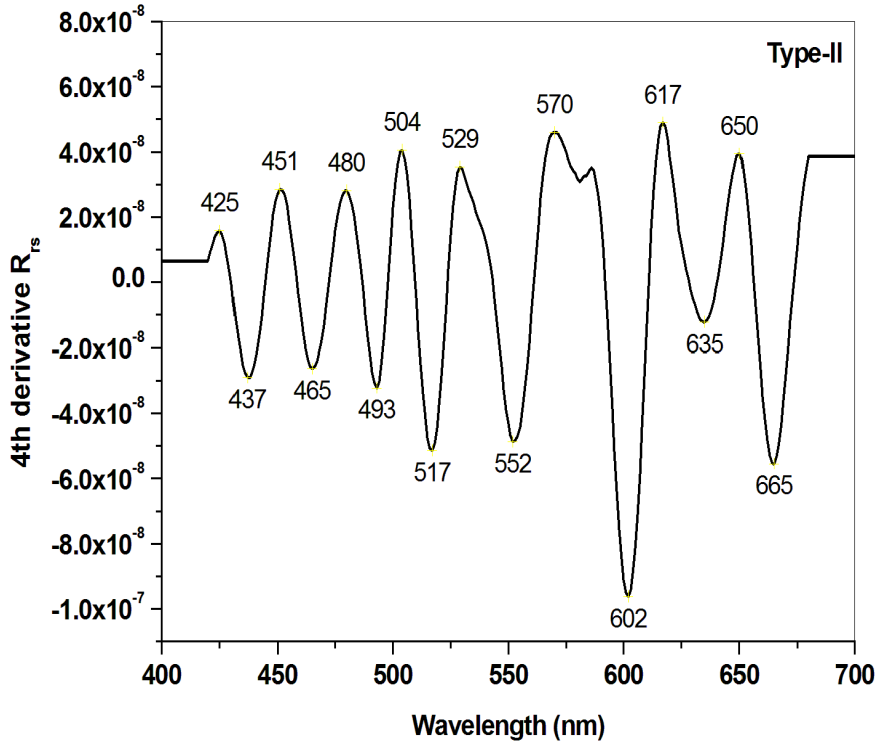

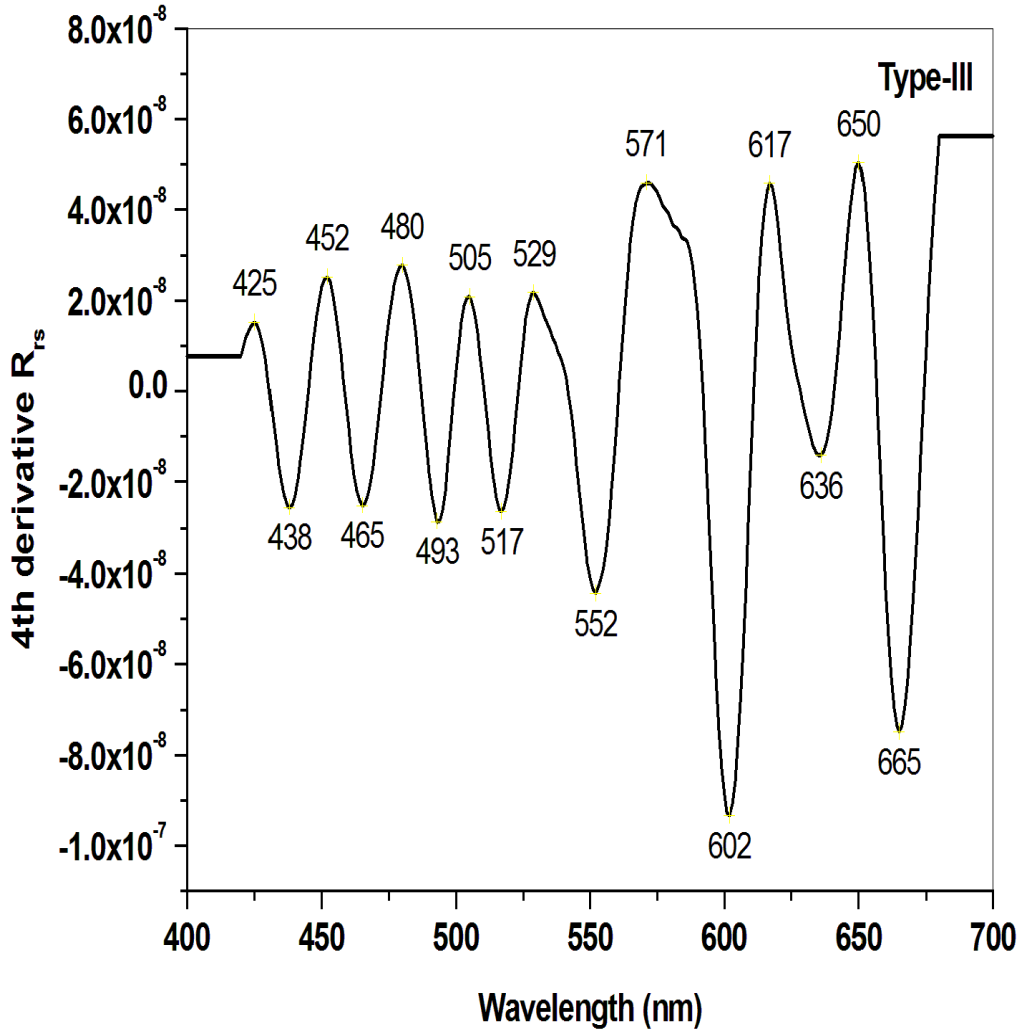

Figure 4.6.Fourth derivative analysis of the three types of Remote sensing reflectance spectra from the study area. X axis represented by wavelength ranging from 400-700 nm and Y axis by remote sensing reflectance after performing 41 point Savitsky–Golay polynomial smoothing and differentiation.

The positive peaks identified for pigments in the absorption spectra is matching with the negative peaks of remote sensing reflectance spectra. The positive peaks at 451±1 nm identified in the 4th derivative analysis of Type-II and III reflectance spectra corresponds to contribution by picoplankton and at

568±3 nm by microphytoplankton, especially diatoms. Large peaks at 450nm associated with picoplankton (Uitz et al., 2015). The signals for diatoms were evidenced at 570nm of the 4th derivative reflectance spectra (Soja-Wozniak et al., 2017)

4.3.5. The Interrelationship of Chlorophyll a with CDOM and β650

Analysis of inter-relationship of Chla with CDOM and β_{650} in different water types is shown in Fig 4.7. The Chla and CDOM did not show any significant inter-relationship in Type-1 waters. This indicated that the CDOM was independent of the variations in Chla in these waters. However, a large association seen in Type-II and Type-III waters. In these waters, the concentration of Chla and CDOM was very high. The covariance of Chla with CDOM indicated that the source of nutrient, for phytoplankton growth, and organic matter was same. Since the primary source of CDOM was from the riverine sources, it can be inferred that river discharge was one of the primary forcing mechanism for distribution of Chla and CDOM in the study area (Nair, Devassy, and Madhupratap 1992; Jyothibabu et al., 2006;

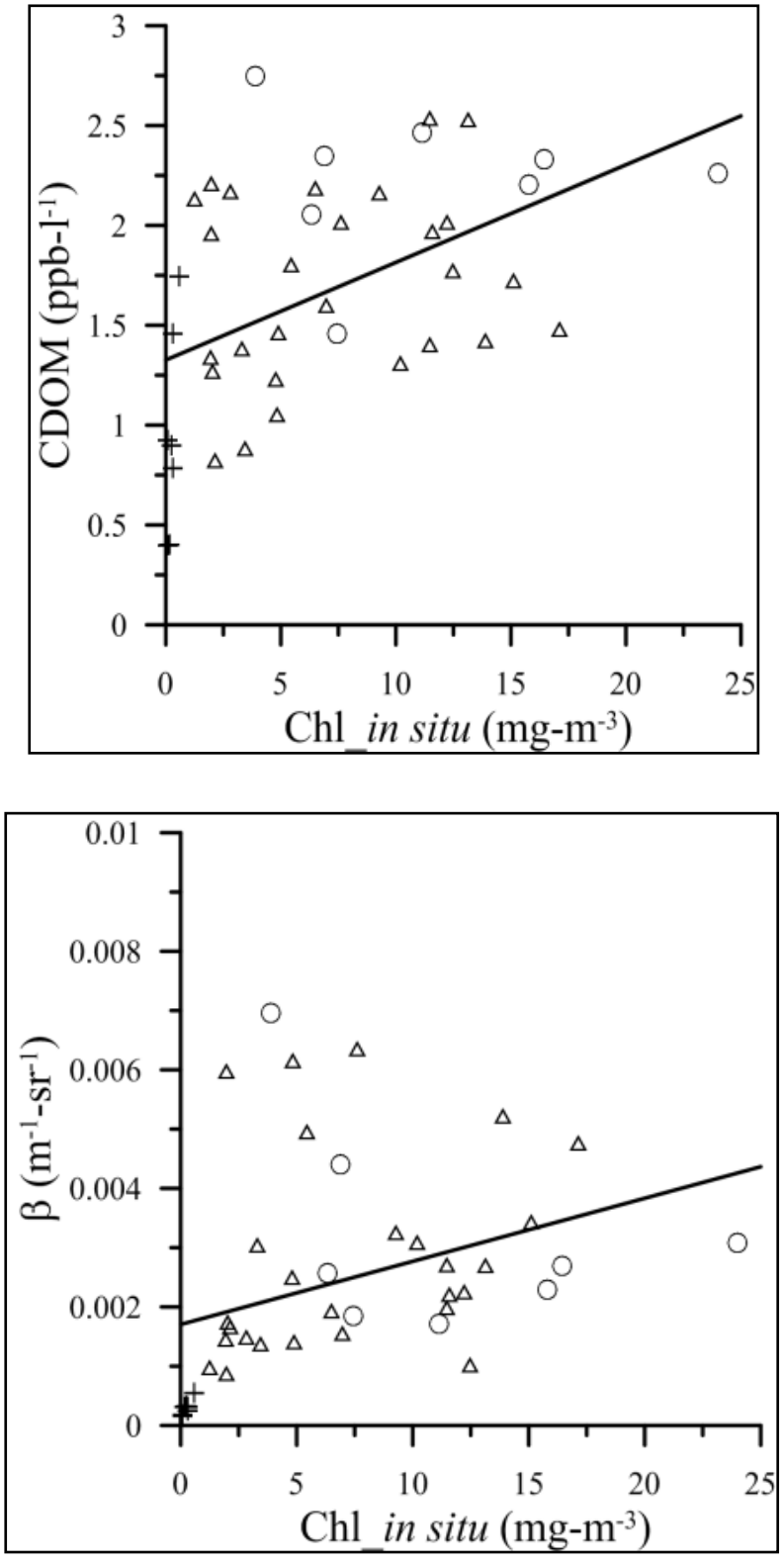

Figure. 4.7. Scatter plot showing relation between (a) insitu chlorophyll-a (Chla) and CDOM in QSDE unit (b) insitu Chla and β. The plus (□) sign corresponds to Type-I, open triangle (Δ) correspond to Type-II and open circles (○) correspond to Type-III waters.

Minu et al., 2014). The β_{650} did not show any significant relationship with Chla in any of the water types. This shows that Chla and suspended matter do not covary in water types. Hence it can be inferred that river discharge is not the primary source of suspended matter in the study area. Studies by Thomas et al., (2004), Srinivas et al., (2003) and Jyothibabu et al., (2006) reported that continuous dredging process in the study area occurring around the year drains increased nutrient and sediment load from the estuary into the coastal waters.

4.4. Conclusion

- Phytoplankton containing pigments such as Chla, Chlb, Chlc, peridinin, diadinoxanthin, fucoxanthin, β carotene and phycoerythrobilin identified from the results of derivative analysis dominated in these waters.
- The R_{rs}spectra exhibited three distinct water types based on its variability.
- Type-I waters exhibited very low Chla, CDOM and β_{650} indicating that these were case-I waters and peak R_{rs} was in the blue band.
- Type-II waters had the peak R_{rs} shifted to the green band which was attributed to the elevated concentration of Chla, CDOM and β_{650}.
- The peak R_{rs} further shifted to longer wavelength in Type-III waters, due to increase in Chla and CDOM.
- Further, Chla was found to be associated with CDOM indicating that river is one of the primary sources for discharging essential parameters for the growth of phytoplankton.
- From the derivative analysis of remotes sensing reflectance, marker peaks for picoplankton and microplankton were evident, while it failed to distinct peaks for nanophytoplankton.

- The strong water absorption can be studied from reflectance peaks corresponding to 571nm to 602 nm, picophytoplankton from 451±1, nanophytoplankton from negative peaks around 515±2 nm and 600±2 nm and microplankton from 568±3 nm in the study area.
- Apart from this, picoplankton dominates in the Type-II and Type-III waters.

4.5. References

Aiken J, Fishwick J, Moore G, Pemberton K. 2004. The annual cycle of phytoplankton photosynthetic quantum efficiency, pigment composition and optical properties in the western English Channel. Journal of the Marine Biological Association of the United Kingdom, 84 (2), 301–313.

Babin M, Therriault J C, Legendre L and Condal A. 1993. Variations in the specific absorption coefficient for natural phytoplankton assemblages: Impact on estimates of primary production. Limnology and Oceanography, 38,154-177.

Balch W M, Drapeau D T, Fritz J J, Bowler B C, Nolan J. 2001. Optical backscattering in the Arabian Sea—continuous underway measurements of particulate inorganic and organic carbon. Deep-Sea Research I ,48, 2423–2452.

Barlow R G, Aiken J, Holligan P M, Cummings D G, Maritorena S, Hooker S. 2002. Phytoplankton pigment and absorption characteristics along meriodinal transects in the Atlantic Ocean. Deep-Sea Res Part I, 49, 637–660.

Barlow R G, Aiken J, Moore G F, Holligan P M, Lavender S. 2004. Pigment adaptations in surface phytoplankton along the eastern boundary of the Atlantic Ocean. Marine Ecology Progress Series, 281, 13−26.

Barrón, R.K., Siegel, D.A. and Guillocheau, N., 2014. Evaluating the importance of phytoplankton community structure to the optical properties of the Santa Barbara Channel, California. Limnology and Oceanography, 59(3), pp.927-946.

Beardsley G F, Zaneveld J R V. 1969. Theoretical dependence of the near asymptotic apparent optical properties on the inherent optical properties of seawater. Journal of the Optical Society of America, 59, 373–377.

Bricaud A and Stramski D. 1990. Spectral absorption coefficients of living phytoplankton and nonalgal biogenous matter: a comparison between the Peru upwelling area and the Sargasso Sea. Limnology and Oceanography, 35, 562–582.

Bricaud A, Babin M, Morel A, Claustre H. 1995. Variability in the chlorophyll-specific absorption coefficients of natural phytoplankton: analysis and parameterization. Journal of Geophysical Research ,100 (C7), 13321-13332.

Brito, A.C., Sá, C., Brotas, V., Brewin, R.J., Silva, T., Vitorino, J., Platt, T. and Sathyendranath, S., 2015. Effect of phytoplankton size classes on bio-optical properties of phytoplankton in the Western Iberian coast: Application of models. Remote Sensing of Environment, 156, pp.537-550.

Buiteveld H, Hakvoort J H M, Donze M. 1994. The optical properties of pure water. Ocean Optics XII SPIE, 2258, 174–183.

Cannizaro J P, Carder K L. 2006. Estimating chlorophyll a concentrations from remotesensing reflectance in optically shallow waters. Remote Sensing of Environment, 101, 13–24.

Carder K L, Chen FR, Lee Z P, and Hawes S K. 1999. Semianalytic Moderate-Resolution Imaging Spectrometer algorithms for chlorophyll a and absorption with bio-optical domains based on nitrate-depletio temperatures. Journal of Geophysical Research, 104, 5403-5421.

Ciotti A M, Cullen J J, Lewis M R. 1999. A semi-analytical model of the influence of phytoplankton community structure on the relationship between light attenuation and ocean color. Journal of Geophysical Research, 104(C1), 1559–1578.

Ciotti A M, Lewis M R, Cullen J J. 2002. Assessment of the relationships between dominant cell size in natural phytoplankton communities and the spectral shape of the absorption coefficient. Limnology and Oceanography, 47, 404–417.

Devred, E., Sathyendranath, S., Stuart, V. and Platt, T., 2011. A three component classification of phytoplankton absorption spectra: Application to ocean-color data. Remote Sensing of Environment, 115(9), pp.2255-2266.

Fishwick J, Aiken J, Barlow R, Sessions H, Bernard S, Ras J. 2006. Functional relationships and bio-optical properties derived from phytoplankton pigments, optical and photosynthetic parameters; a case study of the Benguela ecosystem. Journal of the Marine Biological Association of the United Kingdom, 86, 1267–1280.

Fujiwara, A., Hirawake, T., Suzuki, K. and Saitoh, S.I., 2011. Remote sensing of size structure of phytoplankton communities using optical properties of the Chukchi and Bering Sea shelf region. Biogeosciences, 8(12), p.3567.

Gomez Aguirre R, Weeks A R, Boxall S R. 2001. The identification of phytoplankton pigments from absorption spectra. International Journal of Remote sensing, 22 (2 & 3), 315–338.

Gomez Aguirre R. 2014. Spectral Reflectance Analysis of the Caribbean Sea. Geofísica Internacional, 53 (4), 385–398.

Gordon H R, Brown O B, Evans R H, Brown J W, Smith R C, Baker K S, Clark D K. 1988. A semianalytic radiance model of ocean color. Journal of Geophysical Research, 93, 10909–10924.

Gordon H R, Clark D K, Brown J W, Brown O B, Evans R H, Broenkow W W. 1983. Phytoplankton pigment concentrations in the Middle Atlantic Bight: comparison of ship determinations and CZCS estimates. Applied Optics, 22, 20–36.

Gordon J H R and Morel A .1983. Remote assessment of ocean color for interpretation of satellite visible imagery. A review. In Barber, R.T., Mooers, N. K., Bowman, M.J. and Zeitzschel. B- (eds). Lecture Notes on Coastal and Estuarine Studies. Springer-Verlag, New York.

Hsiu-Ping L, Gwo-Ching G, Tung-Ming H. 2002. Phytoplankton pigment analysis by HPLC and its application in algal community investigations. Botanical Bulletin of Academia Sinica, 43: 283 – 290.

Johnsen G, Nelson N B, Jovine R V M and Prèzelin B B. 1994. Chromoprotein and pigment-dependent modeling of spectral light absorption in two dinoflagellates, Prorocentrum minimum and Heterocapsa pygmaea. Marine Ecology Progress Series, 114, 245–258.

Jorgenson S V.1999. Standard Case 1 algorithms in Danish coastal waters. International journal of remote sensing, 20, 1289-1301.

Jyothibabu R, Madhu N V, Jayalakshmi K V, Balachandran K K, Shiyas C A, Martin G D, Nair K K C. 2006. Impact of fresh water influx on microzooplankton

mediated food web in a tropical estuary (Cochin backwaters - India). Estuarine, Coastal and Shelf Science, 69, 505 - 518.

Kahru M and Mitchell B G. 1998. Spectral reflectance and absorption of a massive red tide off southern California. Journal of Geophysical Research ,103, 21601–21609.

Kirk J T O. 2011. Light and photosynthesis in aquatic Ecosystems (Cambridge: Cambridge University Press), Third Edition.

Kirkpatrick G J, Millie D F, Moline M A, Schofield O. 2000. Optical discrimination of a phytoplankton species in natural mixed populations. Limnology and Oceanography, 45, 467–471.

Kutser T, Vahtma E, and Martin G. 2006. Assessing suitability of multispectral satellites for mapping benthic macroalgal cover in turbid coastal waters by means of model simulations. Estuarine Coastal and Shelf Science, 67: 521–529.

Lee M E, and Lewis M R. 2003. A new method for the measurement of the optical volume scattering function in the upper ocean. Journal of Atmospheric and Oceanic Technology, 20: 563–571.

Lee Z, Carder K L, Arnone R A. 2002. Deriving inherent optical properties from water color: a multiband quasi-analytical algorithm for optically deep waters. Applied Optics, 41(27), 5755 - 5772.

Louchard, E.M., Reid, R.P., Stephens, C.F., Davis, C.O., Leathers, R.A., Downes, T.V. and Maffione, R., 2002. Derivative analysis of absorption features in hyperspectral remote sensing data of carbonate sediments. Optics Express, 10(26), pp.1573-1584.

Marghany M and Hashim M. 2010. MODIS satellite data for modeling chlorophyll-a concentrations in Malaysian coastal waters. International Journal of the Physical Sciences , 5(10), 1489-1495.

Mckee D, and Cunningham A. 2006. Identification and characterization of two optical water types in the Irish Sea from insitu inherent optical properties and seawater constituents. Estuarine, Coastal and. Shelf Science, 68: 305–316.

Menon H B, Lotliker A A, Nayak S R. 2005. Pre-monsoon bio-optical properties in estuarine, coastal and Lakshadweep waters. Estuarine, Coastal and Shelf Science, 63, 211-223.

Menon, H.B., Lotliker, A.A. and Nayak, S.R., 2006. Analysis of estuarine colour components during non-monsoon period through Ocean Colour Monitor. Estuarine, Coastal and Shelf Science, 66(3), pp.523-531.

Millie, D.F., Kirkpatrick, G.J. and Vinyard, B.T., 1995. Relating photosynthetic pigments and in vivo optical density spectra to irradiance for the Florida red-tide dinoflagellate Gymnodinium breve. Marine ecology progress series. Oldendorf, 120(1), pp.65-75.

Millie, D.F., Schofield, O.M., Kirkpatrick, G.J., Johnsen, G., Tester, P.A. and Vinyard, B.T., 1997. Detection of harmful algal blooms using photopigments and absorption signatures: A case study of the Florida red tide dinoflagellate, Gymnodinium breve. Limnology and Oceanography, 42(5part2), pp.1240-1251.

Minu, P., Shaju, S.S., Ashraf, P.M. and Meenakumari, B., 2014. Phytoplankton community characteristics in the coastal waters of the southeastern Arabian Sea. Acta Oceanologica Sinica, 33(12), pp.170-179.

Mishra S, Mishra D R. 2012. Normalized Difference Chlorophyll Index: A novel model for remote estimation of chlorophyll-a concentration in turbid productive waters. Remote Sensing of Environment,117: 394-406, doi: 10.1016/ j.rse.2011. 10.016.

Mitchell B, Kahru M. 1998. Algorithms for SeaWiFS standard products developed with the CalCOFI bio-optical data set. Technical reports, Vol. 30: California Cooperative Fisheries Investigation.

Mobley C D. 1994. The optical properties of water. In. Handbook of optics. Vol. I. 2nd Ed. M Bass, Ed., MacGraw-Hill. New York, USA. 43.3-43.56 pp.

Montres-Hugo M A, Vernet M, Smith R. Carders K. 2008. Phytoplankton Size-Structure on the Western Shelf of the Antarctic Peninsula: A Remote Sensing Approach. International journal of remote sensing, 29(3-4), 801-829.

Moore C M, Lucas M I, Sanders R and Davidson R. 2005. Basin-scale variability of phytoplankton bio-optical characteristics in relation to bloom state and community structure in the Northeast Atlantic. Deep-Sea Research I, 52, 401-419.

Morel A .1991. Light and marine photosynthesis: A spectral model with geo-chemical and climatological implications. Progress in Oceanography, 26, 263– 306.

Morel A, Ahn Y H. 1990. Optical efficiency factors of free living marine bacteria: Influence of bacterioplankton upon the optical properties and particulate organic carbon in oceanic water. Journal of Marine Research, 48: 145-175.

Morel A, and Prieur L. 1977. Analysis of variations in ocean color. Limnology and Oceanography, 22: 709-720.

Morel A, Claustre H, Antoine D, Gentili B. 2007. Natural variability of bio-optical properties in Case 1 waters: attenuation and reflectance within the visible and near-UV spectral domains, as observed in South Pacific and Mediterranean waters. Biogeosciences Discussions, 4, 2147 – 2178.

Morel A. 1997. Consequences of a Synechococcus bloom upon the optical properties of oceanic (case 1) waters. Limnology and Oceanography, 42, 1746–1754.

Nair S S, Devassy V P, Madhupratap M. 1992. Blooms of phytoplankton along the west coast of India associated with nutrient enrichment and the response of zooplankton. Science of the Total Environment, 26, 819–828.

Neukermans, G., Reynolds, R.A. and Stramski, D., 2014. Contrasting inherent optical properties and particle characteristics between an under-ice phytoplankton bloom and open water in the Chukchi Sea. Deep Sea Research Part II: Topical Studies in Oceanography, 105, pp.59-73.

O'Reilly J E, Maritorena S, Siegel D, O'Brien M C, Toole D, Mitchell B G, et al. 2000. Ocean color chlorophyll a algorithms for SeaWiFS, OC2, and OC4: Version 4. In S. B. Hooker, & E. R. Firestone (Eds.), SeaWiFS postlaunch technical report series. SeaWiFS post- launch calibration and validation analyses, Part 3, vol. 11, NASA/GSFC, 9–23 pp.

Ong, L.J., Glazer, A.N. and Waterbury, J.B., 1984. An unusual phycoerythrin from a marine cyanobacterium. Science, 224, pp.80-84.

O'Reilly J E, Maritorena S, Mitchell B G, Siegel D A, Carder K L, Garver S A, Kahru M, and McClain C R. 1998. Ocean colour chlorophyll algorithms for SeaWiFS: Journal of Geophysical Research, 103, 24937-24953.

Ouillon S, and Petrenko A . 2005. Above-water measurements of reflectance and chlorophyll-a algorithms in the Gulf of Lions, NW Mediterranean Sea. Optics Express, 13: 2531–2548.

Pierson D C, and Strombeck N. 2000. A Modelling approach to evaluate preliminary remote sensing algorithms: Use of water quality data from Swedish Great Lakes. Geophysica, 36: 177–202.

Pierson, D.C. and Strömbeck, N., 2001. Estimation of radiance reflectance and the concentrations of optically active substances in Lake Mälaren, Sweden, based on direct and inverse solutions of a simple model. Science of the total environment, 268(1), pp.171-188.

Prézelin, B.B. and Alberte, R.S., 1978. Photosynthetic characteristics and organization of chlorophyll in marine dinoflagellates. Proceedings of the National Academy of Sciences, 75(4), pp.1801-1804.

Prezelin, B.B. and Boczar, B.A., 1986. Molecular bases of phytoplankton spectral properties, and their potential applications to studies in optical oceanography. Progress in Phycological Research.(F. Round and D. Chapman, eds.) pp, pp.349-464.

Pulliainen J, Kallio K, Eloheimo S, Koponen H, Servomaa T, Hannonen S, et al. 2001. A semioperative approach to lake water quality retrieval from remote sensing data. The Science of the Total Environment, 268, 79−93.

Ralf Goericke, D.J.R., 1993. Chlorophylls a and b and divinyl chlorophylls a and b in the open subtropical North Atlantic Ocean. Marine Ecology Progress Series, 101, pp.307-313.

Sathyendranath S, Hoge F E, Platt T, and Swift R N. 1994. Detection of phytoplankton pigments from ocean color: Improved algorithms, Applied Optics, 33, 1081–1089.

Sauer, M.J. and Roesler, C.S., 2013. Unraveling phytoplankton optical variability in the Gulf of Maine during the spring and fall transition period. Continental Shelf Research, 61, pp.125-136.

Savitzky A, Golay M J E. 1964. Smoothing and differentiation of data by simplified least squares procedures. Journal of Analytical Chemistry, 36: 1627 – 1639.

Siegal D A, Maritorena S, Nelson N B, Hansel, D A, Lorenzi-Kayser M. 2002. Global distribution and synamics of colored dissolved and detrital organic materials. Journal of Geophysical Research, 107, 3228.

Srinivas K, Revichandran C, Maheswaran P A, Ashraf M TT, Murukesh N. 2003. Propagation of tides in the Cochin estuarine system South west coast of India. Indian Journal of Marine Sciences, 32(1), 14-24.

Stramski D, Bricaud A, Morel A. 2001. Modeling the inherent optical properties of the ocean based on the detailed composition of the planktonic community. Applied Optics, 40, 2929-2945.

Stuart V, Sathyendranath S, Platt T, Maass H, Irwin B. 1998. Pigments and species composition of natural phytoplankton populations: effect on the absorption spectra. Journal of Plankton Research, 20, 187–217.

Subramaniam A, Carpenter E J. 1994. An empirically derived protocol for the detection of blooms of the marine cyanobacterium Trichodesmium using CZCS imagery. International journal of remote sensing, 15, 1559–1569.

Thomas J V, Premlal P, Sreedevi C, Kurup M B. 2004. Immediate effect of bottom trawling on the physicochemical parameters in the inshore waters (Cochin-Munambum) of Kerala. Indian Journal of Fisheries, 51(3), 277-286.

Tzortziou M, Subramaniam A, Herman J R, Gallegos C L, Neale P J, Harding Jr., L W. 2007. Remote sensing reflectance and inherent optical properties in the mid Chesapeake Bay. Estuarine, Coastal and Shelf Science, 72,16–32.

Uitz J, Stramski D, Reynolds R A, Dubranna J. 2015. Assessing phytoplankton community composition from hyperspectral measurements of phytoplankton absorption coefficient and remotesensing reflectance in open ocean environments. Remote Sensing of Environment, 171, 58–74.

Varunan T and shanmugam P. 2015. A model for estimating size fractionated phytoplankton absorption coefficients in coastal and oceanic waters from satellite data . Remote sensing of environment, 158, 235-254.

Whitmire, A.L., Pegau, W.S., Karp-Boss, L., Boss, E. and Cowles, T.J., 2010. Spectral backscattering properties of marine phytoplankton cultures. Optics Express, 18(14), pp.15073-15093.

Yentsch C S and Phinney D A. 1989. A bridge between ocean optics and microbial ecology. Limnology and Oceanography, 34, 1694-1705.

Chapter 5

You can't cross the sea merely by standing and staring at the water
-Rabindranatha Tagore

5. Performance of Operational Empirical Algorithms

5.1. Introduction

Validation of Chl algorithms have been widely done in Arabian Sea(AS). The phytoplankton distribution in the Arabian Sea (AS) using IRS-P4 OCM (Indian Remote Sensing Satellite- P4 Ocean Colour Monitor) data exhibited relatively low Chla concentration in the southern part compared to northern part of the Sea. The retrieval of Chla using sea-leaving radiance from Modular Optoelectronics Scanner (MOS-B) showed failure of single ratio of Coastal Zone Colour Scanner (CZCS) algorithm in AS (Sathe and Jadhav 2001). They also reported that the two factor algorithm of SeaWIFS fails in 30% of the cases. Further, Nagamani et al., (2008) reported that OC4v4 algorithm overestimates Chla in northern AS when compared to Maximum Band Ratio (MBR) based OCM-2 algorithm. In addition to these Chauhan et al., (2002) evaluated the accuracy, precision and suitability of different ocean colour algorithms for AS. According to his study OC2 and OC4 algorithms performed well in Case 1 waters of AS. But both algorithms failed to estimate Chl in *Trichodesmium* dominated waters. Tilstone et al., (2011) also assessed three algorithms, OC4v6, Carder and OC5, for retrieving Chla in coastal areas of the Bay of Bengal and open ocean areas of the AS. Based on the accuracy of assessment, they recommended the use of OC5 algorithm in the area of study.

The development of Ocean chlorophyll 2-band (OC2) and ocean chlorophyll 4-band (OC4) algorithms was done using SeaBAM data set. The OC2 algorithm was revised (OC2 v2) based on an extensive data set of

1,174 in-situ observations and thereafter with the SIMBIOS data set (McClain and Fargion 1999). O'Reilly et al., (2000) updated OC2 and OC4 with 2,853 insitudata sets (OC2v2 and OC4v4) and suggested the need to determine accuracy of these revised algorithms in lowest Chl concentrations.

The distributions of CDOM and DOC in coastal waters of south China were studied by Chen et al., (2004) and research on the absorption of CDOM fluorescence in the Pearl River estuary were done by Hong et al., (2005). According to them, the regionality and complexity of Case 2 waters ruled out employing universally applicable model. The retrieval of Chla based on phytoplankton abundance failed in the turbid coastal waters and enclosed marine basins which are mainly influenced by suspended particles and CDOM of terrigenous origin. (Gordon et al., 1980, 1983; Smith and Baker 1982; Kowalzuk et al., 2005). CDOM absorption, as a major variable in remote sensing algorithms, was included during evaluation of data from the CZCS mission. The relationship between CDOM, phytoplankton pigments and suspended detrital particles were established from the model simulations but failed to quantify these optical substances which is necessary for model evaluation, testing and optimization (Prieur and Sathyendranath 1981; Sathyendranath et al., 1989; Carder et al., 1991; Tassan 1994). The spatial and temporal distribution of a_{CDOM} (440) in Mandovi and Zuari estuaries, carried out using OCM after applying an algorithm developed for the site, exhibited a good correlation between satellite derived CDOM and insitu data (Menon et al., 2011). The effect of CDOM concentration can prevail up to 650 nm of the optical spectrum of electromagnetic radiation, if it exists in high concentration (Menon et al., 2005).

Table 5.1. Table showing the Characteristics of Sensors with their respective algorithms

	Ocean Colour Monitor	**MODIS-AQUA**	**SeaWIFS**	**OCTS**	**CZCS**	**MERIS**
	OCM 2	OC3M-547	OC4	OC4O	OC3C	OC4E
Agency	ISRO (India)	NASA (USA)	NASA (USA)	NASDA (Japan)	NASA (USA)	ESA (Europe)
Satellite	Oceansat-2 (India)	Aqua (EOS-PM1)	OrbView-2 (USA)	ADEOS (Japan)	Nimbus-7 (USA)	Envisat-1 (Europe)
Launch Date	23/09/2009	04/05/02	01/08/97	17/08/96 - 01/07/97	24/10/78 - 22/06/86	01/03/02
Swath (Km)	1420	2330	2806	1400	1556	1150
Resolution (M)	1-4 km	1000	1100	700	825	300/1200
# Of Bands	8	36	8	12	6	15
Spectral Covrage (Nm)	400 - 900	405-14385	402-885	402-12500	433-12500	412-1050

(Source IOCCG Report No. 1)

Numerous bio-optical algorithms have been developed to retrieve CDOM absorption or closely related products from ocean colour satellite observations including SeaWiFS, MODIS and MERIS. These algorithms determines the a_{CDOM} and detrital (non-pigmented) particles as a single parameter (a_{dg}), since CDOM and detritus have similar spectral responses in the visible spectrum (Bricaud et al 2012; Carder et al 1999; Doerffer and Schiller 2007; Hoge et al 2001; Lee et al 2010; Lee et al 2002; Maritorena et al 2002; Siegel et al 2005; Siegel et al 2005; Tilstone et al., 2012; Werdell et al., 2013).The empirical algorithms presently used for retrieving SeaWIFS and MODIS data based on ratios of algorithms aims at simultaneous retrieval of several inherent optical properties. The maximal absorption by yellow substance (CDOM) (at 400 nm) and by algae (at ~440 nm) are found within the violet-blue region (Morel 1980) of the visible spectrum. It is found that the slopes in the 400 to 440 nm domain of the absorption spectra by CDOM decreases and by that of phytoplankton increases. This information can be used to discriminate a_{CDOM} and a_{ph} (Morel and Gentili 2009). An algorithm has been developed for the MODIS, which uses both the 412 and the 443 nm band to derive the absorption due to CDOM (Carder et al., 1999). This algorithm takes advantage of the fact that CDOM absorbs more strongly at 412 than at 443 nm, while phytoplankton absorbs more strongly at 443 than at 412 nm. In Case 1 waters, retrieval of a_{dg} using inversion algorithms yields reasonable

results (Siegel, Maritorena, Nelson, Behrenfeld, & McClain 2005; Siegel et al., 2002), but in coastal waters it fails due to high levels of CDOM, coloured detrital particles, and phytoplankton (Aurin & Dierssen 2012). Remote sensing algorithms for estimating CDOM in coastal waters by linking the CDOM absorption with apparent optical properties have been initiated by Kowalczuk et al., (2003). The spatial and temporal variability of CDOM in the California Current has been studied by applying SeaWIFS imagery (Kahru and Mitchell 1999, 2001). A quantitative understanding of autochthonous production or removal of CDOM allows us to better identify occasions where (Kowalczuk et al., 2006) suitable algorithms can be used for its retrieval from space. Regionally tuned Tassan's or Carder's a_g440 algorithm retrieved a_g440 with uncertainties as high as 35% when applied in the Yellow and East China Sea (Siswanto et al., 2011). Tehrani et al., (2013) developed seasonal band ratio empirical algorithms to estimate DOC using the relationships between CDOM and R_{rs} and seasonal CDOM and DOC for SeaWiFS, MODIS and MERIS. Results revealed accurate estimation of DOC during summer time and underestimation during spring-winter time by both MODIS and MERIS.

A study performed with R_{rs}'s of HICO at estuaries of the river Indus and GBM of North Indian Ocean suggested the need for ocean colour sensors with central wavelength's of 426, 484, 490, 581 and 610 nm to estimate the concentrations of Chla, Suspended Sediments and CDOM in case-2 waters (Rao et al., 2016). Only a few algorithms have undergone rigorous validation involving direct comparison of field measurements with coincident satellite data. The primary limitation to rigorous validation is the

lack of sufficient data of coincident field measurements and satellite observations that are independent from the data used to develop the algorithm. Hence a study was carried to understand the dynamics of CDOM and the performance of MODIS $a_{dg}443$ retrieval algorithm in the coastal waters off Cochin, SEAS.

5.2. Materials and Methods

5.2.1. Chlorophyll Algorithms

Six operational empirical algorithms (OC3C, OC4O, OC4, OC4E, OC3M, OC4O2) were selected for this study. The data used for the study were between April 2009 and 2011. The algorithms selected have been operationally implemented as default algorithms for Coastal Zone Colour Scanner (CZCS), Ocean Colour and Temperature Scanner (OCTS), Sea-viewing Wide Field-of-view Sensor (SeaWiFS), Medium Resolution Imaging Spectrometer (MERIS), Moderate Resolution Imaging Spectroradiometer (MODIS) and Ocean Colour Monitor (OCM2). The characteristics of sensors with their respective algorithms are shown in Table 5.1 and the functional forms of these algorithms are given in Table 5.2**.**

The algorithms designed for ocean colour sensors such as Coastal Zone Colour Scanner (CZCS), Ocean Colour and Temperature Scanner (OCTS), Medium Resolution Imaging Spectrometer (MERIS), Sea-viewing Wide Field-of-view Sensor (SeaWiFS) and Moderate Resolution Imaging Spectroradiometer (MODIS) have undergone several revisions based on the insitu data generated from different water types.

The OC2 algorithm, designed for CZCS, has undergone eight versions (OC2a, OC2b, OC2c, OC2d, OC2e, OC2, OC2v2 and OC2v4). OC2a algorithm was a modified cubic polynomial using R_{rs} at 412 and 555nm. OC2b uses R_{rs} at 443nm instead of 412 nm in OC2a. OC2c uses $R_{rs}520$ and OC2d $R_{rs}510$ instead of $R_{rs}412$ in the original algorithm. These algorithms were very sensitive and produced unrealistically high Chl estimates in cases of high gelbstoff, detrital and accessory pigment absorption, hence in 1998, NASA announced a revised version of OC2 algorithm(OC2v2), which eliminated overestimation at high concentrations of Chl (O'Reilley et al.,1998). OC2v2, a modified cubic polynomial uses band ratio of $R_{rs}490$ and $R_{rs}555$ but it highlighted the underestimation in the intermediate Chl range (Kahru and Mitchell 1998). The OC2v2 algorithm is similar to OC2 except for the value of coefficients. OC2v4 algorithm operates with five coefficients and has a modified cubic polynomial form and it differswith only the value of coefficients of OC2v2. The latest of which is OC3C which has a modified cubic polynomial form.

The OC4O algorithm, designed for OCTS (Ocean Chlorophyll 4-Band OCTS) is a 4^{th}-order polynomial function relating the maximum of three band ratios and has version 4 (O'Reilly et al., 2000). The OC4O algorithm uses band ratio of $R_{rs}443$,490 and 520 with R_{rs} 565.

The OC4E algorithm, designed for MERIS uses $R_{rs}443$, $R_{rs}443$, 490 and 510 and 565.All the bands are as same as OC4 algorithm except in the reference wavelength (In OC4 R_{rs} 555 is used).OC4E algorithm is the tuned version of OC4v4 (O'Reilly et al. 2000).

The OC4 algorithm, designed for SeaWiFS has two versions (OC4 and OC4v4). The first version of OC4 (O'Reilly et al. 1998) was a modified cubic polynomial (i.e., a third order polynomial plus an extra coefficient) with 4 bands of R_{rs} spectra and the current version of OC4 uses a fourth order polynomial with five coefficients(O'Reilley et al., 2000, Maritorena and O'Reilley 2000).

The OC3 algorithm, designed for MODIS had undergone two versions (OC3d, and OC3e). OC3 algorithm incorporates 443 nm and 488 nm bands. OC3M also uses a fourth order polynomial function.

The default algorithm for OCM-2 is third order modified cubic polynomial which used the maximum ratio of four bands (Nagamani et al., 2008).

5.2.2. CDOM Algorithm

CDOM algorithm used in MODIS aqua sensor was used for validation. MODIS-Aqua Level-2 (L2) data over the study areas were acquired from https://oceancolor.gsfc.nasa.gov/cgi/browse.pl?sen=am, official website of Ocean Colour NASA. L2- IOP files were downloaded and data were processed using SeaDAS software. MODIS-A uses six R_{rs} bands (412, 443, 488, 531, 547 and 667 nm) for CDOM retrieval, with a spatial resolution of 1.1 km and the data were acquired on the same dates of the field measurements from 2010–2015 (temporal window between satellite overpass and the time of field sampling = ±12 h). The algorithm, developed by Carder et al., (1999), used in MODIS retrieves the absorption coefficients of the sum (a_{dg} m^{-1}) of CDOM (a_g m^{-1}) and detritus (a_d m^{-1}),

collectively named as CDM. This algorithm does not separate a_{dg} into a_g and a_d analytically and hence for this study the combined effect of a_{dg} is used.

The functional form of algorithm used to retrieve a_{dg} (443) in MODIS is an empirical power function based on the ratio of R_{rs}.

$$a_{dg}(443) = 10^{(0.043 - 0.185a0 - 1.081a1 + 1.234a2)}$$

where $a0 = \frac{R_{rs}(443)}{R_{rs}(551)}$, $a1 = \frac{R_{rs}(488)}{R_{rs}(551)}$ and $a2 = \frac{R_{rs}(667)}{R_{rs}(551)}$.

5.3. Results and Discussion

5.3.1. Validation of Chlorophyll Algorithms

The scatter plot showing relation between insitu measured Chla and that derived using OC4, OC3C, OC4O, OC4E, OC3M and OC4O2 algorithm is given as Fig 5.1. The validation statistics has been computed using data from all water types. The corresponding statistical indicators are given in Table 5.3. The R^2 was better in case of OC4 (0.70), which was also comparable with that of OC3M (0.68). Further OC4 and OC3M showed least Log_{10}- Root Mean Square Error (Log_{10}-RMSE=0.37). However, Absolute Percentage Difference (APD) (35.9%) was better in case of OC4 whereas OC3M showed better slope (0.69), Relative percentage difference (RPD) was (4.8%) and Unbiased percentage difference (UPD) was (17.1%). The intercept (i=0.07) was least in the case of OC4O and regression coefficient, 'r' was closer to unity in case of OC4O2.

The inverse transform ratios also showed that OC3M performs better at the median scale with F_{med} close to unity. The overall statistical analysis

showed that OC3M and OC4 produced comparable results having least significant difference between estimated and measured Chla.

Table 5.2.: Table showing the functional forms of the algorithms used to generate Chla from Coastal Zone Colour Scanner (CZCS), Ocean Colour and Temperature Scanner (OCTS), Sea-viewing Wide Field-of-view Sensor (SeaWiFS), Medium Resolution Imaging Spectrometer (MERIS), Moderate Resolution Imaging Spectroradiometer (MODIS) and Ocean Colour Monitor 2 (OC4O2).

Algorithm	**EQUATION**	**Model Type**
OC2M	$\mathrm{R} = \log_{10}\left(\frac{Rrs488}{Rrs547}\right)$ $a = [0.25, -2.4752, 1.4061, -2.8237, 0.5405]$ $C = 10^{(a_0+a_1R+a_2R^2+a_3R^3)} + a4$	Modified Cubic Polynomial
OCM2 MBR	$R = \log_{10}\{\max\left[\left(\frac{Rrs443}{Rrs555}\right), \left(\frac{Rrs490}{Rrs555}\right), \left(\frac{Rrs510}{Rrs555}\right)\right]\}$ $a = [0.475, -3.029, 2.240, -1.253, -0.027]$ $C = 10^{(a_0+a_1R+a_2R^2+a_3R^3)} + a4$	Modified Cubic Polynomial
OC3M MBR	$R = \log_{10}\left\{\max\left[\left(\frac{RRs443}{RRs547}\right)\left(\frac{Rrs488}{Rrs547}\right)\right]\right\}$ $a = [0.2424, -2.7423, 1.8017, 0.0015, -1.228]$ $C = 10^{(a_0+a_1R+a_2R^2+a_3R^3+a_4R^4)}$	Fourth Order Polynomial
OC4 MBR	$R = \log_{10}\{\max\left[\left(\frac{Rrs443}{Rrs555}\right), \left(\frac{Rrs489}{Rrs555}\right), \left(\frac{Rrs510}{Rrs555}\right)\right]\}$ $a = [0.3272, -2.9940, 2.7218, -1.2259, -0.5683]$ $C = 10^{(a_0+a_1R+a_2R^2+a_4R^4)}$	4th Order Polynomial
OC4O MBR	$R = \log_{10}\{\max[(\frac{Rrs443}{Rrs565}), \left(\frac{Rrs490}{Rrs565}\right), (\frac{Rrs520}{Rrs565})]\}$ $a = [0.3325, -2.8275, 3.0939, -2.0917, -0.0257]$ $C = 10^{(a_0+a_1R+a_2R^2+a_3R^3+a_4R^4)}$	4th Order Polynomial
OC3C MBR	$R = \log_{10}\{\max[\left(\frac{Rrs443}{Rrs550}\right), \left(\frac{Rrs520}{Rrs550}\right)]\}$ $a = [0.330, -4.377, 7.6267, -7.1457, 1.6673]$ $C = 10^{(a_0+a_1R+a_2R^2+a_3R^3+a_4R^4)}$	4th Order Polynomial
OC4E MBR	$R = \log_{10}\{[(\frac{Rrs443}{Rrs560}), \left(\frac{Rrs490}{Rrs560}\right), (\frac{Rrs510}{Rrs560})]\}$ $a = [0.3255, -2.7677, 2.4409, -1.1288, -0.4990]$ $C = 10^{a_{0+}a_1R+a_2R^2+a_3R^3+a_4R^4}$	4th Order Polynomial

Although the validation has been carried out for the entire data set, the accuracy of the algorithms was also evaluated in the different water types. The assessment of measured and estimated Chla in type-1 waters (Details in Chapter 4) showed a good agreement with a coefficient of determination (R^2) of 0.93 in the case of OC4O, OC4, OC4E and OC3M and 0.89 in the case of OC3C. The Chla estimated using OC4O2 algorithm showed relatively lower correlation (R^2=0.74). However, the measured Chla was lower in magnitude than the estimated Chla, having a slope of 1.06, 0.60, 0.68, 0.67, 0.71 and 0.68 for OC3C, OC4O, OC4, OC4E, OC3M and OC4O2 respectively.

The result based on the statistical analysis indicated that OC3M performs better than other algorithm in Type-I waters. In Type-II waters, it was observed that a cluster of points having Chla concentration between 9.0 to 13 mg-m^{-3} had a poor relation between estimated and measured Chla. At these points, β_{650} was tenfold higher than that in Type-I waters. In addition, the CDOM was higher than the average value (2.1 to 2.5 ppb Quinine Sulphate Dihydrate Equivalents, QSDE). In the absence of this cluster, the estimated and measured Chla had moderate agreement in case of OC3C (R^2=0.52), OC4 (R^2=0.67), OC4E (R^2=0.67), OC3M (R^2=0.67) and OC4O2 (R^2=0.67). In this water type estimated Chla was lower in magnitude than the measured with a slope of 0.59, 0.50, 0.63, 0.63, 0.90 and 0.88 for OC3C, OC4O, OC4, OC4E, OC3M and OC4O2 respectively. Based on the statistical analysis comparable result was seen between OC3M and OC4O2. The performance of both these algorithms was better than other algorithm in Type-II waters. In Type-III waters estimated Chlawas found to be higher in

magnitude as compared to measured Chla. The slope of regression was 1.46, 1.45, 1.39, 1.65, 1.44 and 1.84 for OC3C, OC4O, OC4, OC4E, OC3M and OC4O2 respectively. Although the estimated and measured Chlawas found to be variable in magnitude, the trend was in good agreement. The R^2 was 0.68, 0.63, 0.69, 0.66, 0.70 and 0.70 for OC3C, OC4O, OC4, OC4E, OC3M and OC4O2 respectively. The result based on the statistical analysis, in Type-III waters, indicated that OC3M and OC4 performs better.

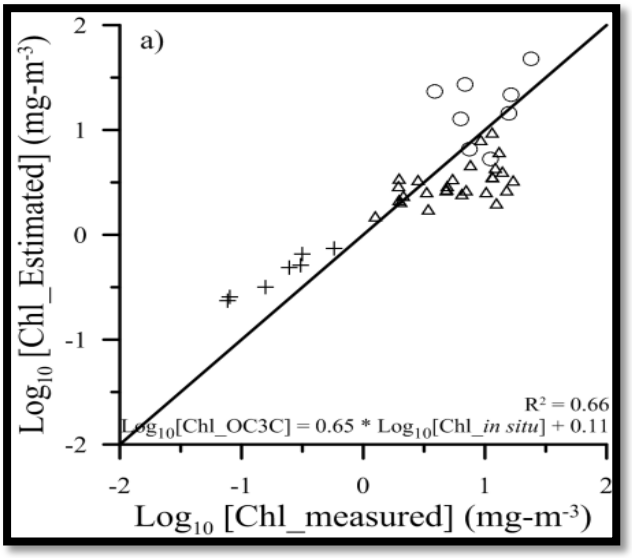

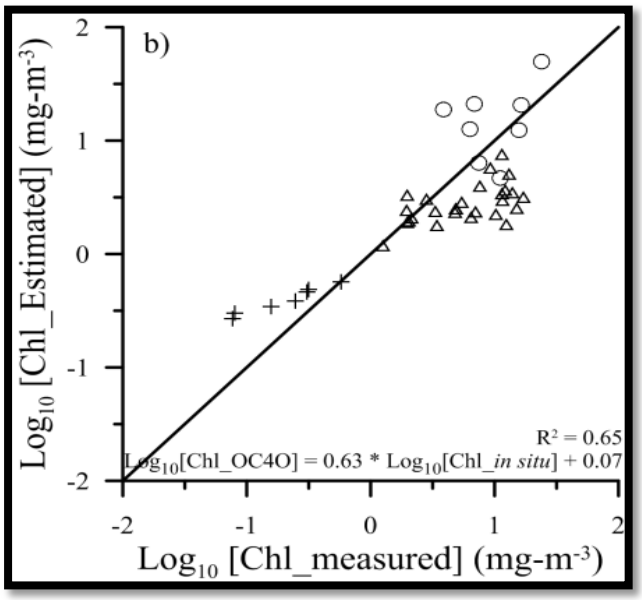

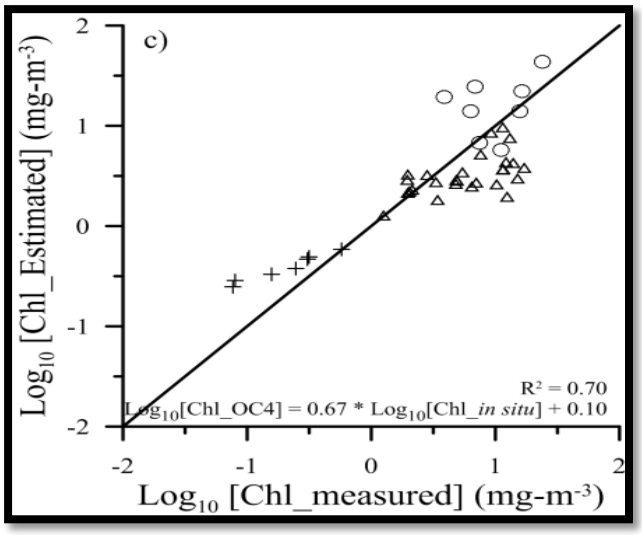
c)
Log10 [Chl_Estimated] (mg-m-3)
Log10 [Chl_measured] (mg-m-3)
R² = 0.70
Log10[Chl_OC4] = 0.67 * Log10[Chl_in situ] + 0.10

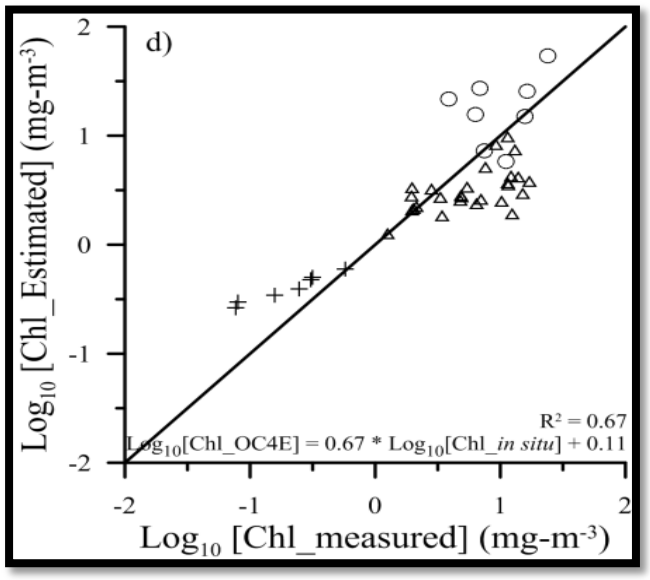
d)
Log10 [Chl_Estimated] (mg-m-3)
Log10 [Chl_measured] (mg-m-3)
R² = 0.67
Log10[Chl_OC4E] = 0.67 * Log10[Chl_in situ] + 0.11

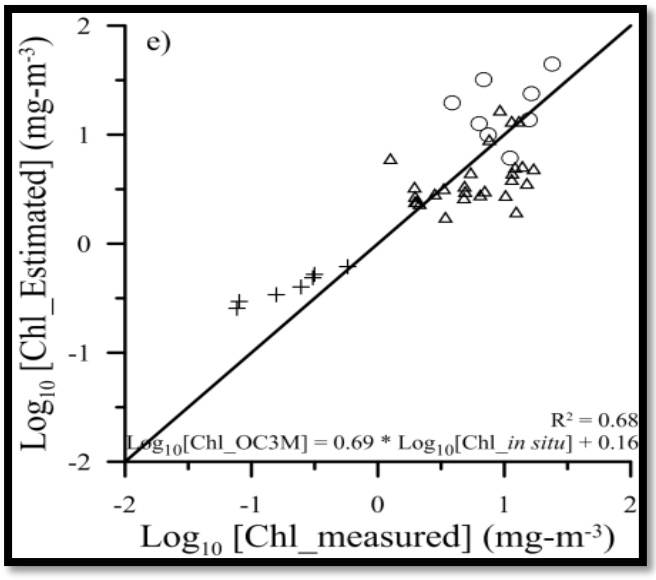
e)
Log10 [Chl_Estimated] (mg-m-3)
Log10 [Chl_measured] (mg-m-3)
R² = 0.68
Log10[Chl_OC3M] = 0.69 * Log10[Chl_in situ] + 0.16

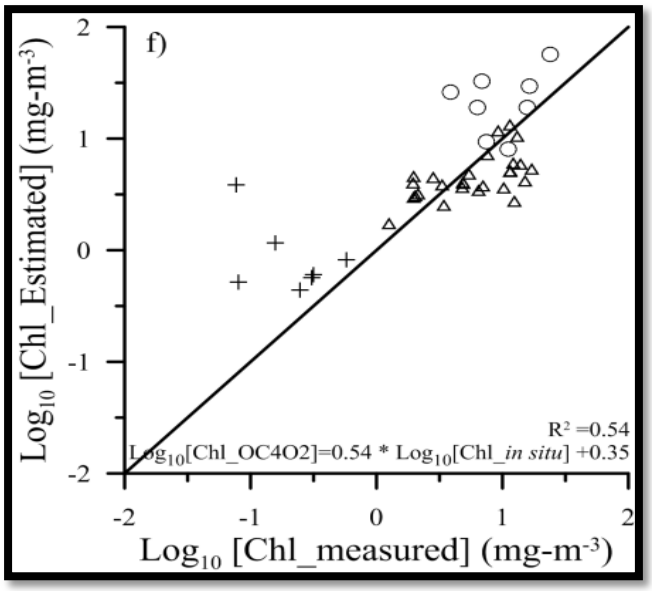

Figure. 5.1.Correlation between insitu Chla and that derived using OC4, OC3C, OC4O, OC4E, OC3M and OC4O2 algorithms in Type-I (plus), II (triangle) and III (circle) waters. The solid line indicate the trend and the dottedlinecorrespondsto1:1.

Among all the algorithms OC3M and OC4 performed better in the study area. In general all algorithms showed that, in Type-I waters, the measured Chla was less than that of estimated Chl. These waters were having typical case-1 characteristics. Also, the R_{rs} signals were dominated in 443 nm band(Chapter 4. Fig.4.4). In Type-II waters cluster of points was found to be weakly correlated. Further in Type-II waters the dominant signal in R_{rs} was from blue-green band.

In the case of OC4, OC4E and OC4O2 the dominant R_{rs} signal was from 510 nm whereas it was 520 nm in the case of OC3C and OC4O. For OC3M R_{rs} signal was dominated by the 488 nm band. Similar conditions were observed in Type-III waters. The performance of all the algorithms were poor in Type-II waters where as it was comparatively better in Type-III waters. Although the Type-II and Type-III waters were having Chla and

Table 5.3. : Performance indices for relative errors between insitu measured and estimated Chla from insitu R_{rs} using OC3C, OC4O, OC4, OC4E, OC3M and OC4O2 algorithms. These indices include correlation coeffcient (R^2), slope (s), intercept (I), summation of ratio of measured to estimated (r), root mean squared error (RMSE), absolute percentage difference (APD), relative percentage difference (RPD) and unbiased percentage difference (UPD). The geometric mean and one-sigma range of the ratio (F =$Value_{alg}$/$Value_{meas}$) are given by Fmed, Fmin, and Fmax, respectively. The values closer to 1 are more accurate. Total 42 data points were used for the analysis.

Algorithm	R^2	S	I	r	RMSE	APD	RPD	UPD	Fmin	Fmed	Fmax
OC3C	0.66	0.65	0.11	1.74	0.39	41.0	17.2	29.8	0.50	1.21	2.94
OC4O	0.65	0.63	**0.07**	1.95	0.41	40.3	23.6	36.5	**0.56**	1.36	3.34
OC4	**0.70**	0.67	0.10	1.69	**0.37**	**35.9**	16.3	26.7	0.53	1.22	2.82
OC4E	0.67	0.67	0.10	1.70	0.38	37.2	16.6	27.7	0.50	1.20	2.88
OC3M	0.68	**0.69**	0.16	1.47	**0.37**	50.4	4.8	**17.1**	0.44	**1.04**	2.45
OC4O2	0.54	0.54	0.35	**1.21**	0.45	47.1	3.26	30.1	0.29	0.82	2.29

CDOM concentration tenfold higher than Type-I waters. The covariance between Chla and CDOM was significantly higher in Type-III waters.

Desa et al. (2001) showed that the ratio of R_{rs} at 490 to 555 nm is a better indicator of Chlain eastern AS. They illustrated significant improvement in R^2(0.93), slope (0.96) and intercept (0.26) by modifying SeaWiFS OC4v4 coefficients. HoweverShanmugam (2011) suggested that although OC3 reliably estimates Chlain open ocean waters, it tends to fails in the coastal waters of the AS. The Chlaand CDOM compete for absorption of light in almost similar wavelengths in the blue region. As a result the signal emerging out from the water column carries signature of both Chlaand CDOM. The empirical algorithms takes the ratio of blue to green band with an assumption that water leaving radiance decreases in blue band width increase in Chla concentration. However, if the water column is dominated by Chla and CDOM, both significantly contribute for decrease in water leaving radiance in blue band. In such a scenario the performance of ratio based algorithms weakens for retrieval of Chla. In the earlier studies Tzortziou et al. (2007) also reported that the failure of MODIS algorithm in inshore waters of Chesapeake Bay was due the large contribution by non co-varying CDOM and non-algal particles to total light absorption in the blue. The study concludes that OCM and OC4 algorithms can be used in retrieval of Chla in the area. The performance of these algorithms is better during eutrophic conditions, where waters are of Type-III. Further, the ratio R_{rs} 490 to R_{rs} 555 can be used in estimating Chl from R_{rs} data.

5.3.2. Validation of CDOM Algorithms

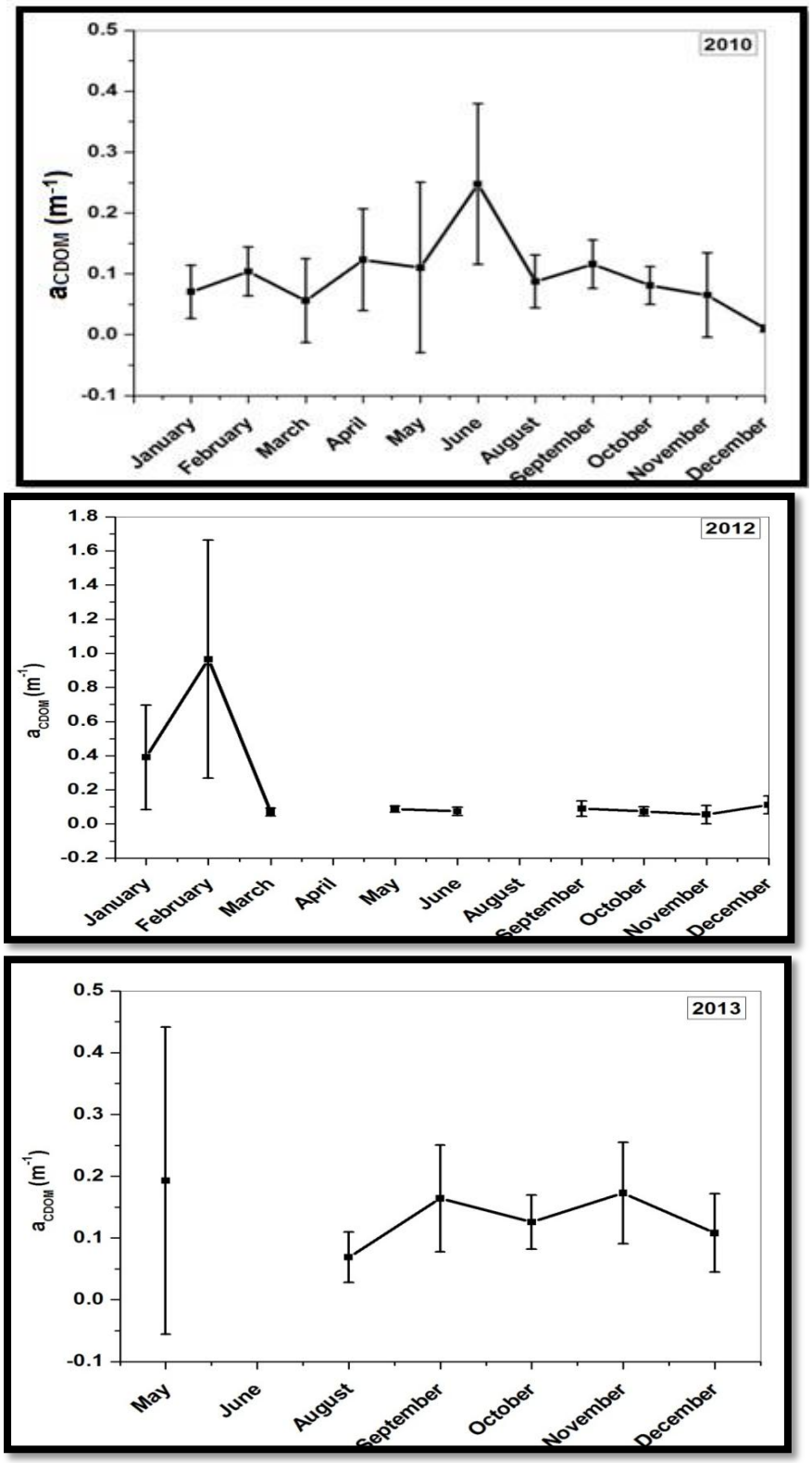

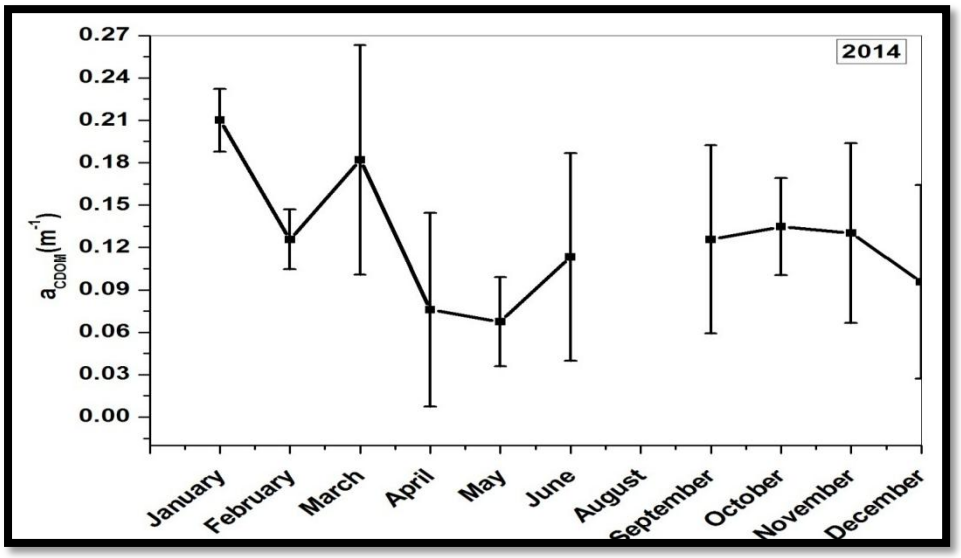

Figure 5.2. Monthly variation of Absorption by CDOM at 443nm during 2010, 2011, 2012, 2013 and 2014. X axis represents Months and Y axis represents coefficient of absorption by CDOM at 443nm.$a_{CDOM}(m^{-1})$

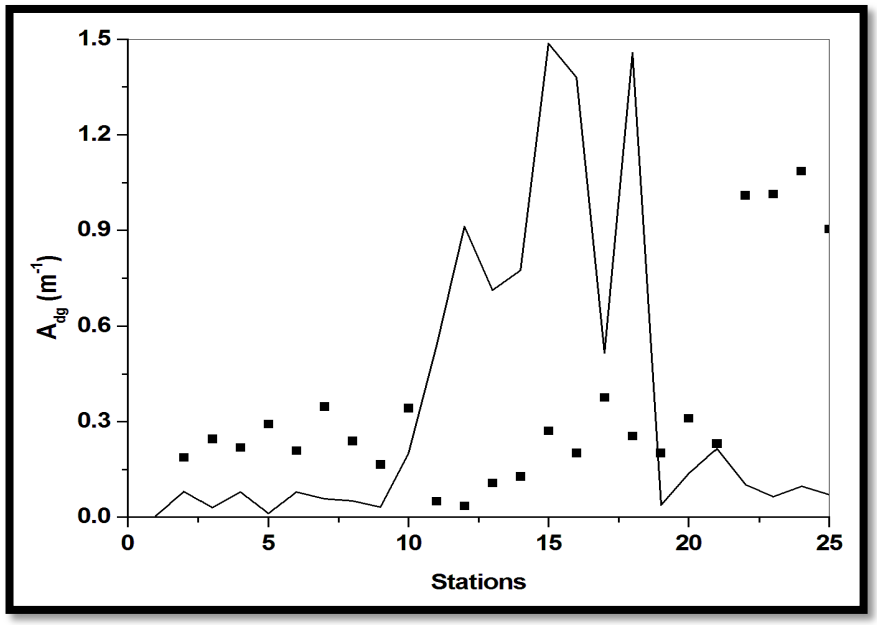

Figure 5.3. Matchup analysis between insitu (solid line) $a_{dg}(443)$ data and MODISA (symbols) data. In X axis stations are plotted and in Y axis a_{dg} (443) coefficients are plotted.

The monthly variation in a_{CDOM} (443) spanning 5 years were studied from 2010 to 2014 in the study area (Fig. 5.2). Monthly variations in the 2010 -2014 showed similar trends in monthly variation of absorption by CDOM at

443nm. The trend followed a zig-zag pattern with maximum during June in 2010 and 2011. After June, eventhough the pattern remained same, the absorption showed a decreasing trend. In 2012 February, the absorption was very high. 2014 also had high absorption values with maximum during January.

Matchup analysis between insitu measured absorption by detritus and gelbstoff at 443 nm ($a_{dg}443$) and a_g443_M from MODIS Aqua sensor were done (Figure 5.3.). All together 25 matchup data were obtained from MODISA during the period 2010 to 2014 December. Due to heavy cloud coverage satellite data over SEASare limited. The raw data exhibited a few matchups between insitu and satellite data. The insitu data ranged from 0.003 m^{-1} to 1.49 m^{-1} while satellite data ranged between 0.0344 m^{-1} and 1.0847 m^{-1}. In Stations 0 to 10 and 22-26, insitu data was over estimated by satellite data whereas Stations 11-19 underestimation of insitu data was observed. A few matchups were observed when the insitu data falls between 0.15 and 0.3 m^{-1}.

Since the matchup analysis didn't work for raw data, another correlation analysis was performed using insitu data and ratio of Chla and CDOM data obtained from satellite (Figure 5.4). The analysis exhibited a negative correlation between the two with R^2 0.484. To know the influence of seasons, the data corresponding to two seasons were analysed separately and correlation analyses were performed.

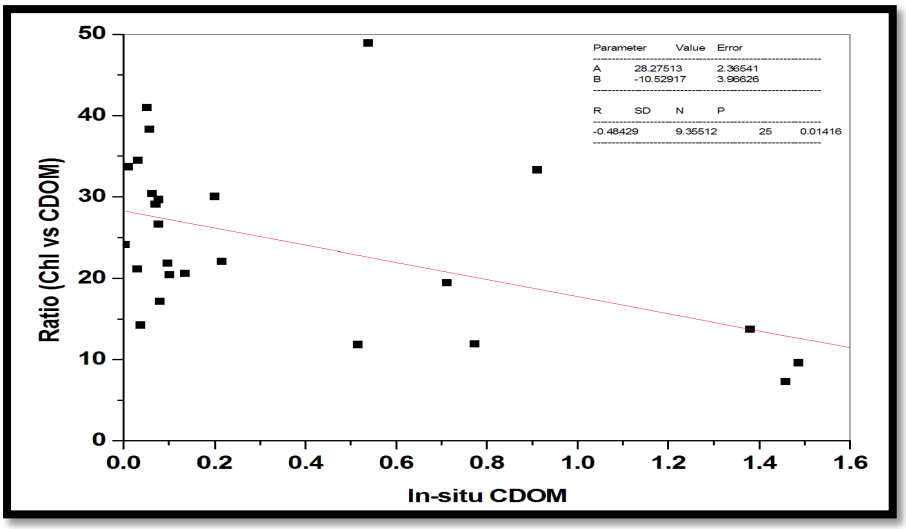

Figure 5.4. Matchup analysis between insitua$_{dg}$(443) data and ratio between MODISA Chl and CDOM.

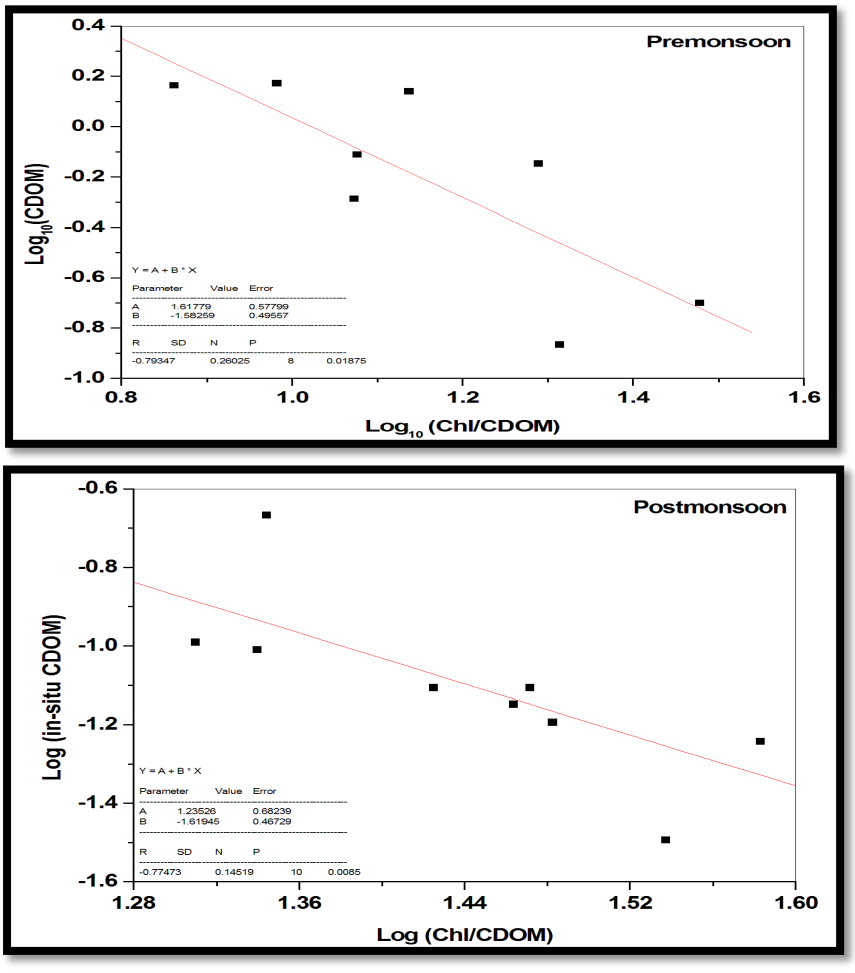

Figure 5.5. Matchup analysis between insitua$_{dg}$(443) data and ratio between MODISA Chla and CDOM during Premonsoon and Postmonsoon.

Premonsoon season exhibited a tuned algorithm as follows

$$Log_{10} (insitu\ CDOM) = 1.61779 - 1.58259 * Log_{10} (Chl/CDOM)$$

For post monsoon season, the algorithm was as follows

$$Log_{10} (insitu\ CDOM) = 1.23526 - 1.61945 * Log_{10} (Chl/CDOM)$$

Both data exhibited negative correlation. The R^2 value for premonsoon season and postmonsoon season were 0.79 and 0.77 respectively. The data points from satellite for both the seasons were low because of cloud coverage in the area.

The origin of CDOM in marine waters was mainly by the decomposition of biological activity and by terrestrial input such as river discharge. Hence, CDOM absorption may be related to phytoplankton biomass or salinity. However, $a_{dg}(443)$ in Cochin coastal waters did not correlate with Chla (Minu et al., 2014). During January and February (late postmonsoon and early premonsoon) occurs phytoplankton blooms along with preshowers of southwest monsoon. The high phytoplankton density results in increased decomposition of organic matter during the senescence of bloom. This results in high CDOM production. The peaks found during January and February coincides with the phytoplankton blooms.

MODIS aqua data was biased when the annual data were taken for correlation. Since the CDOM absorption showed monthly variations, the data when taken as a whole exhibited bias. This bias was reduced when the data were splitted to two seasons and when the ratio of Chl and CDOM were taken. It was expected that during monsoon and postmonsoon season the CDOM absorption should exceed Chl, however, the coastal waters off

Cochin are considered as eutrophic environment promoting phytoplankton production far more than organic matter production (Lathika et al 2013, Bhavya et al 2016).

The study concludes that algorithms for retrieving $a_{dg}(443)$ has to be season specific.

5.4. Conclusion

- The present study primarily focussed on the evaluation of six empirical algorithms (OC3C, OC4O, OC4, OC4E, OC3M and OC4O2), operationally used to retrieve Chla from CZCS, OCTS, SeaWiFS, MERIS, MODIS and OCM-2.
- The algorithms were applied to the spectral R_{rs} measured in situ using hyperspectral radiometer with an intention to assess the functional form and the coefficients.
- The overall statistical analysis showed that the performance of OC3M and OC4 was better as compared to other algorithms.
- Further in the case of Chlamore than 1.0 mg-m^{-3} it was found that the ratio of higher wavelength (488, 510 and 520 nm) dominates.
- The assessment of algorithms in different water types indicated better performance of all the algorithms in Type-I waters.
- The performance was poor in Type-II and Type-III waters. The errors associated with the estimation of Chlaco-varied with CDOM in Type-III waters.
- CDOM absorption algorithms need to be tuned for different seasons in the area. Therefore, in the regions where there is dominance of OAS

other than Chla, developing IOP based algorithm that takes into account of absorption and scattering due to individual OAS is required.

5.5. References

Aurin, D.A. and Dierssen, H.M., 2012. Advantages and limitations of ocean color remote sensing in CDOM-dominated, mineral-rich coastal and estuarine waters. Remote Sensing of Environment, 125, pp.181-197.

Bhavya P S, Kumar S, Gupta G V M, Sudheesh V, Sudharma K V, Varrier D S, Dhanya K R and Saravanane N. 2015. Nitrogen Uptake Dynamics in a Tropical Eutrophic Estuary (Cochin, India) and Adjacent Coastal Waters. Estuaries and Coasts, 1-14.

Bricaud, A., Ciotti, A.M. and Gentili, B., 2012. Spatial-temporal variations in phytoplankton size and colored detrital matter absorption at global and regional scales, as derived from twelve years of SeaWiFS data (1998–2009). Global Biogeochemical Cycles, 26(1).

Carder, K.L., Hawes, S.K., Baker, K.A., Smith, R.C., Steward, R.G. and Mitchell, B.G., 1991. Reflectance model for quantifying chlorophyll a in the presence of productivity degradation products. Journal of Geophysical Research: Oceans, 96(C11), pp.20599-20611.

Carder K L, Chen F R, Lee Z P and Hawes S K. 1999. Semi-analytic Moderate- Resolution Imaging Spectrometer algorithms for chlorophyll-a and absorption with bio-optical domains based on nitrate-depletion temperatures. Journal of Geophysical Research, 104, 5403–5421.

Chauhan P, Mohan M, Sarangi R K, Kumari B, Nayak S, Matondkar S G P. 2002. Surface chlorophyll estimation in the Arabian Sea using IRS-P4 OCM Ocean Color Monitor (OCM) satellite data. International Journal of Remote Sensing, 23(8): 1663–1676.

Chen Y L L, Chen H , Karl D M and Takahashi M. 2004. Nitrogen modulates phytoplankton growth in spring in the South China Sea. Continental Shelf Research, 24, 527–541.

Desa E S, Suresh T, Matondkar S G P, Desa E. 2001. Sea truth validation of sea WiFS ocean colour sensor in the coastal waters of the eastern Arabian Sea. Current Science, 80(7): 854-860.

Doerffer, R. and Schiller, H., 2007. The MERIS Case 2 water algorithm. International Journal of Remote Sensing, 28(3-4), pp.517-535.

Gordon H R, Clark D K, Brown J W, Brown O B, Evans R H, and Broenkow W W. 1983. Phytoplankton pigment concentrations in the Middle Atlantic Bight: comparison of ship determinations and CZCS estimates. Applied Optics, 22, 20–36.

Gordon H R, Clark D K, Muller J L and Hovis W A. 1980. Phytoplankton pigments derived from from Nimbus-7 CZCS: Initial comparisons with surface measurements, Science, 210:63-66.

Hoge, F.E., Wright, C.W., Lyon, P.E., Swift, R.N. and Yungel, J.K., 2001. Inherent optical properties imagery of the western North Atlantic Ocean: Horizontal spatial variability of the upper mixed layer. Journal of Geophysical Research: Oceans, 106(C12), pp.31129-31140.

Hong H S, Wu J Y and Shang S L. 2005. Absorption and fluorescence of Chromophoric dissolved organic matter in the Pearl River estuary, South China. Marine Chemistry, 97: 78-89.

IOCCG. 1998. Minimum requirements for an operational ocean-colour sensor for the open ocean. International Ocean Colour Coordinating Group, Dartmouth, Canada (Rep No. 1, IOCCG).

Kahru M and Mitchell B G. 1998. Spectral reflectance and absorption of a massive red tide off southern California. Journal of Geophysical Research, 103, 21601–21609.

Kahru, M. and Mitchell, B.G., 1999. Empirical chlorophyll algorithm and preliminary SeaWiFS validation for the California Current. International Journal of Remote Sensing, 20(17), pp.3423-3429.

Kahru, M. and Mitchell, B.G., 2001. Seasonal and nonseasonal variability of satellite-derived chlorophyll and colored dissolved organic matter concentration in the California Current. Journal of Geophysical Research: Oceans, 106(C2), pp.2517-2529.

Kowalczuk, P., Stedmon, C.A. and Markager, S., 2006. Modeling absorption by CDOM in the Baltic Sea from season, salinity and chlorophyll. Marine Chemistry, 101(1), pp.1-11.

Kowalczuk Piotr, Joanna Ston´-Egiert, William J. Cooper, Robert F. Whitehead, Michael J. Durako. 2005. Characterization of chromophoric dissolved organic matter (CDOM) in the Baltic Sea by excitation emission matrix fluorescence spectroscopy. Marine Chemistry, 96. 273-292.

Kowalczuk, P., Cooper, W.J., Whitehead, R.F., Durako, M.J. and Sheldon, W., 2003. Characterization of CDOM in an organic-rich river and surrounding coastal ocean in the South Atlantic Bight. Aquatic Sciences, 65(4), pp.384-401.

Lee, Z., Arnone, R., Hu, C., Werdell, P.J. and Lubac, B., 2010. Uncertainties of optical parameters and their propagations in an analytical ocean color inversion algorithm. Applied Optics, 49(3), pp.369-381.

Lee, Z., Carder, K.L. and Arnone, R.A., 2002. Deriving inherent optical properties from water color: a multiband quasi-analytical algorithm for optically deep waters. Applied optics, 41(27), pp.5755-5772.

Maritorena, S., Siegel, D.A. and Peterson, A.R., 2002. Optimization of a semianalytical ocean color model for global-scale applications. Applied Optics, 41(15), pp.2705-2714.

Maritorena S and O'Reilly J E. 2000. OC2v2: Update on the initial operational SeaWiFS chlorophyll-a algorithm, In J. E. O'Reilly & co-authors, (Eds.), SeaWiFSPostlaunch Calibration and Validation Analyses: Part 3. NASA Tech. Memo. 2000-206892, vol. 11.InS.B. Hooker & E. R. Firestone, NASA Goddard Space Flight Center, Greenbelt, Maryland, 3–8.

McClain M E and Fargion G S. 1999. Simbios project annual report. N.T. M. Greenbelt, MD: NASA, Goddard Space Flight Center.

Menon H B, Lotliker A A, Nayak S R. 2005. Pre-monsoon bio-optical properties in estuarine, coastal and Lakshadweep waters. Estuarine, Coastal and. Shelf Science, 63: 211-223.

Menon H B, Sangekar N P, Lotliker A A and Vethamony P. 2011. Dynamics of chromophoric dissolved organic matter in Mandovi and Zuari estuaries—A study through in situ and satellite data. ISPRS Journal of Photogrammetry and Remote Sensing, 66(4), 545-552.

Minu P, Lotliker A A, Shaju S S, SanthoshKumar B, Ashraf P M and Meenakumari B. 2014. Effect of optically active substances and atmospheric correction schemes on remote-sensing reflectance at a coastal site off Kochi. International Journal of Remote Sensing, 35(14), 5434-5447.

Morel A and Gentili B. 2009. A simple band ratio technique to quantify the colored dissolved and detrital organic material from ocean color remotely sensed data. Remote Sensing of Environment, 113 , 998–1011.

Morel A. 1980. In-water and remote measurements of ocean color. Boundary Layer Meteorology, 18, 177-201.

Nagamani P V, Chauhan P, Dwivedi R M. 2008. Development of Chlorophyll a Algorithm for Ocean Colour Monitor onboard OCEANSAT-2 Satellite. IEEE Geosciences and Remote Sensing Letters, 5(3): 527-531.

O'Reilly J E, Maritorena S, Siegel D, O'Brien M C, Toole D, Mitchell B G, et al. 2000. Ocean color chlorophyll a algorithms for SeaWiFS, OC2, and OC4: Version 4. In S. B. Hooker, & E. R. Firestone (Eds.), SeaWiFSpostlaunch technical report series. SeaWiFS post- launch calibration and validation analyses, Part 3, vol. 11, NASA/GSFC, 9–23 pp.

O'Reilly J E, Maritorena S, Mitchell B G, Siegel D A, Carder K L, Garver S A, Kahru M, and McClain C R. 1998. Ocean colour chlorophyll algorithms for SeaWiFS: Journal of Geophysical Research, 103:24937-24953.

Prieur L, Sathyendranath S. 1981. An optical classification of coastal and oceanic waters based on the specific spectral absorption curves of phytoplankton pigments, dissolved organic matter, and other particulate materials. Limnology and Oceanography, 26:671–689.

Rao, S., Ramarao, E.P. and Srinivas, K., 2016, May. Classification of case-II waters using hyperspectral (HICO) data over North Indian Ocean. In SPIE Asia-Pacific Remote Sensing (pp. 98780X-98780X). International Society for Optics and Photonics.

Sarangi R K, Chauhan P, Mohan M, Nayak S R and Navalgund R R. 2001. Phytoplankton distribution in the Arabian Sea using IRS-P4 OCM satellite data. International Journal of Remote Sensing, 22(15), 2863-2866.

Sathe P V, and Jadhav N. 2001. Retrieval of Chlorophyll from the Sea-Leaving Radiance in the Arabian Sea. Journal of the Indian Society of Remote Sensing, Vol. 29, No. 1&2.

Sathyendranath S, Stuart V, Nair A, Oka K, Nakane T, Bouman H, Forget M H. et al. 2009. Carbon-to-chlorophyll ratio and growth rate of phytoplankton in the sea. Marine Ecology Progress Series, 383: 73–84.

Sathyendranath, S., Prieur, L. and Morel, A., 1989. A three-component model of ocean colour and its application to remote sensing of phytoplankton pigments in coastal waters. International Journal of Remote Sensing, 10(8), pp.1373-1394.

Shanmugam P. 2011. A new bio-optical algorithm for the remote sensing of algal blooms in 682 complex ocean waters. Journal of Geophysical Research-Oceans, 116.

Siegel, D.A., Maritorena, S., Nelson, N.B. and Behrenfeld, M.J., 2005. Independence and interdependencies among global ocean color properties: Reassessing the bio-optical assumption. Journal of Geophysical Research: Oceans, 110(C7).

Siegel, D.A., Maritorena, S., Nelson, N.B., Behrenfeld, M.J. and McClain, C.R., 2005. Colored dissolved organic matter and its influence on the satellite-based characterization of the ocean biosphere. Geophysical Research Letters, 32(20).

Siegel, D.A., Maritorena, S., Nelson, N.B., Hansell, D.A. and Lorenzi-Kayser, M., 2002. Global distribution and dynamics of colored dissolved and detrital organic materials. Journal of Geophysical Research: Oceans, 107(C12).

Siswanto, E., Tang, J., Yamaguchi, H., Ahn, Y.H., Ishizaka, J., Yoo, S., Kim, S.W., Kiyomoto, Y., Yamada, K., Chiang, C. and Kawamura, H., 2011. Empirical ocean-color algorithms to retrieve chlorophyll-a, total suspended matter, and colored dissolved organic matter absorption coefficient in the Yellow and East China Seas. Journal of oceanography, 67(5), p.627.

Smith R C and Baker K S. 1982 Oceanic chlorophyll concentration as determined by satellite (Nimbus-7 Coastal Zone Color Scanner). Marine Biology, 66, pp. 269–279.

Tassan S. 1994. Local algorithm using SeaWiFS data for retrieval of phytoplankton pigment, suspended sediments and yellow substance in coastal waters. Applied Optics, 12, 2369-2378.

Tehrani, N.C., D'Sa, E.J., Osburn, C.L., Bianchi, T.S. and Schaeffer, B.A., 2013. Chromophoric dissolved organic matter and dissolved organic carbon from sea-viewing wide field-of-view sensor (SeaWiFS), Moderate Resolution Imaging Spectroradiometer (MODIS) and MERIS Sensors: Case study for the Northern Gulf of Mexico. Remote Sensing, 5(3), pp.1439-1464.

Thomas L C, Padmakumar K B, Smitha B R, Devi C A, Nandan S B and Sanjeevan V N. 2013. Spatio-temporal variation of microphytoplankton in the upwelling system of the south-eastern Arabian Sea during the summer monsoon of 2009. Oceanologia, 55(1), 185-204.

Tilstone, G.H., Peters, S.W., van der Woerd, H.J., Eleveld, M.A., Ruddick, K., Schönfeld, W., Krasemann, H., Martinez-Vicente, V., Blondeau-Patissier, D., Röttgers, R. and Sørensen, K., 2012. Variability in specific-absorption properties and their use in a semi-analytical ocean colour algorithm for MERIS in North Sea and Western English Channel Coastal Waters. Remote Sensing of Environment, 118, pp.320-338.

Tilstone G H, Ingrid M, Benavides A, Pradhan Y, Shutler J D, Groom, Sathyendranath S. 2011. An assessment of chlorophyll-a algorithms available for SeaWiFS in coastal and open areas of the Bay of Bengal and Arabian Sea. Remote sensing of environment., 115, 2277-2291.

Tzortziou M, Subramaniam A, Herman J R, Gallegos C L, Neale P J, Harding Jr., L W. 2007. Remote sensing reflectance and inherent optical properties in the mid Chesapeake Bay. Estuarine, Coastal and Shelf Science, 72, 16–32.

Werdell, P.J., Franz, B.A., Bailey, S.W., Feldman, G.C., Boss, E., Brando, V.E., Dowell, M., Hirata, T., Lavender, S.J., Lee, Z. and Loisel, H., 2013. Generalized ocean color inversion model for retrieving marine inherent optical properties. Applied optics, 52(10), pp.2019-2037.

Chapter 6

All the rivers run into the sea; yet the sea is not full.

-King Solomon

6. Summary and Conclusion

The studies on phytoplankton dynamics in the coastal waters of the Southeastern Arabian Sea in different seasons exhibited 73 genera of phytoplankton from 19 orders and 41 families. The numerical abundance of phytoplankton varied from 14.235×10^{3} to 55.075×10^{6}cells L^{-1}. Centric diatoms dominated in the region and the largest family identified was Thalassiosiraceae with main genera as *Skeletonema* spp., *Planktionella* spp. and *Thalassiosira* spp. Annual variations in abundance of phytoplankton showed a typical one-peak cycle, with the highest recorded during premonsoon season and the lowest during monsoon season. The species diversity index of phytoplankton exhibited low diversity during monsoon season.

Phytoplankton diversity also played a major role in determining the inherent optical properties in the area. The absorption coefficients and wavelength at peak absorption varied significantly with high and low diversity irrespective of seasons. Phytoplankton with pigments Chla, Chlb, Chlc, peridinin, diadinoxanthin, fucoxanthin, β-carotene and phycoerythrobilin dominated in these waters. From the derivative analysis of R_{rs}, marker peaks for picoplankton and microplankton was evident, while it failed to distinct peaks for nanophytoplankton. The strong water absorption can be studied from reflectance peaks corresponding to 571nm to 602 nm, picophytoplankton from 451±1nm, nanophytoplankton from negative peaks around 515±2 nm and 600±2 nm and microplankton from 568±3 nm in the

study area. Apart from this, picoplankton dominates in the Type-II and Type-III waters.

The alteration of dominance between the groups from diatoms to dinoflagellate and cyanobacteria, in different seasons can result in significant changes in the light absorption by phytoplankton pigments in the region. This inturn affects the ocean colour estimation used for various applications. Thus the data on the phytoplankton numerical abundance and diversity along with its absorption properties in the present study will provide insight to community dynamics and to the phytoplankton pigment composition of this water mass.

The concentration of Chla, an index of phytoplankton biomass, played a major role in the spectral variance of apparent optical properties. The variations in OAS such as Chla, CDOM and β_{650} showed three distinct water types associated with 3 different spectral R_{rs}. Low Chla resulted in spectral R_{rs} peak at 470 nm in the blue band in the Type-I waters. The tenfold increase in Chla concentration and β_{650} resulted in reflectance peaking at 560 nm. 64% increase in Chla concentration further resulted in shifting of R_{rs} peak at 570 nm. The study concluded that an increase in concentration of OAS results in shifting of the peak R_{rs} at the longer wavelength.

The six bio-optical algorithms (OC3C, OC4O, OC4, OC4E, OC3M and OC4O2) used operationally to retrieve Chla from CZCS, OCTS, SeaWiFS, MERIS, MODIS and OCM2. For Chla concentration greater than 1.0 mg m^{-3}, algorithms based on the reference band ratios 488/510/520 nm

to547/550/555/560/565 nm have to be considered. The assessment of algorithms showed better performance of OC3M and OC4. All the algorithms exhibited better performance in Type-I waters. However, the performance was poor in Type-II and Type-III waters which could be attributed to the significant co-variance of Chla with CDOM.

The Chla and CDOM compete for absorption of light at almost similar wavelengths in the blue region. As a result, the signal emerging from the water column carries signatures of both Chla and CDOM. The empirical algorithms take the ratio of the blue to the green band with an assumption that the water leaving radiance decreases in the blue band with an increase in Chla concentration. If the water column is dominated by Chla and CDOM, both significantly contribute to the decrease in the water leaving radiance in the blue band. In such a scenario, the performance of a ratio based algorithms weakens the retrieval of Chla.

Future Recommendations

- Understanding the dynamics of individual phytoplankton and their absorption studies can be used to indicate major differences in phytoplankton absorption spectra, which forms the basis of ocean colour remote sensing, with respect to seasons in the area.
- Interpretation of pigment data can improved by analysis of pure strains of local algal cultures under a range of conditions
- Size fractionation of samples will facilitate studies by removing large diatoms from the nanoplankton and picoplankton, thereby

understand their contribution to the inherent and apparent optical properties in the region.

- Hyperspectral radiometer measurements has to be carried out continuously irrespective of seasons to records the spectral underwater light field at depth, reaching the depths of phytoplankton maxima (10 to 30meters) and deeper.
- The concentration of optically active substances has to be validated using valuable ocean colour remote-sensing measurements.